Space-Time-Frequency Block Codes for MIMO-OFDM in Next Generation Wireless Systems

Min Zhang

A THESIS SUBMITTED FOR THE DEGREE OF DOCTOR OF PHILOSOPHY OF THE AUSTRALIAN NATIONAL UNIVERSITY

Department of Information Engineering
Research School of Information Sciences and Engineering
The Australian National University

April 2010

I hereby declare that the work in this thesis are my own, or partially in collaboration with others, except where otherwise stated and that, to the best of my knowledge and belief, it contains no material previously published or written by another person nor material which to a substantial extent has been accepted for the award of any other degree of diploma of the university or other institute of higher learning. My contributions to results of collaborative work presented in this thesis are at least 85%.

Min Zhang
26 April 2010

Dedication

This thesis is dedicated to my wife Mengmeng Tian, who have supported me along these years.

Acknowledgements

The thesis would not have been possible without the support and encouragement of many people who guided and supported me along these years. Firstly, I am very grateful to my supervisor Professor Thushara D. Abhayapala and Dr. Dhammika Jayalath. Thushara became my chief supervisor at the second year but he has been incredibly supportive since I just started my PhD study. He gave me a lot of freedom of pursuing my research interest, and valuable suggestions in potential research directions and academic career. I also want to express my gratitude to Dhammika for taking an interest in me, giving me an opportunity to working with him, providing me the PhD scholarship and most importantly inspiring me such a fascinating but challenging topic in MIMO-OFDM communication systems. Even he went to QUT at my second year, his suggestions and cooperations are still critical throughout my whole PhD study.

I would like to thank to Dr. David Smith, who has supported me in so many ways including joint discussions in the code design, his valuable suggestions for my publications and etc. I would also like to thank to Dr. Chandra Athaudage, who supported me in the research of decoding in the MIMO-OFDM system. The paper of classifier based decoding would not possible without his contribution. Many thanks also go to Professor Rod Kennedy who supported me in various aspects of my study and professional development. I am also deeply grateful to Dr. Mansoor Shafi, as my mentor, friend, and family member, who supported and urged me on the PhD study and career development along many years.

I would also like to thank to ANU, NICTA and ACoRN for the award of international PhD scholarship which supported me during three and half years of research, and for the travel grants of conference attendance and visiting which encouraged me to build the relationship with other researchers.

In May 2008, I was fortunate to have had an opportunity to visit engineering department of University of Victoria in New Zealand and I would like to thank to Dr. Peter Komisarczuk for his hospitality and financial support during my visiting. I am also grateful to my current boss Andrew Mackay for his valuable support and comments of thesis, and also Alcatel-Lucent New Zealand for generously giving me free time and resources to finish my thesis writing.

Finally, I also gratefully acknowledge the assistance I have received from ANU administration, Ms Debbie Pioch, Ms Elspeth Davies, and Ms Lesley Goldburg and IT staff for their enduring support.

The work is funded by Australian Research council Discovery grant DP0558865.

List of Publications

This thesis is based on following collection of papers which have either been published in or accepted by peer-reviewed journal or conference.

1. Min Zhang, Dhammika Jayalath, Thushara D. Abhayapala, David Smith, and Chandra Athaudage, "Compensation Decoding in Space Time Frequency Block Coding", *IEEE Communication Letters*, Vol 11, No 7, Page 610-612, July 2007.

2. Chandra Athaudage, Min Zhang, Dhammika Jayalath, and Thushara D. Abhayapala, "Classifier Based Low-Complexity MIMO Detection for Spatial Multiplexing Systems", *Australian Communication Theory Workshop*, Page 1-5, Jan. 2008.

3. Min Zhang and Thushara D. Abhayapala and Dhammika Jayalath and David Smith and Chandra Athaudage, "Multirate space-time-frequency linear block coding", *IEEE International Conference on Communications*, Page 4084-4089, May 2008.

4. Min Zhang, Thushara D. Abhayapala, Dhammika Jayalath, David Smith and Chandra Athaudage, "Matched Rotation Precoding: A new Paradigm in Space-Frequency Coding", *IEEE International Conference on Communications*, 2009.

5. Min Zhang, Thushara D. Abhayapala, Dhammika Jayalath, David Smith and Chandra Athaudage, "Space-frequency block coding with matched rotation for MIMO-OFDM system with limited feedback", *accepted by EURASIP Journal on Advances in Signal Processing*, 2008.

Abstract

In this thesis the use of space-frequency block codes (SFBC) and space-time-frequency block codes (STFBC) in wireless systems are investigated. A variety of SFBC and STFBC schemes are proposed for particular propagation scenarios and system settings where each has its own advantages and disadvantages. The objective is to propose coding strategies with improved flexibility, feasibility and spectral efficiency, and reduce the decoding complexity in an MIMO-OFDM system.

Firstly an efficient SFBC with improved system performance is proposed for MIMO-OFDM systems. The proposed SFBC incorporates the concept of matched rotation precoding (MRP) to achieve full transmit diversity and optimal system performance for an arbitrary number of transmit antennas, subcarrier interval and subcarrier grouping. The MRP is proposed to exploit the inherent rotation and repetition properties of SFBC, arising from the channel power delay profile, in order to fully capture both space and frequency diversity of SFBC in a MIMO-OFDM system. It is able to relax restrictions on subcarrier interval and subcarrier grouping, making it ideal for adaptive/time-varying systems or multiuser systems. The SFBC without an optimization process is unstable in terms of achievable system performance and diversity order, and also risks diversity loss within a specific propagation scenario. Such loss or risk is prominent while wireless propagation channel has a limited number of dominant paths, e.g. relatively close to transmitters or relatively flat topography. Hence in order to improve the feasibility of SFBC in dynamic scenarios, the lower bound of the coding gain for MRP is derived. The SFBC with MRP is proposed for more practical scenarios when only partial channel power delay profile information is known at the transmit end, for example the wireless channel has dominant propagation paths. The proposed rate one MRP has a relatively simple optimization process that can be transformed into an explicit diagram and hence an optimal result can be derived intuitively without calculations.

Next, a multi-rate transmission strategy is proposed for both SFBC and STFBC to balance the system performance and transmission rate. A variety of rate adaptive coding matrices are obtained by a simple truncation of the coding matrix, or by parameter optimization for coding matrices for a given transmission rate and constellation. Proposed strategy can easily and gradually adjust the achievable diversity order. As a result it is capable of achieving a relatively smooth balance between system perfor-

mance and transmission rate in both SFBC and STFBC, without a significant change of coding structure or constellation size. Such tradeoff would be useful to maintain stable Quality of Service (QoS) for users by providing more scalability of achievable performance in a time-varying channel.

Finally the decoding procedure of space-time block code (STBC), SFBC and STFBC is discussed. The decoding of all existing STBC/SFBC/STFBC is unified at first, in order to show a concise procedure and make fair comparisons. Then maximum likelihood decoding (MLD) and arbitrary sphere decoding (SD) can be adopted. To reduce the complexity of decoding further, a novel decoding method called compensation decoding (CD) is presented for a given space-time-frequency coding scheme. By taking advantage of the simplicity of zero-forcing decoding (ZFD) we are able to calculate a compensation vector for the output of ZFD. After modification by utilizing the compensation vector, the BER performance can be improved significantly. The decoding procedure is relatively simple and is independent of the constellation size. The performance of the proposed decoding method is close to maximum-likelihood decoding for low to medium SNR.

A low complexity detection scheme, classifier based decoding (CBD), is further proposed for MIMO systems incorporating spatial multiplexing. The CBD is a hybrid of an equalizer-based technique and an algorithmic search stage. Based on an error matrix and its probability density functions for different classes of error, a particular search region is selected for the algorithmic stage. As the probability of occurrence of error classes with larger search regions is small, overall complexity of the proposed technique remains low, whilst providing a significant improvement in the bit error rate performance.

List of Abbreviations

AoA	Angle of arrival
AoD	Angle of departure
BS	Base station
BER	Bit error rate
CD	Compensation Decoding
CBD	Classifier based decoding
CP	Cyclic prefix
FDM	Frequency-division multiplexing
FDD	Frequency division duplexing
FFT	Fast Fourier transform
IFFT	Inverse fast Fourier transform
ISI	Inter symbol interference
LDC	Linear Dispersion Code
LTE	Long Term Evolution
LTE-A	Long Term Evolution Advance
LoS	Light of sight
MIMO	Multiple-input Multiple-output
MISO	Multiple-input Single-output
MLD	Maximum likelihood Detection
MS	Mobile station
NLoS	Non light of sight
OFDM	Orthogonal frequency-division multiplexing
QAM	Quadrature amplitude modulation
PSK	Phase shift keying
PDP	Power delay profile
STBC	Space-time block code
SFBC	Space-frequency block code
STFBC	Space-time-frequency block code
STF	Space-time-frequency
SF	Spatial-frequency
SISO	Single-input Single-output
SCM	3GPP spatial channel model

TDD	Time division Duplexing
ZFD	Zero-forcing Decoding

List of Notations

$\mathbb{E}$	Expectation
$(.)^T$	Matrix transpose
$(.)^*$	Complex conjugate
$(.)^\dagger$	Adjoint complex conjugate transpose
vec	Matrix reconstruction which stacks a matrix columnwise to form a column vector
$\otimes$	Kronecker product
$\circ$	Hadamard product
$\mathbf{1}_a$	$a \times a$ all one matrix
$\mathbf{1}_{a\times b}$	$a \times b$ all one matrix
$\mathbf{I}_a$	$a \times a$ Identity matrix
$\mathbf{R}_{BS}(m, m')$	BS spatial correlation coefficient between the mth and the m'th transmitters
$\mathbf{R}_{BS}$	BS spatial correlation matrix
$\mathbf{R}_{MS}(n, n')$	MS spatial correlation coefficient between the nth and the n'th receivers
$\mathbf{R}_{MS}$	MS spatial correlation matrix
$\mathbf{R}_F(f, f')$	Frequency correlation coefficient between the fth and the f'th subcarriers
$\mathbf{R}_F$	Frequency correlation matrix
$\mathbf{R}_T(k, k')$	Temporal correlation coefficient between the kth and the k'th symbol periods
$\mathbf{R}_T$	Temporal correlation matrix
N_t	Number of transmitters at BS
N_r	Number of receivers at MS
F	Number of subcarriers of a MIMO-OFDM system
K	Number of symbol periods of a MIMO-OFDM system
P	Number of subcarriers of a MIMO-OFDM subsystem
τ_ℓ	Time delay of the ℓth path
$\hbar_{mn,\ell}$	Complex amplitude coefficient of the ℓth path
T_s	OFDM symbol period
$\mathbb{R}$	Real
$\mathbb{Z}$	Integer
$\mathbb{C}$	Complex

Contents

Dedication v

Acknowledgements vii

Publications ix

Abstract xi

1 Thesis Introduction 1
- 1.1 MIMO-OFDM System . . . 1
- 1.2 Motivations of the Thesis . . . 2
- 1.3 Chapter Outline . . . 3
- 1.4 Original Contributions . . . 5

2 MIMO-OFDM System Model 7
- 2.1 Introduction . . . 7
- 2.2 MIMO System . . . 8
- 2.3 OFDM System . . . 10
- 2.4 MIMO-OFDM System Model . . . 11
- 2.5 Correlations of STF domains . . . 13
- 2.6 Separability of Cross-Correlation . . . 14
- 2.7 Frequency Correlation . . . 16
  - 2.7.1 Uniform PDP . . . 16
  - 2.7.2 COST207 . . . 19
  - 2.7.3 SCM . . . 19
- 2.8 MIMO-OFDM Subsystem . . . 21
  - 2.8.1 Subcarrier Grouping . . . 21
  - 2.8.2 Correlation Structure of Subsystem . . . 22
- 2.9 Summary . . . 24

3 Review of STBC/SFBC/STFBC 27
- 3.1 Introduction . . . 27
- 3.2 Spatial Diversity . . . 27

3.2.1 Orthogonal STBC 28
3.2.2 Quasi-orthogonal STBC 29
3.2.3 Linear Dispersion Code 29
3.2.4 High Rate STBC 30
3.2.5 STBC Applications in the MIMO-OFDM System 31
3.3 Space and Frequency Diversity 32
3.4 STF Diversity 37
3.5 Multiuser SFBC 38

4 Space-Frequency Block Codes with Matched Rotation Precoding 41
4.1 Introduction 41
4.2 Brief Survey of Space-Time Block Codes 43
4.3 MIMO-OFDM System Modelling 44
4.3.1 Subcarrier Grouping for the MIMO-OFDM Model 44
4.3.2 Correlation Structure of the MIMO-OFDM subsystem 46
4.4 Analysis of SFBC Design 47
4.4.1 Design Criteria 47
4.4.2 Structure Analysis with Full PDP 49
4.4.3 Structure Analysis with Limited PDP 51
4.5 Rate One Matched Rotation Precoding 53
4.5.1 Rate One SFBC 53
4.5.2 Optimization process for $\check{\xi}_{\mathcal{A}}$ 55
4.5.3 Optimization Process for $\check{\xi}_{ECG}$ 56
4.5.4 Visualization of Optimization 59
4.5.5 Examples 61
4.6 Multirate Matched Rotation Precoding 62
4.6.1 Multirate SFBC 63
4.6.2 Optimization Process 65
4.6.3 Examples 66
4.7 Simulation Results 67
4.7.1 Diversity Loss 68
4.7.2 Rate one MRP 69
4.7.3 Multirate MRP 70
4.8 Summary 71
4.9 Conclusions 74

5 Space-Time-Frequency Block Codes 75
5.1 Introduction 75

5.2 Brief survey of Space-Time-Frequency Block Codes 76
5.3 MIMO-OFDM System Modelling 77
5.4 Multirate STFBC coding scheme 78
5.4.1 Coding Process 79
5.4.2 Coding Gain 80
5.4.3 Coding Design 81
5.4.4 Example of the multirate STFBC 83
5.5 Simulations and comparisons 84
5.6 Summary 87
5.7 Conclusions 88

6 Simplified Decoding for MIMO-OFDM Systems **89**
6.1 Introduction 89
6.2 Summary of Decoding 90
6.3 Unified Decoding 91
6.4 Compensation Decoding 92
6.4.1 Channel Modelling and Coding 92
6.4.2 MIMO-OFDM Decoding 95
6.4.3 Simulations and Comparisons 99
6.5 Classifier Based Decoding 102
6.6 Summary 105
6.7 Conclusions 107

7 Conclusion **109**

A Derivation of Equation (4.9) **113**

B Derivation of Equation (4.14) **115**

C Proof of Remark 1 in Chapter 5 **117**

Bibliography **119**

Chapter 1

Thesis Introduction

1.1 MIMO-OFDM System

The fast growing high data-rate applications such as new multimedia services and video on demand require wireless systems to provide higher data-rate and offer better Quality of Service (QoS). First, the scarcity of available spectrum places a limitation on the available data-rate. Secondly, the multi-path fading makes broadband radio propagation more prone to transmission errors. Consequently, it is of practical significance to enable an evolution on transmission architecture itself in order to use the radio resources flexibly in multi-user environments.

The system spectral efficiency in a wireless channel can be increased by introducing a multiple-input multiple-output (MIMO) communication system. It can provide both high rate transmission, high spatial diversity or trade-off between diversity and multiplexing. Moreover, the orthogonal frequency division multiplexing (OFDM) system transforms the frequency-selective fading channel into a number of parallel narrowband MIMO subsystems with flat fading. The inter symbol interference (ISI) can be eliminated completely by inserting a long enough cyclic prefix (CP). The system combining both MIMO and OFDM techniques has already been implemented in IEEE 802.11n, LTE [1,2] and WiMax system [3] and attracted much attention for future broadband wireless systems [4].

Space-time coding strategy achieves spatial diversity by transmitting signals through multiple transmit antennas and multiple time blocks. The simplest form of diversity gain was introduced by Alamouti [5]. Alamouti code is a simple $2x2$ MIMO scheme that achieves full transmit and receive diversity gain with an efficent maximum likelihood decoding algorithm. Furthermore, all existing space-time block codes (STBC), e.g. [5–7], can be converted to space-frequency block codes (SFBC) or space-time-frequency block codes (STFBCs) simply by spreading time domain signals of STBC within frequency domain or a combination of time and frequency domains. This conversion works well if adjacent subcarrier channels are highly correlated, e.g.

an OFDM system with relatively large number of subcarriers. However this kind of direct conversion is not optimal and fails to achieve valuable frequency diversity. Moreover, it neither increases diversity gain nor improves coding gain. Therefore the performance of the code is generally related to the MIMO-OFDM channels and the signal to noise ratio only. The codes based on such domain conversion method are still regarded as STBC, and reviewed in Chapter 3.

1.2 Motivations of the Thesis

The main purpose of this doctoral thesis is to design space-frequency and space-time-frequency coding strategies with improved flexibility, feasibility and spectral efficiency, and reduce the decoding complexity in the MIMO-OFDM system. Since space, time and frequency domains might have different channel characteristics/assumptions, SFBC and STFBC are treated separately to incorporate a variety of design concepts and desired performance goal.

To achieve full spatial and frequency diversity, the SFBCs were proposed in [8–10] by exploiting a mass of subcarriers. The advantages of the SFBC are better diversity gain and coding gain (which are related to actual channel conditions), without increasing the number of transmitters. Hence the traditional design criteria of the STBC should be modified to deal with the special characteristics of SFBC. By employing a large number of subcarriers, e.g. $N_t(L+1)$, and proper interleaving, full spatial and frequency diversity can be obtained where L is the fixed channel order and N_t is the number of transmitters. However the channel order L might be enormous in a wireless propagation channel, e.g. $L+1 = 20, 21$ in [11], and be rapidly changed with time and users. Hence such requirements will increase the difficulty of practical implementation of the SFBC in communication systems. To mitigate such requirements, a novel SFBC of the MIMO-OFDM system is discussed in Chapter 4.

The optimization process of the SFBC has a requirement of perfect knowledge of channel power delay profile (PDP) at the transmit end. It was proposed in [12, 13] by a subcarrier grouping strategy. The subcarrier grouping is often considered in the MIMO-OFDM system to reduce the design complexity and the system complexity. Hence the second-order characteristics of a MIMO-OFDM subsystem after grouping is varied with different subcarrier grouping strategies so that corresponding coding gain of the SFBC can be maximized. However inherent limitation of subcarrier grouping is the choices of subcarrier interval, if the efficient use of all available subcarriers is the goal of optimization. And it will be even more difficult in a multiuser scenario since each user might have independent self-optimized subcarrier grouping strategy. Adjusting subcarrier grouping strategy leads to additional difficulty of resource schedul-

ing in a multiuser MIMO-OFDM system. To optimize system performance whilst mitigating the requirement of subcarrier grouping, the SFBC design of the MIMO-OFDM system is further discussed in Chapter 4.

The high rate SFBC/STFBC with full transmit diversity can further increase the spectral efficiency of the MIMO-OFDM system. Hence the design of high rate SFBC/STFBC were proposed in [12, 13] by a layered algebraic design. The design of high rate SFBC/STFBC is more challenging in the MIMO-OFDM system, compared to the high rate STBC in the MIMO system, e.g. perfect code in [14]. The design criteria of high rate SFBC/STFBC becomes entangled in time-varying channel conditions and also be inseparable. An optimal high rate SFBC/STFBC, in terms of the spectral efficiency, should be time-varying, and also system-dependent. On the other hand, higher symbol transmission rate also reduces the coding gain and BER performance if symbol constellation is fixed. In Chapter 4 and Chapter 5 a tradeoff of spectral efficiency and performance is proposed, with a flexible system transmission rate (high rate or low rate) and fully achieved SF diversity. The multirate code in Chapter 4 can achieve full frequency diversity gain in the MIMO-OFDM system. The multirate code in Chapter 5 can only achieve partial frequency diversity because of more strict channel assumptions.

The decoding procedure should be considered as well in the MIMO-OFDM system. Most existing decoding procedures of SFBC/STFBC in the MIMO-OFDM system focus on the maximum likelihood decoding (MLD) with exponential complexity, the sphere decoding (SD) with a polynomial complexity, the zero-forcing decoding (ZFD) with a polynomial complexity and serious diversity loss, and the minimum mean-squared error decoding (MMSE) with a polynomial complexity and a complex process of channel inverse. With the increase of size of the MIMO-OFDM system (e.g. number of subcarriers, constellation size and number of antennas), corresponding decoding procedure might be extremely time-consuming, e.g. MLD and SD. On the other hand, the ZFD and MMSE are relatively time saving. However they suffer from serious performance loss and require a channel inverse process. In order to balance decoding complexity and system decoding performance some strategies are discussed in Chapter 6 for the MIMO-OFDM system utilizing compensation decoding, or prior statistical channel information.

1.3 Chapter Outline

The rest of the thesis is organized as follows:

In Chapter 2 basic properties of the MIMO-OFDM channel are reviewed and investigated. The correlation structure of the system is derived to satisfy requirements

of a concise design structure and complexity of channel modeling. The special characteristics of the MIMO-OFDM system inspires the development of coding strategies.

Chapter 3 provides a review of STBCs, SFBCs and STFBCs. These existing codes are designed for different communication systems with particular channel assumptions. Hence the diversity gain and coding gain achieved by these codes vary from case to case, with their own advantages and disadvantages.

In Chapter 4 an efficient SFBC is proposed. The proposed SFBC incorporates a concept of matched rotation precoding (MRP) to achieve full diversity and an optimal system performance for the MIMO-OFDM system. A SFBC with rate one MRP and a SFBC with multirate MRP are proposed for more practical scenarios, both of which are capable of achieving full transmit diversity for the MIMO-OFDM system with an arbitrary subcarrier interval, subcarrier grouping, or number of transmitters, with partial channel knowledge at the transmit end.

In Chapter 5, the design structure of all existing STBC/SFBC/STFBC for the MIMO-OFDM system is unified in order to get an in-depth understanding and make fair comparisons. Based on this unified structure, a multirate STFBC with full STF transmit diversity is proposed. A variety of rate adaptive coding matrices are obtained by a simple truncation of the coding matrix, or by parameter optimization for coding matrices with a given transmission rate and constellation. The proposed multirate STFBC can achieve a relatively smooth balance between the transmission rate and the performance without changing constellation size.

In Chapter 6, the decoding procedures of STBC/SFBC/STFBC in the MIMO-OFDM system are investigated. The decoding of all existing STBC/SFBC/STFBC for the MIMO-OFDM system is unified at first in order to show a concise procedure. Then the MLD or the SD can be adopted. Furthermore, a novel decoding method called as compensation decoding (CD) is represented for a given space-time-frequency coding scheme to reduce the complexity of decoding. Taking advantage of the simplicity of the ZFD, we develop a method to calculate a compensation vector for the output of ZFD. A trade-off between the system performance and complexity is demonstrated for the implementation of CD. Furthermore, a low complexity detection scheme, classifier based decoding (CBD), is proposed in chapter 6 for MIMO systems incorporating spatial multiplexing. The CBD is a hybrid of an equalizer-based technique and an algorithmic search stage. Based on an error matrix and its probability density functions for different classes of error, a particular search region is selected for the algorithmic stage.

1.4 Original Contributions

Several contributions have been made for the academic research in this doctoral thesis and given by following

1. A concise design structure is proposed. It can unify all existing linear SFBC / STBC / STFBC into a flexible structure. Distinct patterns of coding reveal special characteristics of the SFBC / STFBC in the MIMO-OFDM system.

2. An efficient SFBC is proposed. It has a high spectral efficiency, improved system flexibility and feasibility, and reduced complexity of system optimization process.

3. A multi-rate STFBC is proposed. It has a high spectral efficiency, and can achieve relatively smooth balance between system performance and precoding complexity.

4. Two simple decoding procedures are proposed. They can take advantage of the simplicity of zero-forcing decoding and improve the decoding performance with a small incremental complexity.

The content of Chapter 4 can be found in following publications:

- Min Zhang, Thushara D. Abhayapala, Dhammika Jayalath, David Smith and Chandra Athaudage, "Matched Rotation Precoding: A new Paradigm in Space-Frequency Coding", *IEEE International Conference on Communications*, 2009.

- Min Zhang, Thushara D. Abhayapala, Dhammika Jayalath, David Smith and Chandra Athaudage, "Space-frequency block coding with matched rotation for MIMO-OFDM system with limited feedback", *Accepted by EURASIP Journal on Advances in Signal Processing and under a second review*, 2008.

The content of this chapter 5 can be found in the following publication:

- Min Zhang, Thushara D. Abhayapala, Dhammika Jayalath, David Smith and Chandra Athaudage, "Multirate space-time-frequency linear block coding", *IEEE International Conference on Communications*, Page 4084-4089, May 2008, Beijing, China.

The content of this chapter 6 can be found in following publication:

- Min Zhang, Dhammika Jayalath, Thushara D. Abhayapala, David Smith, and Chandra Athaudage, "Compensation Decoding in Space Time Frequency Block Coding", *IEEE Communication Letters*, Vol 11, No 7, Page 610-612, July 2007.

- Chandra Athaudage, Min Zhang, Dhammika Jayalath, and Thushara D. Abhayapala, "Classifier Based Low-Complexity MIMO Detection for Spatial Multiplexing Systems", *Australian Communication Theory Workshop*, Page 1-5, Jan. 2008.

- Min Zhang, Thushara D. Abhayapala, Dhammika Jayalath, David Smith and Chandra Athaudage, "Multirate space-time-frequency linear block coding", *IEEE International Conference on Communications*, Page 4084-4089, May 2008.

Chapter 2

MIMO-OFDM System Model

2.1 Introduction

Motivated by the huge demands for fast and reliable wireless communication networks, a multiple-input multiple-output (MIMO) technique is proposed for next generation communication systems, e.g. 3G LTE [2] and WiMax [3], since it offers significant increase in data throughput, link reliability and link range without additional bandwidth or transmit power, compared with single-input single-output (SISO) technique. It can achieve higher spectral efficiency (more bits per second per Hertz) and transmit-receive diversity (better link reliability) in space, and/or time, and /or frequency domains.

Orthogonal frequency-division multiplexing (OFDM) is a frequency-division multiplexing (FDM) scheme regarded as a digital multi-carrier modulation method. A large number of closely-spaced orthogonal subcarriers are used to carry data. The data are divided into a number of parallel low-rate data streams or subchannels, typically dozens to thousands, to be carried by each subcarrier. Each subcarrier is modulated with a conventional modulation scheme (such as quadrature amplitude modulation (QAM) or phase shift keying (PSK)) at a low symbol rate.

The primary advantage of OFDM over single-carrier schemes is its ability to cope with severe channel conditions, e.g., narrowband interference and frequency-selective fading due to multipath. Therefore the OFDM system can avoid complex equalization processes. It can also transform the frequency-selective fading channel into a number of parallel MIMO subsystems with flat fading. The OFDM systems eliminate the inter-symbol-interference (ISI) completely by inserting a long enough cyclic prefix (CP).

The MIMO-OFDM system has attracted much attention for future broadband wireless systems. It has already been implemented in IEEE802.11n, WiMax [3] and 3G-LTE systems [1]. The results of lab and field tests of the MIMO-OFDM system can be found in [15, 16]. Increased capacity, coverage and reliability of the system can be found in articles [15, 16]. This chapter will provide a review of some typical MIMO-OFDM sys-

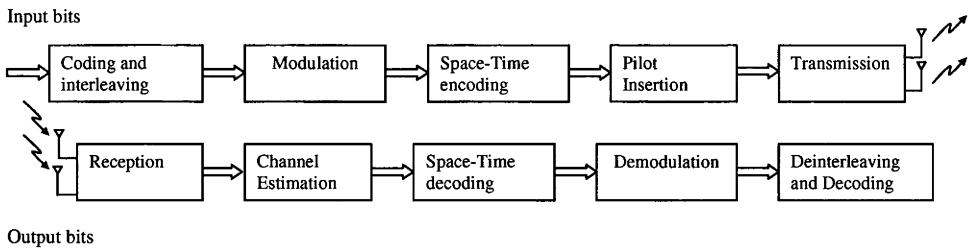

Figure 2.1: Block diagram for a MIMO system

tem models. However the strategy of MIMO-OFDM modelling has to cater for the code design process so that model simplification should be considered with certain degree. Hence the wireless channel models discussed in this chapter are commonly used for the code design process, rather than used for channel research or system level simulations. Furthermore, some basic rules of simplification for the MIMO-OFDM system modelling are reviewed. Hence we are able to understand limitations of each channel model that might significantly affect the code design process and determine the feasibility of coding strategy.

Firstly this chapter will review background and major characteristics of the MIMO-OFDM system. A generalized MIMO-OFDM system model is then proposed. The correlation properties of space-time-frequency (STF) domains are discussed based on the MIMO-OFDM system model. Several rules of simplification for channel correlation properties are reviewed so that a concise structure can be proposed for later code design and optimization. The frequency domain is a distinct domain which makes SFBC/STFBC special. Therefore the frequency correlation is discussed further with respect to different channel modelling strategies. Finally the property of a MIMO-OFDM subsystem after subcarrier grouping is reviewed since subcarrier grouping is commonly adopted in a wireless OFDM system so that the code design process can focus on a subsystem only.

2.2 MIMO System

Figure 2.1 is a block diagram of a typical MIMO system. The input bits first go through a error control code, e.g. a turbo code or a convolutional code, and then interleaved. The interleaved codeword is modulated into data symbols by a given digital modulation scheme, e.g. QAM or PSK. The data symbols are then input into a space-time encoder, e.g. Alamouti code [5] or linear dispersion code [6]. The output of the space-time encoder is then added with some pilot symbols. Data symbols are mapped into multiple transmit antennas (transmitters) and launched from these antennas with a

given transmission power. The wireless signals arrive at the receive antennas (receivers) after traveling through the propagation channel experiencing fading and time delay. The receivers collect the signal from every antenna. The pilot symbols are removed at first and used to estimate the channel impulse response coefficients. Then received symbols go through corresponding space-time decoder with estimated channel coefficients, demodulation, de-interleaving and decoding. Each block in Figure 2.1 provides great challenge of design. And many research outcomes can be found in existing literature, e.g. [17].

In order to design a efficient space-time encoder for a MIMO system, it is important to understand the MIMO channel. For a MIMO system with N_t transmitters and N_r receivers in a frequency-flat fading channel (time delays of paths are negligible), the channel impulse response at a given time instance is expressed as a $N_t \times N_r$ matrix:

$$\mathbf{H} = \begin{bmatrix} h_{11} & \cdots & h_{1N_r} \\ \vdots & \vdots & \vdots \\ h_{N_t1} & \cdots & h_{N_tN_r} \end{bmatrix} \tag{2.1}$$

where h_{mn} is the channel impulse response of the mth transmitter and the nth receiver at a given time instance, $m \in [1, \cdots, N_t]$ and $n \in [1, \cdots, N_r]$. The channel matrix $\mathbf{H}$ might be represented as $N_r \times N_t$ matrix for the representation of system coding and decoding process. The individual h_{mn} is commonly modeled as zero-mean circular symmetrical complex Gaussian random variable. Hence the amplitudes of h_{mn} are random Rayleigh distributed and the power $\|h_{mn}\|^2$ are random exponential distributed.

The transmit spatial correlation at the base station (BS) is denoted as

$$\mathbf{R}_{BS} = \mathbb{E}\left[\mathbf{H}\mathbf{H}^\dagger\right], \tag{2.2}$$

and the receive spatial correlation at the mobile station (MS) is denoted as

$$\mathbf{R}_{MS} = \mathbb{E}\left[\mathbf{H}^\dagger\mathbf{H}\right]. \tag{2.3}$$

The relative geometry configuration of antennas and the conditions of propagation channel determine the correlation of transmit signals and the correlation of receive signals. Ideally the signals should be uncorrelated so that the correlation matrices $\mathbf{R}_{BS}$ and $\mathbf{R}_{MS}$ are diagonal matrices. This is particularly important when the independent data streams are launched from the transmitters in the case of spatial multiplexing. However this property is strictly limited by the available antenna spacing so that it might not be feasible in some practical implementations.

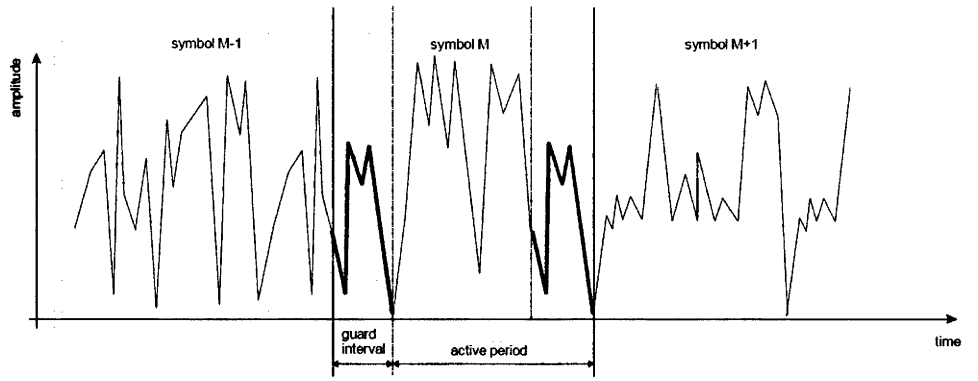

Figure 2.2: Example of the cyclic prefix (CP). Each OFDM symbol is made up of two parts: one is active period, the last part of active period is repeated at the start of the symbol which is called as the CP or guard interval.

2.3 OFDM System

The concept of OFDM was initially proposed in the mid 1960s [18–20] utilizing the technique of FDM, where fast fading was not a problem. The principle was to use several data streams with smaller size data package and FDM without overlapping subchannels. Hence high speed equalization can be avoided and the efficiency of bandwidth can be improved by parallel transmission over frequency domain. The initial applications were in the military communications because of high cost of applications.

The orthogonality of the OFDM indicates that there is a precise mathematical relationship between the subcarriers in the system. In a traditional FDM system, the subcarriers are separated from each other so that the signals can be transmitted or received using conventional filters and equalizations. However, the subcarriers in an OFDM system can be overlapped and the signals can be received without adjacent subcarrier interference. Hence the subcarriers must be exactly mathematically orthogonal [21].

Each subcarrier can be expressed as a complex wave:

$$s_f(t) = A_f e^{j(\omega_f t + \phi_f)} \tag{2.4}$$

where A_f and ϕ_f are the amplitude and phase of a signal and stay constant over an OFDM symbol period of T_s. Then the complex wave of all subcarriers is represented by

$$s(t) = \frac{1}{F} \sum_{f=0}^{F-1} A_f e^{j(\omega_f t + \phi_f)} \tag{2.5}$$

where $\omega_f = \omega_0 + f\Delta\omega$. If the signal $s(t)$ is sampled using a sampling frequency of $1/T$ and $T = T_s/F$, without loss of generality by letting $\omega_0 = 0$, the signal is simplified as

$$s(kT) = \frac{1}{F}\sum_{f=0}^{F-1} A_f e^{j\phi_f} e^{j(f\Delta\omega kT)}. \tag{2.6}$$

Furthermore, if the system has exactly subcarrier separation $\Delta\omega = 1/T_s$, we have

$$s(kT) = \frac{1}{F}\sum_{f=0}^{F-1} A_f e^{j\phi_f} e^{j(2\pi fk/F)} \tag{2.7}$$

which is the general form of inverse discrete Fourier transform. The inverse fast Fourier transformation (IFFT) and the fast Fourier transformation (FFT) are merely rapid mathematical methods easily implemented for computer applications. With the development of integrated circuit, the technology of the OFDM can now be realized.

The orthogonality of the OFDM system must be maintained. And the individual subcarrier can be exactly separated at the receive end as long as the ISI introduced by the channel transmission delays are removed. One way of preventing ISI is to create a CP, also called as guard interval. The CP is a periodic extension of the signal itself and appended at the head of the signal before transmission. It is shown in Figure 2.2. At the receive end, the CP is removed at first, then goes through FFT operation. When the time of the CP is longer than the channel impulse response, or the propagation delays, the ISI can be eliminated completely. The insertion of the CP will reduce the data throughput, so the time of the CP is usually less than $T_s/4$.

2.4 MIMO-OFDM System Model

We consider a MIMO-OFDM system with N_t transmitters, N_r receivers, K OFDM symbol periods and F subcarriers. Figure 2.3 (a) is a single-input single-output OFDM system and Figure 2.3 (b) is a MIMO-OFDM system. The frequency-selective fading channel is assumed to be static (time invariant) within at least one OFDM symbol period of T_s. Each transmit and receiver pair has $L+1$ resolvable delay paths with the same power delay profile (PDP) but the PDP may vary from one OFDM symbol period to another depending on the channel. The channel impulse response coefficient between the mth transmitter and the n receiver at the kth OFDM period is expressed as:

$$h_{mn,k}(\tau) = \sum_{\ell=0}^{L} \hbar_{mn,\ell}^{k}\delta(\tau - \tau_\ell) \tag{2.8}$$

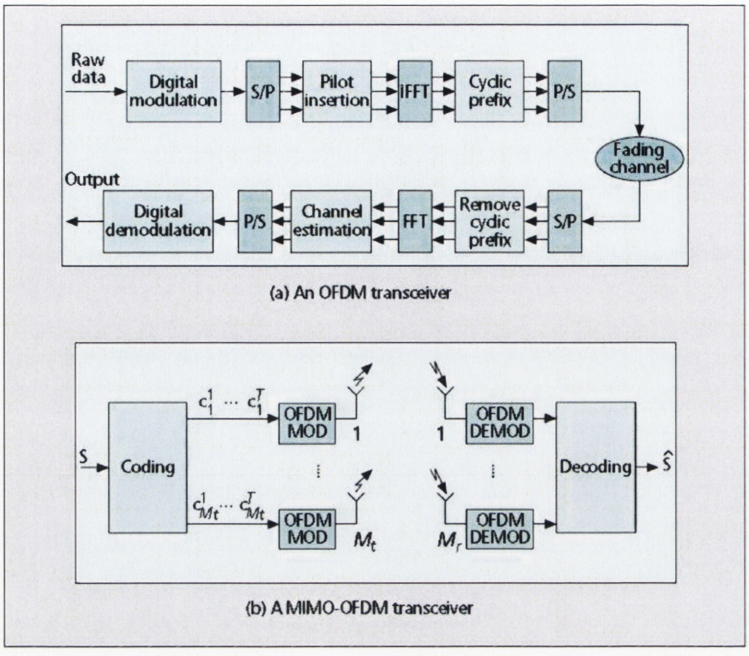

Figure 2.3: Block Diagram for a MIMO-OFDM system [22]

where τ_ℓ and $\hbar_{mn,\ell}$ are the delay and complex amplitude coefficient of the ℓth path respectively. And $\delta(.)$ is the Dirac delta function.

A block of data symbols is transmitted over each transmitter passed through a F-point IFFT and a CP is appended following. The length of CP is chosen to be long enough to remove the ISI completely so that the OFDM system does not require a complicated equalizer. At each receiver, the CP is removed and then a FFT is applied. Hence the frequency selective MIMO channel is decoupled into F parallel frequency flat fading channels. And the channel frequency response coefficient between the mth ($m \in [1, \cdots, N_t]$) transmitter and the n receiver ($n \in [1, \cdots, N_t]$) at the kth ($k \in [1, \cdots, K]$) OFDM symbol period is expressed as:

$$h_{mn,k}(f) = \sum_{\ell=0}^{L} \hbar_{mn,\ell}^{k} e^{-j2\pi f \tau_\ell / T_s} \tag{2.9}$$

where $j = \sqrt{-1}$ and T_s is the OFDM symbol period. For the purpose of coding and decoding, it is assumed that the system has perfect knowledge of channel frequency response coefficients $h_{mn,k}(f)$ at the receive end. But the system does not have such knowledge at the transmit end. The channel frequency response coefficients can be derived by combined pilot insertion at the transmit end and channel estimation process at the receive end. It is also assumed that there is a perfect synchronization between the BS and the MS so that any kind of channel estimation errors are ignored. We only

focus on the performance effect of coding and decoding in the thesis.

The channel frequency response $\mathbf{H}_k(f)$, a complex $N_t \times N_r$ matrix , between transmitters and receivers for the fth subcarrier in the MIMO-OFDM system is denoted by

$$\mathbf{H}_k(f) = \begin{bmatrix} h_{11,k}(f) & \cdots & h_{1N_r,k}(f) \\ \vdots & \cdots & \vdots \\ h_{N_t1,k}(f) & \cdots & h_{N_tN_r,k}(f) \end{bmatrix} \tag{2.10}$$

where each entry $h_{mn,k}(f)$ is denoted by (2.9). If the wireless channel is a frequency-flat channel, then $\mathbf{H}_k(f) = \mathbf{H}_k(f')$ for $\forall f \in [1, \cdots, F]$.

2.5 Correlations of STF domains

The correlation coefficients among STF domains are denoted as transmit spatial correlation coefficient $\mathbf{R}_{BS}(m, m')$, receive spatial correlation coefficient $\mathbf{R}_{MS}(n, n')$, frequency correlation coefficient $\mathbf{R}_F(f, f')$ and temporal correlation coefficient $\mathbf{R}_T(k, k')$. And $\mathbf{R}_{BS}(m, m')$ is the entry of matrix $\mathbf{R}_{BS}$ at the mth row and the m'th column. There are similar definitions for the other three correlation matrices. The entries of these correlation matrices are further given by

$$\begin{aligned} \mathbf{R}_T(k, k') &= \mathbb{E}\{h_{mn,k}(f)h^*_{mn,k'}(f)\}, \\ \mathbf{R}_{BS}(m, m') &= \mathbb{E}\{h_{mn,k}(f)h^*_{m'n,k}(f)\}, \\ \mathbf{R}_{MS}(n, n') &= \mathbb{E}\{h_{mn,k}(f)h^*_{mn',k}(f)\}, \\ \mathbf{R}_F(f, f') &= \mathbb{E}\{h_{mn,k}(f)h^*_{mn,k}(f')\} = \mathbf{w}_f\mathbf{R}_D\mathbf{w}^\dagger_{f'}, \\ \mathbf{R}_D(\ell, \ell') &= \mathbb{E}\{\hbar^k_{mn,\ell}\hbar^{k*}_{mn,\ell'}\}. \end{aligned} \tag{2.11}$$

Furthermore, the frequency correlation matrix $\mathbf{R}_F$ is given by:

$$\mathbf{R}_F = \mathbf{W}\mathbf{R}_D\mathbf{W}^\dagger \tag{2.12}$$

where the $F \times (L+1)$ matrix $\mathbf{W}$ is shown as

$$\mathbf{W} = \left[\mathbf{w}^0, \cdots, \mathbf{w}^L\right] = \begin{bmatrix} \mathbf{w}_1 \\ \vdots \\ \mathbf{w}_F \end{bmatrix} = \begin{bmatrix} 1 & \cdots & 1 \\ \vdots & \cdots & \vdots \\ w_F^0 & \cdots & w_F^L \end{bmatrix}$$

where the entry w_f^ℓ in matrix $\mathbf{W}$ is defined as $w_f^\ell = e^{j2\pi(f-1)\tau_\ell/T_s}$ where $f \in [1, \cdots, F]$ and $\ell \in [0, \cdots, L]$. The matrix $\mathbf{R}_D$ is $(L+1) \times (L+1)$ correlation matrix of multipath. And $\mathbf{R}_D = \frac{1}{L+1}\mathbf{I}_{L+1}$ if delay paths are independent and have equal delay power.

Moreover there is a underlying assumption of $2\pi\tau_\ell/T_s \neq 2k\pi + 2\pi\tau_{\ell'}/T_s$ for $\forall \ell \neq \ell'$, $\ell, \ell' \in [0, \cdots, L]$ and $k \in \mathbb{Z}$. Otherwise the MIMO-OFDM system can not achieve full frequency diversity order of $L+1$.

The frequency correlation coefficient $\mathbf{R}_F(f, f')$ between two subcarriers f and f' will be varied for different propagation scenarios and subcarrier interval $\delta = \|f - f'\|$. Two subcarriers can be highly correlated, e.g. two consecutive subcarriers for an OFDM system with a large value of F, or be non-correlated, e.g. two subcarriers with specific subcarrier interval for an OFDM system with an ideal uniform PDP. Moreover, the temporal correlation coefficient $\mathbf{R}_T(k, k')$ between two OFDM symbol periods k and k' can be highly correlated when total transmission time of these symbol periods is less than the coherence time of propagation channel, or be non-correlated when such condition can not be satisfied, e.g. two well-separated OFDM symbol periods or a fast fading channel.

2.6 Separability of Cross-Correlation

The cross-correlation coefficient ρ between two channel frequency response coefficients $h_{mn,k}(f)$ and $h_{m'n',k}(f')$ is defined as

$$\rho = \mathbb{E}\left[h_{mn,k}(f) h_{m'n',k}(f')\right]. \tag{2.13}$$

The separability of cross-correlation coefficient between STF domains is one of key assumptions of channels so that the code design could be simplified or be extremely complex. Here some basic principles of the separability are discussed in this thesis and they are commonly adopted in all SFBC/STFBC code designs with stated or implied assumptions in the literature.

The separability of coefficient ρ is defined as whether the following equation is satisfied:

$$\rho = \mathbf{R}_T(k, k')\mathbf{R}_{BS}(m, m')\mathbf{R}_{MS}(n, n')\mathbf{R}_F(f, f') \tag{2.14}$$

so that the cross-correlation coefficient can be expressed as a product of independent temporal, transmit spatial, receive spatial and frequency correlations.

The separability is closely related to the statistical distribution of $\hbar^k_{mn,\ell}$ and delays τ_ℓ where $\ell \in [0, \cdots, L]$. The assumptions of distributions are varied from one paper to another. Generally the $\hbar^k_{mn,\ell}$ is modeled as zero-mean, complex Gaussian random variables with variance $\mathbb{E}\left[\|\hbar^k_{mn,\ell}\|^2\right] = \sigma^2_\ell$ where $\sum_{\ell=0}^{L} \sigma^2_\ell = 1$, and time delay τ_ℓ is irrelevant to $\hbar^k_{mn,\ell}$.

The assumptions of wireless channels are varied from case to case so that the sep-

arability is shown with different levels. Some of them are listed and discussed as following:

- SFBCs in [8,9,23] and discussions in [24] do not consider the time domain. The $\hbar^k_{mn,\ell}$ is assumed to be a statistically independent Gaussian distribution. The channel assumptions lead to a perfect separation between SF domains and gives $\mathbf{R}_{BS} = \mathbf{I}_{N_t}$ and $\mathbf{R}_{MS} = \mathbf{I}_{N_r}$. Hence we have $\rho = \mathbf{R}_F(f, f')$ when $m \neq m'$ and $n \neq n'$ otherwise $\rho = 0$.

- SFBC in [25] do not consider time domain. And it is assumed that the $\hbar^k_{mn,\ell}$ is jointly Gaussian distribution but also the AoA and AoD of propagation paths are independent. The assumptions lead to a perfect separation between SF domains. Hence we have $\rho = \mathbf{R}_{BS}(m, m')\mathbf{R}_{MS}(n, n')\mathbf{R}_F(f, f')$.

- STFBC in [26] assume that K consecutive OFDM symbol periods are static so that $\hbar^k_{mn,\ell} = \hbar^{k'}_{mn,\ell}$ for $\forall k, k'$. And it is also assumed that $\hbar^k_{mn,\ell}$ is independent to the receivers so that $\mathbf{R}_{MS} = \mathbf{I}_{N_r}$. Hence we have $\rho = \mathbf{R}(n, n')\mathbf{R}_F(f, f')$ when $n \neq n'$ otherwise $\rho = 0$.

- STFBC in [27,28] assume that K consecutive OFDM intervals are static so that $\hbar^k_{mn,\ell} = \hbar^{k'}_{mn,\ell}$ for $\forall k, k'$. It is also assumed that the AoA and AoD of propagation paths are uncorrelated. The assumption leads to a perfect separation between STF domains. Hence we have $\rho = \mathbf{R}_{MS}(n, n')\mathbf{R}_{BS}(m, m')\mathbf{R}_F(f, f')$.

- STFBC in [29] assume that the $\hbar^k_{mn,\ell}$ is jointly Gaussian distribution but also has independent clusters of scatterers. The assumption leads to a perfect separation between SF domains and temporal domain. The temporal correlation is modeled by a first-order Markovian model [30] in which the constant ε determines the amount of the temporal correlation. When $\varepsilon = 0$, there is no temporal correlation whilst if $\varepsilon = 1$ the channel stays constant over several OFDM symbol periods. Hence we have $\rho = \mathbf{R}_T(k, k')\mathbf{R}(m, m', n, n')\mathbf{R}_F(f, f')$.

- STFBC in [4,12,31] assume that the $\hbar_{mn,\ell}$ is statistically independent Gaussian distribution. The assumption leads to a perfect separation between STF domains and gives $\mathbf{R}_{BS} = \mathbf{I}_{N_t}$, $\mathbf{R}_{MS} = \mathbf{I}_{N_r}$ and $\mathbf{R}_T = \mathbf{I}_K$. Hence we have $\rho = \mathbf{R}_T(k, k')\mathbf{R}_{BS}(m, m')\mathbf{R}_{MS}(n, n')\mathbf{R}_F(f, f')$ when $m \neq m'$, $n \neq n'$ and $k \neq k'$ otherwise $\rho = 0$.

In conclusion, generally the assumptions of PDP leads to different level of separability of STF domains. Some rules are listed here:

1. The channel PDP stays constant during at least one OFDM symbol period otherwise the temporal and frequency domains are jointly correlated. This basic assumption is held for all papers addressing code design. Thus the ISI can be removed completely when a CP is long enough. Then temporal domain is independent to SF domains.

2. The channel PDP is independent of all MIMO transmit and receive pairs. This assumption generally can be realized by closed-spaced antennas at both ends so that all transmit and receive pairs can experience same propagation paths to bring about consistent channel PDP among antenna pairs. Hence the spatial domain is independent of frequency domain.

3. The AoA and AoD are uncorrelated [32]. This assumption generally is suitable for outdoor propagation scenarios without light of sight (LOS) so that the transmit and receive ends are independent of each other.

Generally we could divide all types of MIMO-OFDM channel assumptions into three simplified types in order to simplify code design process:

1. Statistically independent SF domains ignoring temporal domain;

2. Statistically independent SF domains and consecutive OFDM intervals are static;

3. Statistically independent STF domains.

The effect of these types of assumptions will be discussed within later chapters.

2.7 Frequency Correlation

The temporal and spatial correlations will affect the performance but they can not reveal the speciality of SFBC/STFBC. Hence in this section, we only focus on the frequency correlation, $\|\mathbf{R}_F(f, f')\|$ which is the key property for SFBC/STFBC design. The subcarrier interval is denoted by $\delta = \|f - f'\|$. Some results can be found in [24]. They are reviewed here so that the wireless channel characteristics for different modelling strategies can be shown and easily compared. Here several basic types of wireless channel models are presented.

2.7.1 Uniform PDP

The simplest PDP is the uniform PDP which has $\sigma_\ell^2 = \frac{1}{L+1}$ and $\tau_\ell = \ell T_s/F$ where $\ell \in [0, \cdots, L]$. The uniform PDP is considered in [8, 24] etc because of its simplicity. The setting of T_s is irrelevant to frequency correlation after substituting uniform PDP

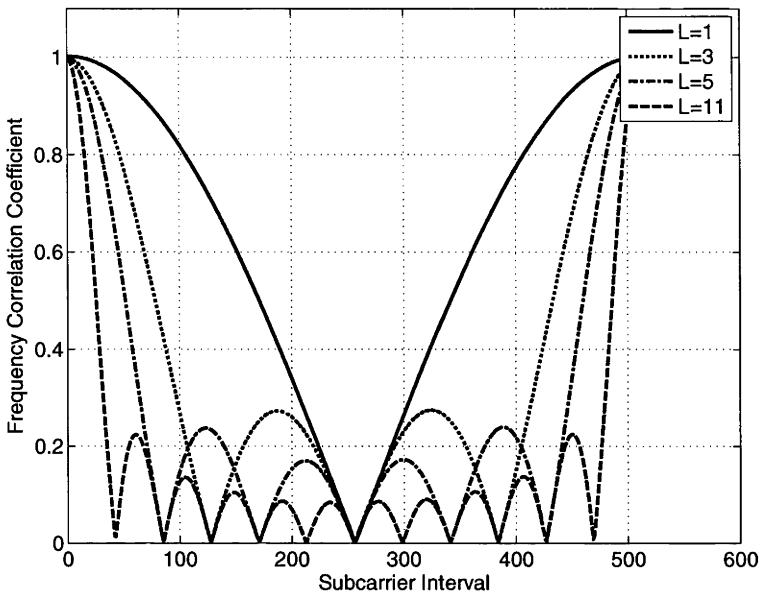

Figure 2.4: Frequency correlation of OFDM system vs subcarrier interval for Uniform PDP

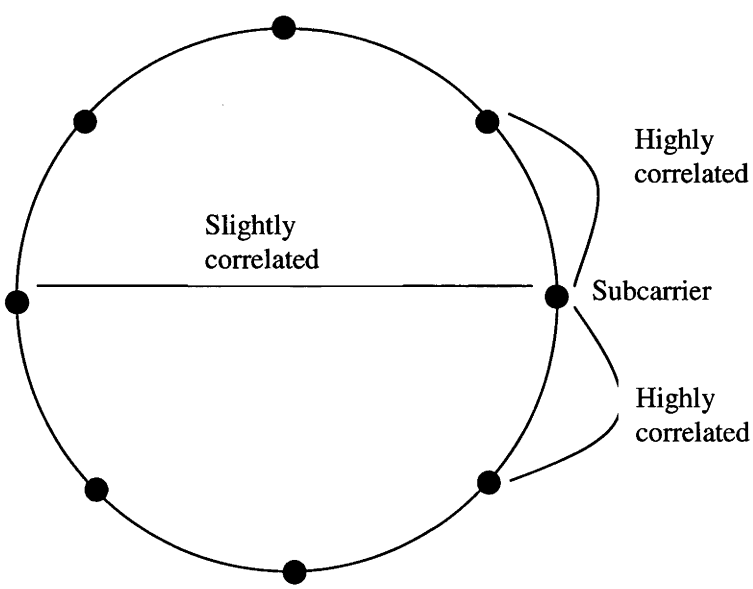

Figure 2.5: Sketch of correlation of Uniform PDP

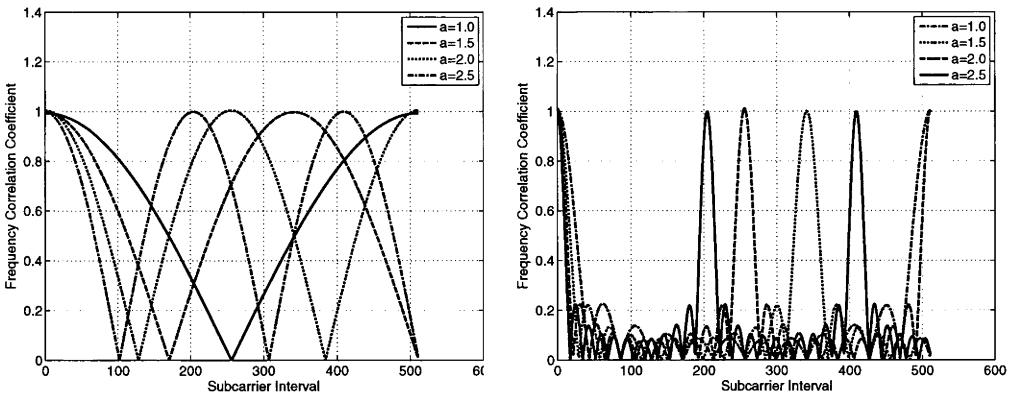

(a) L=1 (b) L=11

Figure 2.6: Frequency correlation of OFDM system vs time delay for Uniform PDP

into equation (2.9). And $T_s = F/BW$ where BW is denoted as allocated bandwidth. As an example, we assume that $F = 512$. Corresponding correlation curves with $L = 1, 3, 5, 11$ are illustrated in Figure 2.4.

Frequency correlation plots for the uniform PDP are symmetrical around the middle of plots. And the first subcarrier is highly correlated with the second subcarrier and also to the last subcarrier. We could uniformly embed all subcarriers into a unit circle one by one in Figure 2.5. Therefore an arbitrary subcarrier will be highly correlated to its closest neighborhood (both sides of itself) and least correlated to the farthest subcarrier (opposite side of itself). Moreover, there are L zero/close-to-zero frequency correlation points in Figure 2.4. Hence theoretically it is feasible to find at most $L + 1$ uncorrelated subcarriers in an OFDM system. And with the increasing of channel order L, the number of oscillations around the bottom of plots also increases so that the variation of frequency correlation is smoother.

A generalized uniform PDP is considered further. The time delay of a uniform PDP is usually assumed to be T_s/F, but it can be relaxed to an arbitrary value. Hence it is assumed that $\tau_\ell = a\ell T_s/F$ where a is arbitrary positive real and $\ell \in [0, \cdots, L]$. Then correlation curves corresponding to different values of a are illustrated in Figure 2.6. It is shown in Figure 2.6(a) that the middle value of subcarrier interval $\delta = 256$ gives the least correlation coefficient when the delay interval of uniform PDP equals to T_s/F, but the highest correlation coefficient when the delay interval equals to $2T_s/F$. Hence we can not simply jump to a conclusion that uniformly allocated subcarriers are the best strategy of subcarrier allocation. It is also shown in Figure 2.6(b) that each plot will repeat a curve of roughly "U" shape a number of a times, e.g. when $a = 2$ there are two "U" shaped curves and when $a = 2.5$ there are two and half. It would give us a hint how to choose the strategy of subcarrier grouping.

COST207 Typical Urban Six-Ray PDP						
Time Delay (μs)	0.2	0.5	0.0	1.6	2.3	5.0
Delay Power	0.379	0.239	0.189	0.095	0.061	0.037
COST207 Hilly Terrain Six-Ray PDP						
Time Delay (μs)	0.0	0.1	0.3	0.5	15.0	17.2
Delay Power	0.413	0.293	0.145	0.074	0.066	0.008

Table 2.1: COST207 Power Delay Profile in the Order of Delay Power

2.7.2 COST207

A COST207 six-ray channel model [33] is next considered. COST 207 provides a relatively simple channel modelling strategy considering multipath propagation and widely adopt for technology evaluation and standardization, e.g. LTE and LTE-A. Two propagation scenarios, typical urban and hilly terrain, are described in Table 2.1, in which the paths are sorted by delay powers in a decreasing order so as to design an optimal code to capture dominant propagation paths. Details of explanation will be given within later chapters. The frequency correlation for COST207 typical urban scenario is presented here with $F = 512$. The value of T_s is varied with an underlying assumption that the wireless channel is always static within a period of T_s. Increasing the value of T_s corresponds to increasing the value of F or reducing the bandwidth. Hence the change of T_s has the same effect of modification of the number of subcarriers F or of the bandwidth BW.

The COST207 has irregular time delays, which obviously has less repetition patterns of frequency correlation coefficient while the OFDM system period is increased, as shown in Figure 2.4 and 2.6. The number and location of zero correlation coefficients are changed with the variation of OFDM symbol period T_s. Moreover, with the increasing of T_s, the frequency correlation is less sensitive to subcarrier interval δ. Hence a group of uncorrelated subcarriers can not be found in a COST207 model.

2.7.3 SCM

The 3GPP spatial channel model (SCM) [34] has been widely used for system level simulations and advanced technology evaluation. It is also a basis of many industrial models, e.g. WINNER [11] and ITU M.2135. It is designed for the bandwidth up to $5MHz$ and frequency up to $2GHz$. SCM considers K_1 ($K_1 = 6$ in SCM) clusters of scatterers and each simulation, or drop, varies the cluster statistics and array orientations. A cluster corresponds to a separate path and within the path, there are K_2 unresolvable subpaths ($K_2 = 20$ in SCM). The channel impulse response $h_{mn}(t, \tau_\ell)$ of the path between the transmitter m at the BS and the receiver n at the MS in [34] is expressed

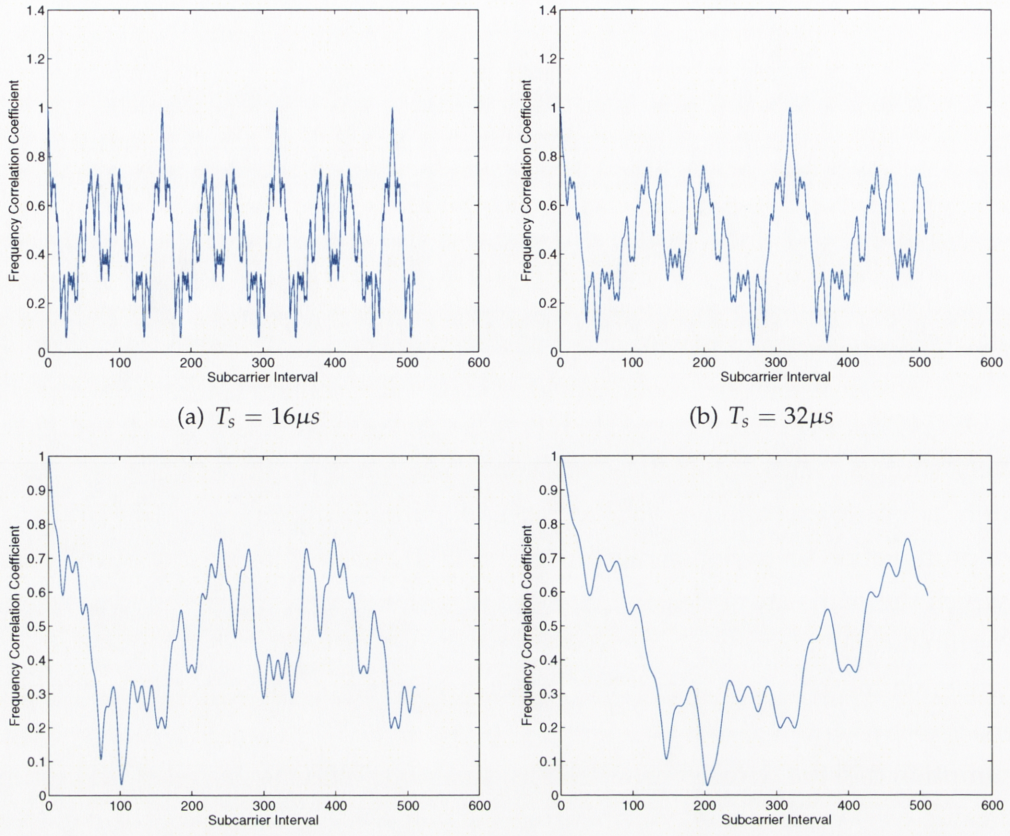

(a) $T_S = 16\mu s$ (b) $T_S = 32\mu s$

(c) $T_S = 64\mu s$ (d) $T_S = 128\mu s$

Figure 2.7: Frequency correlation of OFDM system for COST207 Typical Urban Six-Ray PDP

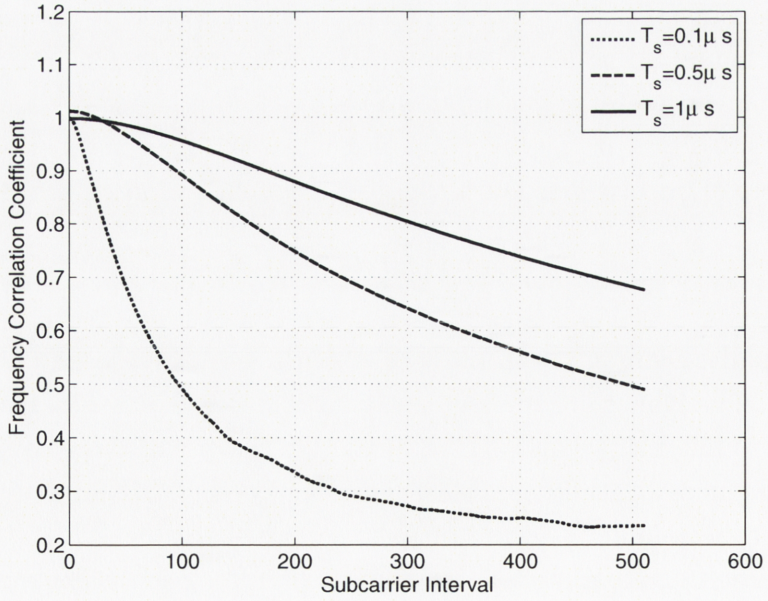

Figure 2.8: Frequency correlation of OFDM system for SCM suburban macro scenario

as

$$h_{mn}(t,\tau_\ell) = \sqrt{\frac{1}{K_2}} \sum_{i=1}^{K_2} \left(\chi^{\dagger}_{m,BS}(\mathbf{k}_{i,BS})\mathbf{H}_i\chi_{n,MS}(\mathbf{k}_{i,MS})e^{-i\mathbf{k}_{i,MS}\cdot\mathbf{v}t}\right) \tag{2.15}$$

where $\ell \in [1,\cdots,K_1]$. Details of SCM will not be reviewed here and the interested reader is referred to [34, 35]. Basically each drop of SCM simulations will independently generate a new PDP. In contrast, COST207 and uniform PDP have a fix PDP but random channel impulse response. Hence the SCM is a systematic model which can be used to describe an averaged system performance. The frequency correlation in Figure 2.8 could be considered as an averaged frequency correlation over dynamic scenario with constantly changed surrounding environment.

Figure 2.8 are plots of frequency correlation for SCM suburban macro scenario. The curves in Figure 2.8 are much smoother than in COST207 or uniform PDP. For the SCM it would be impossible to find completely uncorrelated subcarriers in a OFDM system. In other words, the group of uncorrelated subcarriers are constantly changed in a dynamic scenario. Compared with Figure 2.7, the frequency correlation coefficient between two subcarriers would be changed with the change of the channel PDP or system setting so that averaged frequency correlation does not equal to zero. Moreover, with the increase of OFDM symbol period T_s (equivalent to the decrease of subcarrier bandwidth), the frequency-selective fading channel is closer to a frequency-flat fading channel arising from reduced total bandwidth of subcarriers. And the frequency correlation is also closer to one. Hence the beneficial effect of frequency domain is reduced.

2.8 MIMO-OFDM Subsystem

To reduce system complexity while preserving both diversity gain and ST/STF coding gain, typically a MIMO-OFDM system is partitioned into N_s MIMO-OFDM subsystems where $N_s \geq 1$. Hence the performance of the system is evaluated by averaged performance of all subsystems.

2.8.1 Subcarrier Grouping

The division of the system is performed by subcarrier grouping (also called subcarrier interleaving, subcarrier allocation, resource scheduling) so that a typical MIMO-OFDM subsystem uses all transmitters and receivers but only P subcarriers selected from a total of F subcarriers where P is an arbitrary positive integer. Hence the performance of the system will be evaluated by the averaged performance of all MIMO-OFDM subsystems.

Subcarrier grouping does not affect spatial and temporal correlation as long as the frequency domain is independent of ST domains. For details, readers are referred to the previous discussion of the separability of cross-correlation. But the frequency correlation between subcarriers within a subsystem will be varied depending on specific grouping strategy and wireless channel characteristics. Typically subcarriers in a subsystem are equally separated from each other with positive subcarrier interval δ. However this is not definitive. For example, the subcarrier grouping strategy in [9] requires $N_t(L+1)$ subcarrier in a subsystem but the subcarriers within each set should be separated from each other as far as possible. Each set includes only partial, $L+1$, subcarriers. Furthermore some SFBC/STFBC require coherent subcarriers so that some subcarriers within a subsystem should be very close. The choice of subcarrier grouping strategy depends on the requirement of code design, wireless channel characteristics and limitations of application.

2.8.2 Correlation Structure of Subsystem

Assuming that a MIMO-OFDM subsystem has P uniformly selected subcarriers with a subcarrier interval δ. The channel frequency response $h_{mn,k}(p)$ in the MIMO-OFDM subsystem over the pth subcarrier at the kth symbol period between transmitter m, ($m \in [1, \cdots, N_t]$) and receiver n, ($n \in [1, \cdots, N_r]$) is given by

$$h_{mn,k}(p) = \sum_{\ell=0}^{L} \hbar_{mn,\ell}^{k} e^{-j2\pi((p-1)\delta+1)\tau_\ell/T_s} \tag{2.16}$$

where $p \in [1, \cdots, P]$, $k \in [1, \cdots, K]$ and $\ell \in [0, \cdots, L]$. The channel frequency response matrix between transmitters and receivers for the pth subcarrier in the MIMO-OFDM subsystem is denoted by

$$\mathbf{H}_k(p) = \begin{bmatrix} h_{11,k}(p) & \cdots & h_{1N_r,k}(p) \\ \vdots & \cdots & \vdots \\ h_{N_t1,k}(p) & \cdots & h_{N_tN_r,k}(p) \end{bmatrix} \tag{2.17}$$

where each entry $h_{mn,k}(p)$ is denoted by (2.16). Then the $PKN_t \times N_r$ channel matrix $\tilde{\mathbf{H}}$ is constructed by stacking up these channel matrices $\mathbf{H}_k(p)$ columnwise and shown

as

$$\tilde{\mathbf{H}} = \begin{bmatrix} \mathbf{H}_1(1) \\ \vdots \\ \mathbf{H}_1(P) \\ \vdots \\ \mathbf{H}_K(P) \end{bmatrix}. \tag{2.18}$$

The MIMO-OFDM subsystem is assumed to have arbitrary spatial correlation structure at both BS and MS ends. The spatial correlation matrix between two ends is separable because of independent outgoing and incoming propagation paths (uncorrelated angle of arrival and angle of departure) [36,37]. Furthermore, with the assumption that the space, time and frequency domains are independent of each other [9] (refer to rules of separability of section 2.5), the cross-correlation coefficient between two channel frequency response coefficients $h_{mn,k}(p)$ and $h_{m'n',k}(p')$ with a MIMO-OFDM subsystem is given by the following:

$$\begin{aligned} &\mathbb{E}\{h_{mn,k}(p)h^*_{m'n',k'}(p')\} \\ =&\mathbb{E}\left\{\sum_{\ell=0}^{L}\sum_{\ell'=0}^{L}\hbar^{k}_{mn,\ell}\hbar^{k'*}_{m'n',\ell'}e^{-j2\pi\delta(p\tau_\ell - p'\tau_{\ell'})/T_s}\right\} \\ =&\mathbf{R}_T(k,k')\mathbf{R}_{BS}(m,m')\mathbf{R}_{MS}(n,n')\mathbf{R}_F(p,p') \end{aligned} \tag{2.19}$$

where the frequency correlation matrix $\mathbf{R}_F$ is given by:

$$\mathbf{R}_F = \mathbf{W}\mathbf{R}_D\mathbf{W}^\dagger \tag{2.20}$$

where the $P \times (L+1)$ matrix $\mathbf{W}$ is shown as

$$\mathbf{W} = \left[\mathbf{w}^0, \cdots, \mathbf{w}^L\right] = \begin{bmatrix} \mathbf{w}_1 \\ \vdots \\ \mathbf{w}_P \end{bmatrix} = \begin{bmatrix} 1 & \cdots & 1 \\ \vdots & \cdots & \vdots \\ w_P^0 & \cdots & w_P^L \end{bmatrix}$$

where the entry w_p^ℓ in matrix $\mathbf{W}$ is defined as $w_p^\ell = e^{j2\pi(p-1)\delta\tau_\ell/T_s}$ where $p \in [1, \cdots, P]$. Moreover the system has a underlying assumption of $2\pi\delta\tau_\ell/T_s \neq 2k\pi + 2\pi\delta\tau_{\ell'}/T_s$ for $\forall \ell \neq \ell', \ell, \ell' \in [0, \cdots, L]$ and $k \in \mathbb{Z}$.

Therefore, the covariance matrix after combining (2.19) and (2.18) can be specified as

$$\mathbb{E}[\mathrm{vec}(\tilde{\mathbf{H}})\mathrm{vec}^\dagger(\tilde{\mathbf{H}})] = \mathbf{R}_{MS} \otimes \mathbf{R}_T \otimes \mathbf{R}_F \otimes \mathbf{R}_{BS} \tag{2.21}$$

where entries of correlation matrices $\mathbf{R}_{MS}$, $\mathbf{R}_T$, and $\mathbf{R}_{BS}$ are given by (2.11) and entries

of $\mathbf{R}_F$ are given by (2.20).

A MIMO-OFDM system can be regarded as a special MIMO-OFDM subsystem with all subcarriers selected. Therefore the notation of frequency correlation for a MIMO-OFDM system and a MIMO-OFDM subsystem are similar or exchangeable. The $\mathbf{R}_F$ would be different if the subcarriers within the subsystem are non-uniformly selected and separated. However, this kind of subcarrier grouping is not really common. And in a multiuser system, each user can be allocated one or more MIMO-OFDM subsystems which can be different from each other.

2.9 Summary

Some characteristics of STF domains that have been explained in this chapter can be summarized as following:

- Subcarrier grouping can be replaced with domain switching, which can simply group resource elements with similar second order characteristics across all STF domains. Such domain switching will not alter achievable diversity gain and coding gain. For example, we could use adjacent subcarriers and adjacent symbol periods to realize static subchannels as a consequence of all one correlation matrices. LTE [1] has adopted Alamouti code [5] across SF domain so that Alamouti code in LTE is referred as SFBC, in stead of STBC. Alternatively well-separated subcarriers and well-separated symbol periods can be used to realize nonstatic subchannels as a consequence of identity correlation matrices (also means uncorrelated resource elements). Traditional STBCs have a underlying assumption of static channel coefficients across the temporal domain. Inconsistency of channel assumptions can be found in the literature for SFBC and STFBC designs.

- The major difference between frequency domain and temporal domain is that the frequency correlation matrix has an upperbound of $L+1$ (see equation (2.11)) arising from a limited number of delay paths but the temporal correlation matrix does not have such an upperbound. However such an upperbound of frequency correlation can be found only for a fixed and given channel PDP, e.g. COST207. For a dynamic scenario, e.g. SCM which generates a new channel PDP within each drop, the frequency correlation after averaging over all drops does not have an upperbound either. This is a critical observation which might leads to severe failure for SFBCs, e.g. [9], in which there is a basic assumption that the frequency correlation has a fixed upperbound. This assumption leads to debate upon the

robustness of system performance in terms of achieved diversity gain and coding gain.

- For a fixed channel PDP, e.g. COST207, the frequency correlation between two subcarriers oscillates dramatically. The first subcarrier (e.g. subcarrier index 1) and the last subcarrier (e.g. subcarrier index 512) show the largest subcarrier separation but they do not always give the least correlation. However for a dynamic propagation channel, e.g. SCM, the frequency correlation decreases smoothly. The first and last subcarriers always give the least correlation.

Chapter 3

Review of STBC/SFBC/STFBC

3.1 Introduction

This chapter will provide a review of block coding strategies including space-time block coding (STBC), space-frequency block coding (SFBC) and space-time-frequency block coding (STFBC). Since all three frequency, time and space (STF) domains in a MIMO-OFDM system are involved, the complexity of wireless channel conditions in different block codes often confuses the reader and the underlying idea of each code is difficult to be discovered sometimes. Therefore in this chapter some existing STBC/SFBC/STFBC are summarized in the following sections and classified as: the block codes with full (or partial) spatial diversity; the block codes with both full (or partial) spatial and frequency diversity simultaneously; the block codes with all full (or partial) spatial, temporal and frequency diversity simultaneously. The MIMO-OFDM system is assumed to have N_t transmitters, N_r receivers, F subcarriers and K OFDM symbols.

3.2 Spatial Diversity

STBCs designed for the MIMO system have been widely discussed for roughly ten years. The consecutive time slots in the MIMO system are assumed to be constant or quasi-static for the STBCs. A large capacity gain can be achieved by transmitting symbols simultaneously from multiple transmitters. In a flat-fading environment, where the N_r receivers might not recover all information vectors affected by a deep fade from a single transmitter, different replicas of symbol vectors will be transmitted by the STBCs from multiple transmitters so as to improve the BER performance. Therefore, the spatial diversity gain can be achieved by a STBC with a proper coding among spatial and temporal domains, e.g. code orthogonality [5]. Alternatively, the performance can be improved by a better spectral efficiency so that the symbol transmission rate can be increased by the spatial multiplexing. A more comprehensive review of

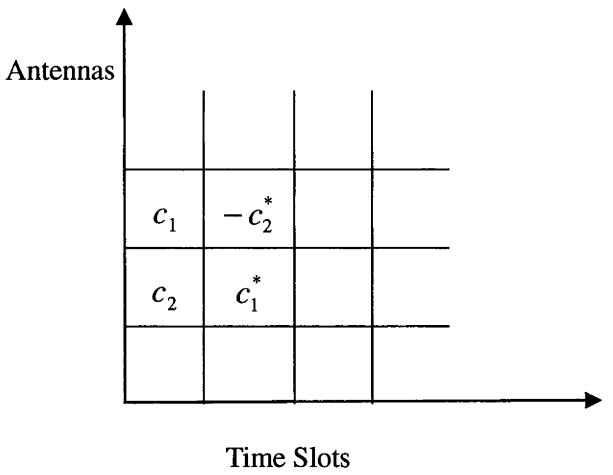

Figure 3.1: Orthogonal STBC-Alamouti Code

STBCs can be found in [38,39]. The theory of STBC design provides a solid foundation of further development of SFBC/STFBC. Most of existing SFBC/STFBC are developed from specific STBC or a combination of STBCs.

3.2.1 Orthogonal STBC

The transmit diversity scheme proposed in [5] and shown in Figure 3.1 is a simple and efficient orthogonal STBC with symbol transmission rate one, designed for a MIMO system with two transmitters and arbitrary number of receivers. It is well known as Alamouti code.

$$\mathbf{S} = \begin{bmatrix} c_1 & c_2 \\ -c_2^* & c_1^* \end{bmatrix} \tag{3.1}$$

The information symbols are transmitted from two transmitters with some modifications so that the orthogonality of the symbol vectors can be satisfied, e.g. $\mathbf{S}\mathbf{S}^\dagger = (\|c_1\|^2 + \|c_2\|^2)\mathbf{I}_2$. Full transmit diversity order of two can be achieved by this Alamouti code in the 2×2 MIMO system. The decoding procedure of the Alamouti code can provide a fast maximum-likelihood detection (MLD) which allows a symbol by symbol MLD. Moreover, this transmit scheme can improve the BER performance, or the capacity of wireless communication systems. Higher modulation schemes, e.g. 64QAM, is allowed so that the effective data rate can be increased. Later the Alamouti code has been generalized to MIMO systems with arbitrary number of transmitters using the theory of orthogonal designs [39,40]. However, the rate one linear complex orthogonal STBC was proven to be not exist for the MIMO systems with more than two transmitters, whilst the rate one real orthogonal STBC was proven to be not exist for the MIMO system with more than eight transmitters. All orthogonal STBCs are

capable of achieving full spatial diversity in the MIMO system. The key advantage of these codes is their low encoding/decoding complexities, which can improve feasibility of coding strategies in a mobile system because of limited battery power. It is also proved that the Alamouti code does achieve the maximal channel capacity for a 2×1 MISO system but not for the MIMO system with more than one receivers [41]. The amount of performance loss of the Alamouti code is substantial at high SNR. Further details about orthogonal STBCs are referred to [17,42,43].

3.2.2 Quasi-orthogonal STBC

The maximal symbol transmission rate of the orthogonal STBC is only 3/4 for a MIMO system with three and four transmitters. It is also difficult to construct orthogonal designs with a rate higher than 1/2 for more than four transmitters. The quasi-orthogonal designs were firstly proposed in [44–46] so that the orthogonality is relaxed to provide higher symbol transmission rate. With the quasi-orthogonal structure, the MLD can be realized by searching pairs of symbols, where the MLD in the orthogonal STBC is to search single symbols. The quasi-orthogonal STBC design with full diversity was discussed in [47–49] further. By rotating part of symbols, resulting quasi-orthogonal STBC can guarantee both full diversity, symbol transmission rate one and a fast MLD. For example, the quasi-orthogonal STBC for four transmitters with full diversity is given by

$$\mathbf{S} = \begin{bmatrix} c_1 & c_2 & c_3 & c_4 \\ -c_2^* & c_1^* & -c_4^* & c_3^* \\ c_3 & c_4 & c_1 & c_2 \\ -c_4^* & c_3^* & -c_2^* & c_1^* \end{bmatrix} \tag{3.2}$$

where $c_1, c_2 \in \mathcal{A}$ and $c_3, c_4 \in e^{j\phi}\mathcal{A}$. The optimal rotation angle ϕ is determined by specific constellation $\mathcal{A}$.

3.2.3 Linear Dispersion Code

The idea of using a linear dispersion code (LDC) to improve performance over fading channels is related to [50, 51] by maximizing the minimum product distance. The LDC is also known as linear constellation code in some literature [6]. The transmitted symbol vector $\mathbf{S}$ is precoded by a matrix Θ and given by

$$\mathbf{S} = \mathbf{C}\Theta \tag{3.3}$$

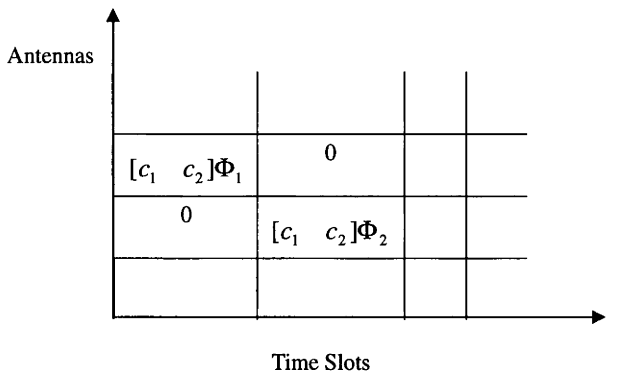

Figure 3.2: Linear Dispersion Code of MIMO with two transmitters

where $\mathbf{C}$ is a $1 \times N_t$ vector of input symbols with given constellation $\mathcal{A}$ and Θ is a $N_t \times N_t$ unitary complex matrix. With an arbitrary number of transmitters and receivers, the LDC always achieves symbol transmission rate one, and full diversity gain over quasi-static fading channels. An example is shown in Figure 3.2 where $\Phi = [\Phi_1, \Phi_2]$ is a 2×2 real or complex unitary matrix whose parameters can be optimized and related to the constellation of symbols c_1, c_2. The zeros in Figure 3.2 mean no signal transmission for specific antenna and time slot. The unitary matrix Θ in [6] was designed with parametrization of unitary matrices, or with algebraic number-theoretic constructions. It is shown that the LDC can achieves the upperbound on the coding gain for certain number of transmitters. Compared with existing orthogonal STBCs, the LDC offers not only better BER performance, but also higher mutual information for the MIMO system with more than two transmitters. The decoding complexity of the LDC is approximately exponential in the number of transmitters, or approximately polynomial if the sphere decoding is applied.

3.2.4 High Rate STBC

In order to achieve higher spectral efficiency over wireless channels, high rate linear dispersion STBCs were introduced in [14,41] with both high symbol transmission rate (> 1) and full transmit diversity. The high rate STBC in [52] constructed a rate two STBC for the MIMO system with two transmitters and two time slots. It is shown that such high rate STBC outperforms the Alamouti code when the number of receivers is greater than one. The improvement of performance is further enhanced when the size of constellation increases. Later in [7] the Golden code for the 2×2 MIMO system was derived using a division algebra, which is rate two, full diversity and has a nonzero lower bound on its coding gain. The Golden code is then extended to be perfect code for 2×2, 3×3, 4×4 and 6×6 MIMO systems in [14]. Furthermore, all linear STBCs

were unified in the coding structure of [41], which is designed to optimize the mutual information between the transmitted and received symbols. Examples of [41] demonstrate a better BER performance than some methods over a wide range of transmission rates and SNR. However [41] can not provide explicit design principles.

3.2.5 STBC Applications in the MIMO-OFDM System

By simply switching adjacent time slots in the MIMO system with the adjacent subcarriers in the MIMO-OFDM system, a STBC can be smoothly transferred into a SFBC (named in some literature), although this conversion will not achieve the frequency diversity or multipath diversity in the MIMO-OFDM system. The major advantage of this kind of transformation is its simplicity and re-utilization of some powerful STBCs. Therefore some articles and applications based on this strategy are reviewed here:

- The Alamouti code has been proposed for the LTE system [1,2]. Thus the LTE system simply replaces two time slots defined in Figure 3.1 with two adjacent subcarriers in the MIMO-OFDM system. For the LTE system with two transmitters, the Alamouti code is applied directly and two adjacent subcarriers are required for the coding process. For the LTE system with four transmitters, the Alamouti code is applied twice. Four subcarriers are required in this case, so that four subcarriers and four transmitters are divided into two independent subsystems each of which has two adjacent subcarriers and two transmitters. Each subcarrier in the LTE system is allocated with $15kHz$ bandwidth. Hence the coherent bandwidth of the propagation channel should be at least greater than $30kHz$.

- The performance of the Alamouti code in the MIMO-OFDM system was also discussed in [53,54]. It was shown that the increasing of the number of subcarriers in the MIMO-OFDM system will improve the BER performance because the variation of channel frequency responses between two adjacent subcarriers are mitigated (finer partitioning of the frequency selective channel). Moreover, the Alamouti code in the MIMO-OFDM system shows the diversity loss when the SNR is high but it demonstrates a relatively good performance when SNR is less than 20dB. Although the STBC in [53,54] can exploit space diversity, the potential multipath diversity or frequency diversity offered by the frequency-selective fading channels can not be exploited.

- To obtain the additional multipath diversity in the MIMO-OFDM systems, space-time trellis codes are mainly concerned during the past. The incoming informa-

tion symbols are trellis coded across both the OFDM subcarriers and transmitters [55–57].

- The code proposed in [58]has utilized the four by four orthogonal STBC with rate 3/4 in the MIMO-OFDM system. Instead of four consecutive time slots in the MIMO system, the code in [58] used two adjacent subcarriers and two adjacent OFDM symbol intervals. From the coding gain respective, it does not make a difference so that the BER performance of this code will be completely determined by the wireless channel conditions (or channel assumptions). Similar strategy was proposed in [59,60] for the MIMO-OFDM system, which deployed a quasi-orthogonal block code and designed zero forcing decoding for symbol pairs. Without constellation rotation, the code in [59] can not achieve full spatial diversity but symbol transmission rate one can be achieved.

- The article [61] proposed an adaptive code for the MIMO-OFDM system with four transmitters across all STF domains. The code in [61] is still the quasi-orthogonal or orthogonal STBC but consecutive subcarriers or consecutive OFDM symbols are adaptively allocated. Hence by exploiting adaptive domain switching, the code can be deployed for highly time-selective and highly frequency-selective channels. However, only spatial diversity can be achieved by [61] in every case.

3.3 Space and Frequency Diversity

Traditional STBCs, e.g. Alamouti code and Golden code, can achieve only spatial diversity in slow and frequency-flat fading channels. They do not work very well in a frequency-selective fading channel. The valuable frequency diversity can not be exploited in a MIMO-OFDM system with these code designs.

The SFBC is developed for the MIMO-OFDM system so that high diversity order can be achieved without coding across multiple OFDM symbol periods and consequently a long delay. Hence the SFBC usually considers only one OFDM symbol, with full or partial frequency diversity gain. The first SFBC with spatial and frequency diversity was proposed roughly six years ago [9, 26, 62]. These works have revealed some basic understanding of SFBC design, for example subcarrier grouping principle and $N_t(L+1)$ subcarriers required for a full space-frequency diversity order. Some conclusions and findings will be reviewed later. However up to now design criteria for these SFBCs were too optimistic in the assumptions about the wireless channel. So the SFBCs were hard to operate in a practical scenario. Furthermore there has been no significant breakthrough to differentiate SFBC from traditional STBC. All existing

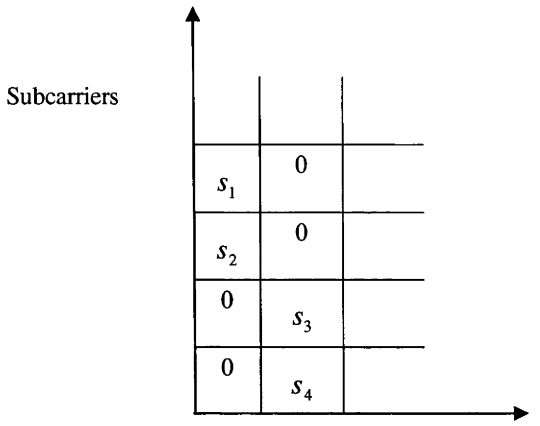

$$[s_1 \quad s_2 \quad s_3 \quad s_4] = [c_1 \quad c_2 \quad c_3 \quad c_4]\Phi$$

Figure 3.3: The SFBC with the LDC for the MIMO-OFDM subsystem with $N_t = 2$ transmitters and $P = 4$ subcarriers

SFBCs can be summarized as a technique combining antenna interleaving and subcarrier interleaving, so that the cross-talk between any pair of transmitters or subcarriers is removed. Then the next step is to deploy a LDC, which is widely adopted in STBCs.

The LDC (or linear constellation code) was firstly introduced into the OFDM system [63, 64] without the consideration of the MIMO. Exploiting the correlation structure of subcarriers, an optimal subcarrier grouping was proposed in [64] to divide the set of subcarriers into subsets (or subsystem in the thesis). Within each subsystem, a LDC is then designed to maximize both frequency diversity gain and coding gain. It is also shown that the subcarrier grouping does not decrease the possible maximum diversity and coding gain, although the underlying assumption of subcarrier grouping comes from the upperbound of the multipath diversity order, which might be infeasible in reality. The LDC in the OFDM system provides considerable flexibility of coding structure and constant symbol transmission rate one using the efficient sphere decoding.

The LDC was expanded into the MIMO-OFDM system in [8–10], which is shown in Figure 3.3 for the MIMO-OFDM subsystem with two transmitters and four equally separated subcarriers after subcarrier grouping. In Figure 3.3, the matrix Φ is a four by four complex or real unitary matrix, whose parameters are related to the constellations of $c_1, \cdots, c_4$. The zeroes mean no transmission for specific transmitter and subcarrier in the system. The LDC proposed in [8] can achieves the maximal spatial diversity over frequency-selective channels. And the LDC is shown to be robust to overestimation or underestimation of the multipath channel order. But this conclu-

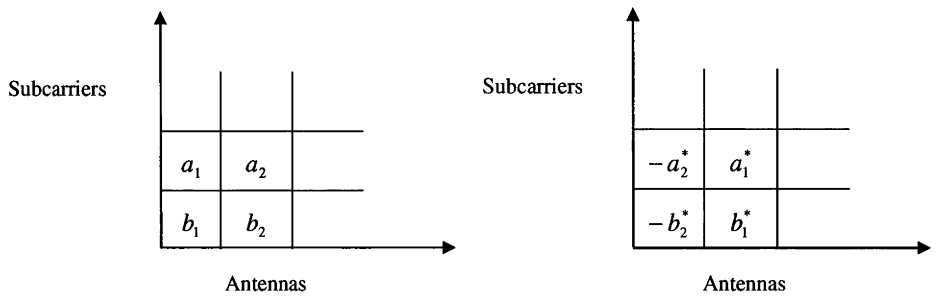

(a) The first OFDM symbol (b) The second OFDM symbol

Figure 3.4: The SFBC with the combination of STBC and LDC for the MIMO-OFDM subsystem with $N_t = 2$ transmitters, $K = 2$ OFDM symbols and $P = 2$ subcarriers

sion is questionable and discussed further in the later Section 4. The key characteristics of the LDC in the MIMO-OFDM system is that the cross talk between any pair of transmitters or subcarriers are removed, so that the MIMO-OFDM system in Figure 3.3 utilizes four parallel subchannels only by interleaving. The achievable frequency diversity of the LDC is varied for the case to case. But to achieve full frequency and spatial diversity, the minimal $N_t(L+1)$ subcarriers are required in the MIMO-OFDM subsystem.

The SFBC proposed in [26] can achieve the maximal diversity gain in space and frequency domains. By combining existing orthogonal STBCs and the LDC, the SFBC can afford low-complexity decoding, symbol transmission rate one and full SF diversity gain. To satisfy the requirement of the orthogonal STBC, consecutive OFDM symbols must be quasi-static (or be constant). Therefore the orthogonal STBC is applied to both space and time domains to achieve full spatial diversity, whilst the LDC is applied to frequency domain only to achieve full frequency diversity. The example is shown in Figure 3.4, in which $[a_1, b_1] = [c_1, c_2]\Theta$ and $[a_2, b_2] = [c_3, c_4]\Theta$. The 2×2 unitary matrix Θ is related to the constellation of $c_1, \cdots, c_4$. Moreover the subcarrier grouping is utilized to reduce the complexity of code design.

The SFBC proposed in [65] used a double Alamouti code in the MIMO-OFDM system so that the number of transmitters can be reduced without sacrificing the symbol transmit rate and transmit diversity order, compared with the orthogonal STBC in [40] proposed for the MIMO system with four transmitters. The SFBC in [65] can achieve transmit diversity order of four, within which the order of two comes from the spatial domain and the other two comes from the frequency domain. The code is actually quite similar to [26] with a reduced rate because of repetition. Compared with [26],

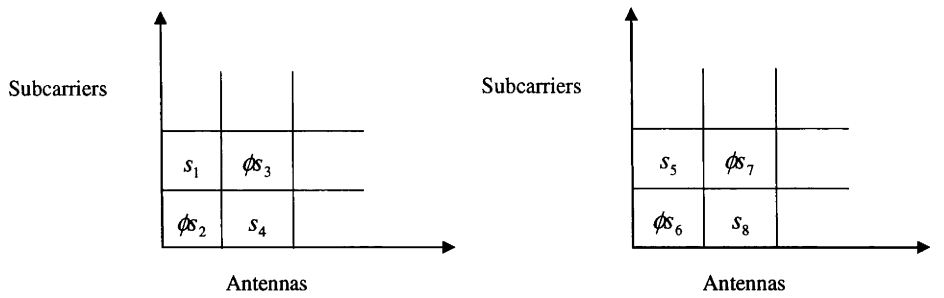

(a) The first OFDM symbol (b) The second OFDM symbol

Figure 3.5: The high rate SFBC for the MIMO-OFDM subsystem with $N_t = 2$ transmitters, and $P = 4$ subcarriers

the double Alamouti code for the MIMO-OFDM system can be shown as:

$$\begin{bmatrix} a_1 & b_1 \end{bmatrix} = \begin{bmatrix} c_1 & c_2 \end{bmatrix} \begin{bmatrix} 1 & 0 \\ 0 & 1 \end{bmatrix} \tag{3.4}$$

$$\begin{bmatrix} a_2 & b_2 \end{bmatrix} = \begin{bmatrix} c_1 & c_2 \end{bmatrix} \begin{bmatrix} 0 & 1 \\ 1 & 0 \end{bmatrix} \tag{3.5}$$

The high rate full diversity SFBC for the MIMO-OFDM systems were investigated in [4, 12, 13, 66–68]. The high rate SFBC usually is constructed from a layer algebraic design, where each layer of algebraic coded symbols is fed into different transmitters, subcarriers and OFDM symbols. For example, the SFBC shown in Figure 3.5 has two layers, one with $[s_1, s_4, s_5, s_8]$ and another one with $[s_2, s_3, s_6, s_7]$. The highest symbol transmission rate of the MIMO-OFDM system is the number of transmitters N_t. The challenge of the high rate SFBC design is that the subcarriers in the MIMO-OFDM system are independent, only for special channel power delay profile and given subcarrier interval. Hence the correlation of subcarriers increases complexity of high rate SFBC design. The high rate STBC, e.g. Golden code, shows a dependence in the number of transmitters, receivers and symbol constellation, whilst the high rate SFBC shows additional relationship with the frequency-selective fading channel. Thus the optimal high rate SFBC for the MIMO-OFDM system would be system-dependent and also time-varying. The optimal SFBC design with high rate, full SF diversity might exist for a MIMO-OFDM subsystem with limited size, e.g. 2 transmitters, 2 receivers, and 3 (or 4) subcarriers. The theory of "perfect code" in [14] can be combined with the design structure proposed in the thesis, and then be applied to the high rate SFBC design.

Some additional articles related to the SFBCs are reviewed here:

- The article [69] proposed an adaptive subcarrier selection as an efficient tech-

nique of improving the BER performance of the OFDM system in the low-to-medium SNR range without significant increase of the decoding complexity. The code in [69] is designed for the OFDM system to achieve partial frequency diversity only. It introduces the redundancy to provide a trade-off between the transmission rate and performance, so that M symbols are transmitted through N subcarriers, where $N > M$. It removes several selected subcarriers with the lowest receiving power, which suppose to have less contributions to the BER performance if the zero-forcing decoding is applied. However, the design of $N \times M$ precoding matrix Φ is not fully discussed in [69]. The matrix Φ is the key parameter which will seriously improve or degrade the performance because of its linear independency.

- The scalable LDC in [70] was proposed to be used in the MIMO-OFDM system. The approach leads a variable tradeoff between improving link reliability (by using diversity) and increasing data rate (by using spatial multiplexing). It describes a method which convert N input symbols into $N_t F$ symbols transmitted by N_t transmitters and F subcarriers. The inner code and outer code proposed in [70] need to be designed for each subcarrier and for each transmission rate. Hence the repetition has to be used in [70] to achieve the diversity and reduce the transmission rate. The scalable LDC provides flexibility but also has a design uncertainty.

- The work in [71] studied the STBC for a single carrier over frequency-selective fading channels. By zero-padding transmissions in stead of cycle prefix in the OFDM system, proposed STBC is similar with the Alamouti code spreading in space and frequency domains. However, its results may be questionable because the zero-forcing decoding and the sphere decoding exploited in [71] show the same diversity order. The explanation is that the simplified channel modelling and relatively large size of precoding matrix might conceal the potential diversity loss.

- The work in [72] proposed space-time multipath coded multi-antenna transmissions over the MIMO-OFDM system. The method of digital phase sweeping proposed in [72] is similar with my work in [25] although the discovery of such method are independent. Hence the description and design criteria of the SFBC are quite different. Proposed digital phase sweeping in [72] is normally difficult to be generalized to practical implementation because of time-varying power delay profile. And the code in [72] is designed for the propagation channels with uniform delay paths, which was proven in [25] to be an optimal channel

assumption and give a best BER performance for a MIMO-OFDM system. It is too optimistic.

- The work in [73] proposed the LDC for the OFDM systems, in which only frequency diversity can be achieved. It proposed a local maximum-likelihood decoding in the neighborhood of the output of MMSE decoding. The basic idea of decoding procedure in [73] is similar with my work in [74] although the precoding/decoding procedure of [74] is completely different with [73].

- The work in [75] proposed a SFBC for the MIMO-OFDM system with four transmitters. The SFBC is designed to achieve diversity order four (two from spatial domain and two from frequency domain) and symbol transmission rate one. Although the quasi-orthogonal design of the SFBC can not achieve full spatial diversity, the repeated transmission through two separated subcarriers, where coordinate interleaving is applied, can achieve frequency diversity order of two which can compensate the diversity loss of the quasi-orthogonal design.

3.4 STF Diversity

To achieve full STF diversity, a basic assumption upon the MIMO-OFDM system is that the channel experiences slow fading so that the channel coefficients (and channel power delay profile) are constant over one OFDM symbol, while channel coefficients (and channel power delay profile) change in subsequent OFDM symbols. At a cost of increased decoding delay arising from transmission of multiple OFDM symbols, the STFBC is capable of achieving full STF diversity. Normally, the STFBC is a logical extension of the STBC/SFBC to all available STF domain, for example the STFBC proposed in [31]. Hence the articles related to the STFBC are reviewed here only:

- The work in [29] shows a general spatial and temporal fading correlation structure on the performance of the MIMO-OFDM system. The conclusion of [29] shows a common upper bound of the maximum achievable STF diversity order, which is $N_t N_r K(L+1)$ where L is the multipath channel order. The STFBC proposed in [29] is a direct repetition of arbitrary SFBC within each OFDM symbol at a price of symbol-rate reduction by a factor of $1/K$, compared with the symbol rate one SFBC.

- The work [13] proposed the LDC to improve the OFDM system performance in multipath fading channels. The code in [13] can not achieve spatial diversity, but temporal and frequency diversity. The MMSE and zero-forcing decoding were investigated for the code in [13]. The precoding matrix of the code is a

special class of codes defined in [41]. Hence the optimal design of the non-square precoding matrix is still an open issue.

- The work in [76] proposed to concatenate the orthogonal STBC as the inner precoder and the conventional channel codes, e.g. convolutional codes or low-density parity-check, as the outer precoder. The orthogonal STBC can provide spatial diversity gain and the additional outer precoder can provide further substantial gain for high SNR range. Adaptivity is proposed in [76] by adjusting the constellation or energy of subcarrier one by one. The adjustment is realized by water-filling procedure, and modifying some parameters, e.g. the code rate and codeword size.

- The work in [77,78] proposed a general framework to analyze the performance of multiband UWB-MIMO systems irrelevant to any specific code. The performance of proposed code was investigated in Nakagami-m frequency-selective fading channels. The analysis shows that the diversity gain does not significantly depend on the fading parameter m. However the STFBC proposed in [31] is reused in [77,78].

3.5 Multiuser SFBC

The downlink multiuser SFBC in [79] proposed a code design criteria, which is based on minimizing the upper bound of pairwise error probability. The key conclusion in [79] is that applying the single user SFBC into a multiuser MIMO-OFDM system is not an optimal solution. The introduction of rotations specified for each user within the system can improve averaged user performance. So if all users might adopt a same SFBC/STBC, the users can be differentiated by user-specific rotation, which performs like finger print. The transmit diversity of each user is still limited by the number of transmitters, receivers and propagation channel order. The improvement of BER performance of the multiuser MIMO-OFDM system comes from the minimized user inference which is resulted from the introduction of same SFBC/STBC strategies to all users. However, there is a wrong assumption which might overturn conclusions of [79]. It was assumed that the channel power delay profiles are the same for all users. However such assumption is impractical in a multiuser system.

The work in [80] proposed a linear precoding scheme which jointly optimizes the power allocation across subcarriers and filters in the MIMO-OFDM system. It requires perfect channel knowledge at both transmit and receive sides. On the other hand, [81] proposed a method combining spreading codes defined in both space and frequency domains.

The multiuser system is relatively easier to be realized in the OFDM system by resource scheduling. The difficulties of the multiuser MIMO-OFDM system, e.g. LTE, come from the issues of synchronization, interference between the cells, etc. The multiuser SFBC/STFBC is less attractive, compared with the single user STBC/SFBC/STFBC. However, the multiuser SFBC/STFBC cooperative system has different characteristics, so that this topic could be further investigated. Moreover [79] proposed an interesting task of designing a user-specific SFBC/STFBC to improve system performance.

Chapter 4

Space-Frequency Block Codes with Matched Rotation Precoding

In chapter 2 we analyzed the correlation structure and properties of the MIMO-OFDM system which is useful for further code design process. And Chapter 3 provides a paper review of block coding strategies of the MIMO-OFDM system. The STBCs play an important role for the development of SFBC/STFBC. Each code is specified for particular communication system with own pros and cons. Therefore in this chapter a new SFBC called matched rotation precoding (MRP) is proposed for the MIMO-OFDM system, and is expected to overcome some drawbacks of existing SFBCs and demonstrate a good system performance.

The proposed rate one MRP and multirate MRP can achieve full transmit diversity and optimal system performance for arbitrary number of antennas, subcarrier intervals, and subcarrier groupings, with limited channel knowledge required by the transmitters. The optimization process of rate one MRP is simple and easily visualized so that the optimal rotation angle can be derived explicitly, or even intuitively for some cases. The multirate MRP has a complex optimization process, but it has a better spectral efficiency and provides a relatively smooth balance between system performance and transmission rate. Simulations show that the proposed SFBC with MRP can overcome the diversity loss in specific propagation scenario, always improve the system performance, and demonstrate flexible performance with large performance gain. Therefore proposed SFBCs with MRP demonstrate flexibility and feasibility so that it is more suitable for a practical MIMO-OFDM system with dynamic parameters.

4.1 Introduction

There are enormous research articles available upon STBCs, e.g. [5,52] and an overview in [38]. But traditional STBCs can achieve only spatial diversity in slow and flat fading

channels. They do not work very well in a frequency-selective fading channel. More importantly valuable frequency diversity can not be exploited in a MIMO-OFDM system with these code designs.

The SFBC is developed for the MIMO-OFDM system so that high diversity order can be achieved without coding across multiple OFDM symbol periods and consequently a long delay. Upon author's knowledge, the first SFBC was proposed roughly in 2002, e.g. [26]. Further publications [9,31] have revealed more basic understanding of SFBC design, for example subcarrier grouping principle and $N_t(L+1)$ subcarriers required for a full space-frequency diversity order. Some conclusions and findings will be reviewed in the next Section. However up to now design criteria for these SFBCs were too optimistic in the assumptions about the wireless channel and the SFBCs were hard to operate in a practical scenario. Furthermore there has been no significant breakthrough to differentiate SFBC from traditional STBC. All existing SFBCs can be summarized as a technique combining antenna interleaving and subcarrier interleaving, so that the cross-talk between any pair of transmitters or subcarriers is removed Then the next step is to deploy a linear dispersion code, which is widely adopted in STBCs.

One premise for this thesis is the question of how to make existing or proposed SFBCs more realistic and practical in a standard dynamic scenario, e.g. a multiuser scenario or an outdoor propagation scenario. Some limitations should be considered. Firstly, because of the relatively large channel order (number of paths) in real propagation scenarios, especially outdoor propagation, achieving full space and frequency diversity is not a top priority. A strategy of achieving a given transmit diversity order efficiently across both space and frequency domains is more desirable. Secondly, considering the difficulty in realization of full channel knowledge at the transmitters, the assumption of limited knowledge is more practical. And the optimization strategy to adjust subcarrier interval significantly increases the difficulty of subcarrier grouping in a multi-user scenario and lacks system flexibility. In order to addressing these difficulties, a novel matched rotation precoding (MRP) is proposed in this chapter.

The rest of the chapter is organized as follows. Section 4.2 briefly reviews the present development of SFBCs. Section 4.3 describes a model for the MIMO-OFDM system, and reviews the correlation structure between space and frequency domains. Section 4.4 presents design criteria of SFBC and reveals the distinct repetition and rotation patterns. Design structures for scenarios with full or limited knowledge of channel PDP are also compared and investigated in this section. Then Section 4.5 and 4.6 introduce a rate one MRP and a multirate MRP respectively with limited feedback knowledge, and corresponding optimization processes are also discussed. Section 4.7 provides simulation results. Section 4.8 summarizes the chapter and proposes some

research challenges which are extended from the chapter content, and might be solved in future research.

4.2 Brief Survey of Space-Time Block Codes

For MIMO-OFDM systems, various space-time/frequency codes have been developed to achieve spatial, multipath and temporal diversities by coding across multiple antennas, subcarriers and OFDM symbol intervals. All existing space-time block codes (STBC), e.g. [5–7], can be converted to space-frequency block codes (SFBC) simply by spreading the time domain signal of STBC within the frequency domain. This conversion works well if adjacent subcarrier channels are highly correlated, e.g. an OFDM system with relatively large number of subcarriers. However this kind of direct conversion [61] is not optimal and fails to achieve valuable frequency diversity that can improve system performance.

The SFBC achieves full spatial and frequency (multipath) diversities by coding across multiple antennas and subcarriers [8–10]. These SFBCs require at least $N_t(L+1)$ subcarriers to achieve full diversity order where L is the fixed channel order and N_t is the number of transmitters. The channel order provides an upperbound in the rank of the frequency correlation matrix of the OFDM system [24]. Hence by employing more than a threshold number of subcarriers, full spatial and frequency diversities can be achieved. However the channel order L might be large, e.g. $L+1=20$ in [11], and vary with users and scatterer movement, raising questions about the practical implementation of these SFBCs.

On the other hand, the design of SFBC provides a fundamental understanding so that a variety of space-time-frequency block codes (STFBC) are proposed for particular system requirements and channel conditions. Essentially these STFBCs do not differ significantly from either SFBC or STBC. Some STFBCs have assumed that consecutive OFDM intervals (OFDM symbol periods) are static during a period of time. For example, a rate one STFBC is proposed in [26] by combining orthogonal STBC [40] and linear dispersion codes [6, 82], and proposed in [28, 59] using quasi-orthogonal block codes [48]. Alternatively some STFBCs have assumed that consecutive OFDM intervals are independent during a period of time so that temporal diversity could be gained. For example, the rate one STFBC proposed in [31] extends SFBC in [9] into all space, time and frequency domains. Furthermore high rate full diversity STFBCs are proposed in [12, 13] using a layered algebraic design.

The SFBC proposed in [8, 31] does not require knowledge of the channel power delay profile (PDP) at the transmit side. However it is verified only for specific channel conditions and provides an upperbound of performance. It will lose the frequency

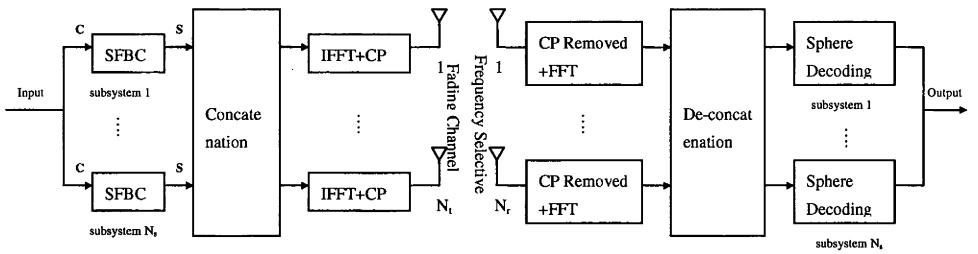

Figure 4.1: SFBC block diagram for a MIMO-OFDM system

diversity for particular propagation scenarios. To overcome this problem and to optimize the performance, perfect channel PDP is required by the transmitters in the optimization process proposed in [9] and a high rate SFBC design proposed in [12, 13]. Such an assumption might not be feasible for a practical implementation. Moreover in order to guarantee one-to-one mapping during the optimization process [9], the subcarrier interval should be a factor of F where F is the number of subcarriers of a MIMO-OFDM system. This property limits the choice of subcarrier interval. Furthermore, a MIMO-OFDM system is usually divided into a number of MIMO-OFDM subsystems by subcarrier grouping. In a multiuser scenario each user will be allocated one or more subsystems. This property leads to diverse optimal subcarrier intervals for subsystems and users. Then a new problem of subcarrier grouping is raised since all users in the system will compete with each other to get a better allocation of subcarriers.

4.3 MIMO-OFDM System Modelling

This section presents a general MIMO-OFDM system model and proposes a concise SFBC design structure that is used to design precoding matrices, optimize coding gain and diversity gain. The MIMO-OFDM system model is simplified with some preliminary assumptions, compared with SCM [34] or WINNER model [11]. Hence it is designed for the code design process. It is assumed that the MIMO-OFDM system model has perfect synchronization between transmitters and receivers, and also among the users, no ISI, uncorrelated AoA and AoD, etc. The effect of these assumptions can be found in Chapter 2.

4.3.1 Subcarrier Grouping for the MIMO-OFDM Model

We consider a MIMO-OFDM system with N_t transmitters, N_r receivers and F subcarriers. The frequency-selective fading channel is assumed to be static (time invariant) within at least one OFDM symbol period T_s. Each transmit and receive pair has $L+1$

resolvable delay paths with the same PDP which is independent of transmitters, receivers, or symbol period. A block of data symbols is transmitted over each transmitter and passed through a F point IFFT and followed by the appending of a CP. The length of CP is chosen to be long enough to remove the ISI. At each receiver the CP is removed at first and then a FFT is applied. Hence the MIMO frequency-selective fading channel is decoupled into F parallel MIMO flat fading channels.

To reduce system complexity while preserving both diversity and coding gain, typically a MIMO-OFDM system is partitioned into N_s MIMO-OFDM subsystems where $N_s \geq 1$. It is pointed out in [83] that the MIMO-OFDM system capacity with grouping can approach the channel capacity without grouping very closely. Hence the performance of the system is evaluated by averaged performance of all subsystems. Here we consider a subsystem with P selected subcarriers from a total of F subcarriers where P can be arbitrary integer greater than N_t. The subcarriers in the subsystem are equally separated from each other with a positive interval δ where $\delta \in \mathbb{Z}$. The optimization process by tuning subcarrier interval δ was proposed in [9]. However for the simplicity of implementation and the efficiency of subcarrier allocation, the subcarrier interval δ is fixed in a MIMO-OFDM subsystem so any two adjacent subcarriers in the subsystem have exact same subcarrier interval. Therefore, it is assumed that $\delta = \lfloor \frac{F}{P} \rfloor$ where $\lfloor a \rfloor$ denotes the largest integer less than or equal to a so that the subcarriers are separated as far as they can in the subsystem. The rest of $(F - \delta P) < P$ subcarriers could be unused or used as guard subcarrier in order to mitigate interference from adjacent bands, e.g. in LTE [1]. Then a MIMO-OFDM system will be partitioned into $N_s = \delta = \lfloor \frac{F}{P} \rfloor$ MIMO-OFDM subsystems who preserve exactly the same second order characteristics with each other. Hence the proposed SFBC design only focuses on an arbitrary MIMO-OFDM subsystem. For a multi-user scenario, each user might be allocated one or more MIMO-OFDM subsystems depending on the system complexity and system requirement. The block diagram of a MIMO-OFDM system is shown in Figure 4.1.

Because only one OFDM symbol period need be considered in the design of the SFBC, the notation of time k of the channel frequency response $h_{mn,k}(p)$ is removed in this chapter. The channel frequency response $h_{mn}(p)$ over the pth subcarrier in the MIMO-OFDM subsystem between transmitter m where $(m \in [1, \cdots, N_t])$ and receiver n where $(n \in [1, \cdots, N_r])$ is given by

$$h_{mn}(p) = \sum_{\ell=0}^{L} \hbar_{mn,\ell} e^{-j2\pi((p-1)\delta+1)\tau_\ell/T_s} \tag{4.1}$$

where $p \in [1, \cdots, P]$ and $\ell \in [0, \cdots, L]$, τ_ℓ and $\hbar_{mn,\ell}$ are the delay and complex ampli-

tude coefficient of the ℓth path respectively, and T_s is the OFDM symbol period. The channel frequency response between transmitters and receivers for the pth subcarrier in the MIMO-OFDM subsystem is a $N_t \times N_r$ matrix and denoted by

$$\mathbf{H}(p) = \begin{bmatrix} h_{11}(p) & \dots & h_{1N_r}(p) \\ \vdots & \dots & \vdots \\ h_{N_t1}(p) & \dots & h_{N_tN_r}(p) \end{bmatrix} \tag{4.2}$$

where each entry $h_{mn}(p)$ is denoted by (4.1). Then the $PN_t \times N_r$ channel matrix $\tilde{\mathbf{H}}$ is constructed by stacking up these channel matrices $\mathbf{H}(p)$ columnwise and shown as

$$\tilde{\mathbf{H}} = \begin{bmatrix} \mathbf{H}(1) \\ \mathbf{H}(2) \\ \vdots \\ \mathbf{H}(P) \end{bmatrix}. \tag{4.3}$$

Suppose that the transmitted symbol vector $\mathbf{S}$ is defined as

$$\mathbf{S} = [s_{1,1}, \cdots, s_{1,N_t}, \cdots, s_{P,1}, \cdots, s_{P,N_t}] \tag{4.4}$$

where two subscripts denotes specific allocated subcarrier and transmitter respectively. Hence the symbol $s_{p,m}$ is transmitted from the pth subcarrier and the mth transmitter. Moreover, the transmission power of vector $\mathbf{S}$ is normalized within each SFBC design and each MIMO-OFDM subsystem. Hence the transmission power will remain constant for all cases and designs. It is given by $\mathbb{E}[\mathbf{S}\mathbf{S}^\dagger] = P$. Hence the receive signal of each subsystem, a $PN_r \times 1$ vector $\mathbf{Y}$, can be expressed as

$$\mathbf{Y} = \sqrt{\frac{\rho}{N_t}}\hat{\mathbf{S}}\mathrm{vec}(\tilde{\mathbf{H}}) + \mathbf{Z} \tag{4.5}$$

where $\hat{\mathbf{S}} = \{(\mathbf{I}_{N_rP} \otimes \mathbf{1}_{1\times N_t}) \circ (\mathbf{1}_{N_rP\times N_r} \otimes \mathbf{S})\}$. The channel state information $\tilde{\mathbf{H}}$ is assumed to be perfectly known at the receive side, but not known at the transmit side. ρ is the average signal to noise ratio (SNR) at each receiver, independent of the number of transmitters and receivers. The noise vector $\mathbf{Z}$ is assumed to be additive white Gaussian noise with zero mean and unit variance.

4.3.2 Correlation Structure of the MIMO-OFDM subsystem

The MIMO-OFDM subsystem is assumed to have arbitrary spatial correlation structures at both transmit and receive sides. The spatial correlation matrix between two

sides is separable because of independent outgoing and incoming propagation (uncorrelated angle of arrival and angle of departure) [36, 37]. Furthermore, with the assumption that the space, time, and frequency domains are independent of each other [9], the correlation coefficient between the channel frequency response $h_{mn}(p)$ and $h_{m'n'}(p')$ is given by:

$$\begin{aligned}&\mathbb{E}\{h_{mn}(p)h^*_{m'n'}(p')\}\\&=\mathbf{R}_{MS}(n,n')\mathbf{R}_F(p,p')\mathbf{R}_{BS}(m,m')\end{aligned} \tag{4.6}$$

where scalars $\mathbf{R}_{BS}(m,m')$, $\mathbf{R}_{MS}(n,n')$, and $\mathbf{R}_F(p,p')$ are transmit spatial, receive spatial, and frequency correlation coefficients respectively. For more detail refer to chapter 2. Therefore we have

$$\mathbb{E}[\mathrm{vec}(\tilde{\mathbf{H}})\mathrm{vec}^\dagger(\tilde{\mathbf{H}})] = \mathbf{R}_{MS}\otimes\mathbf{R}_F\otimes\mathbf{R}_{BS} \tag{4.7}$$

where entries of spatial correlation matrices $\mathbf{R}_{MS}$ and $\mathbf{R}_{BS}$ are given by (2.11), and entries of frequency correlation matrix $\mathbf{R}_F$ of subsystem are given by (2.20).

4.4 Analysis of SFBC Design

In this section the basic design criteria of SFBC are reviewed and distinct rotation / repetition patterns are revealed to show the specialty of SFBC. Some conclusions can be drawn from other literature. However the proposed rotation / repetition patterns discloses the characteristics of SFBC and frequency domain more clearly.

4.4.1 Design Criteria

The average pairwise error probability (PEP) for the codeword difference $\Delta\mathbf{C}$ over all channel realizations can be upper bounded by [29]:

$$P(\Delta\mathbf{C}) \le \left(\frac{\rho}{4N_t}\right)^{-\mathrm{rank}(\mathbf{\Lambda})}\left(\prod_{i=1}^{\mathrm{rank}(\mathbf{\Lambda})}\lambda_i(\mathbf{\Lambda})\right)^{-1} \tag{4.8}$$

where $\mathrm{rank}(\mathbf{\Lambda})$ and $\lambda_i(\mathbf{\Lambda})$ are the rank and the ith nonzero eigenvalue of the covariance matrix $\mathbf{\Lambda}$ respectively. The linear block precoding is applied so that the codeword difference $\mathbf{C}$ can be mapped into a vector $\Delta\hat{\mathbf{S}}$ one by one. The matrix $\mathbf{\Lambda}$ is further given

by:

$$\begin{aligned} \mathbf{\Lambda} &= \mathbb{E}\left[\Delta\hat{\mathbf{S}}\mathrm{vec}(\tilde{\mathbf{H}})\mathrm{vec}^{\dagger}(\tilde{\mathbf{H}})\Delta\hat{\mathbf{S}}^{\dagger}\right] \\ &= \Delta\hat{\mathbf{S}}\left\{\mathbf{R}_{MS}\otimes\mathbf{R}_{F}\otimes\mathbf{R}_{BS}\right\}\Delta\hat{\mathbf{S}}^{\dagger} \\ &= \mathbf{R}_{MS}\otimes\left\{\left(\Delta\tilde{\mathbf{S}}\mathbf{R}_{BS}\Delta\tilde{\mathbf{S}}^{\dagger}\right)\circ\mathbf{R}_{F}\right\} \end{aligned} \tag{4.9}$$

where the $P \times N_t$ matrix $\Delta\tilde{\mathbf{S}}$ is stacked up from $\Delta\mathbf{S}$ and given by

$$\Delta\tilde{\mathbf{S}}^{m} = \begin{bmatrix} \Delta s_{1,m} \\ \Delta s_{2,m} \\ \vdots \\ \Delta s_{P,m} \end{bmatrix} \tag{4.10}$$

$$\Delta\tilde{\mathbf{S}} = [\Delta\tilde{\mathbf{S}}^{1},\cdots,\Delta\tilde{\mathbf{S}}^{N_t}] = \begin{bmatrix} \Delta s_{1,1} & \Delta s_{1,2} & \cdots & \Delta s_{1,N_t} \\ \Delta s_{2,1} & \Delta s_{2,2} & \cdots & \Delta s_{2,N_t} \\ \vdots & \vdots & \vdots & \vdots \\ \Delta s_{P,1} & \Delta s_{P,2} & \cdots & \Delta s_{P,N_t} \end{bmatrix}. \tag{4.11}$$

The details of the derivation of equation (4.9) is shown in Appendix A.

Each row vector of $\Delta\tilde{\mathbf{S}}$ is transmitted by N_t transmitters through the same subcarrier, and each column vector is transmitted by P subcarriers through the same transmitter. The equation (4.9) also shows that the receive correlation matrix $\mathbf{R}_{MS}$ is separable from the SFBC design process. Moreover, the transmit correlation matrix can be absorbed by the matrix $\Delta\tilde{\mathbf{S}}$ by a singular value decomposition. Hence to improve system performance, both coding gain and diversity gain should be optimized by carefully designing $(\Delta\tilde{\mathbf{S}}\Delta\tilde{\mathbf{S}}^{\dagger})\circ\mathbf{R}_{F}$, and the optimization process is independent of spatial correlation matrices.

For instance, if $\mathbf{R}_F \approx \mathbf{1}_P$, e.g. when the subcarrier interval $\delta = 1$ and the value of F is relatively large, the design of SFBC has no difference from traditional STBC, which optimizes the coding gain by a subsequent structure of $\Delta\tilde{\mathbf{S}}\Delta\tilde{\mathbf{S}}^{\dagger}$. Then an arbitrary STBC could be safely converted into SFBC by domain switching, but this conversion suffers the loss of diversity gain at high SNR.

Moreover, if these P subcarriers are independent of each other [26], then $\mathbf{R}_F = \mathbf{I}_P$. The design criterion is simplified as maximizing $\prod_{p=1}^{P}(\sum_{m=1}^{N_t}\|\Delta s_{p,m}\|^2)$. It has a simple lowerbound, $N_t^P\left(\prod_{p=1}^{P}\prod_{m=1}^{N_t}\|\Delta s_{p,m}\|\right)^{2/N_t}$ which could be optimized by linear dispersion codes [64]. Hence if the subcarriers in a MIMO-OFDM subsystem are completely independent, the corresponding optimization process will focus on maximizing $\prod_{p=1}^{P}(\sum_{m=1}^{N_t}\|\Delta s_{p,m}\|^2)$ or its lowerbound $\prod_{p=1}^{P}\prod_{m=1}^{N_t}\|\Delta s_{p,m}\|^2$.

4.4.2 Structure Analysis with Full PDP

Some further assumptions are made in this section. It is assumed that the channel PDP is fed back to the transmitters through uplink transmission or data feedback. Hence the propagation environment should be relatively stable. Otherwise this kind of statistical information is hard to gain. Therefore time delays τ_ℓ and corresponding delay power σ_ℓ^2 where $\ell \in [0, \cdots, L]$ of each drop are perfectly known by the transmit side. The SFBC design with limited knowledge of PDP will be discussed next and compared with the scenario of full knowledge of PDP. Therefore it is assumed that the transmit side knows the channel PDP perfectly for coding design. And at the same time the receive side knows the channel frequency responses for the process of decoding.

The information of channel PDP of system can be obtained by monitoring uplink channel and using pilot symbols. The second order characteristic information would be relatively stable if users are stationary or have low mobility. Furthermore the information can be updated with a low frequency, e.g. one or several microseconds, so that overhead of channel information can be reduced in the MIMO-OFDM system. The channel frequency responses are known by transmitters in 4G standard and used for precoding and multiplxing, e.g. LTE [1]. Monitoring channel PDP would be even simpler than estimation of channel frequency responses, since such information are differentiated by users, but not subcarriers. Also because of channel reciprocity, the channel PDP can be relatively accurate, even for FDD system. Within later section the requirements of channel PDP information can be reduced for further simplicity.

The channel between the mth transmitter and the nth receiver experiences frequency-selective fading induced by $L+1$ independent wireless propagation paths. The coefficient $\hbar_{mn,\ell}$ is assumed to be an uncorrelated circularly symmetric complex Gaussian random variable with zero mean and variance σ_ℓ^2 given by the channel PDP, which is sorted in a decreasing order as $\sigma_0^2 \geq \cdots \geq \sigma_L^2$, e.g. COST207 shown in Table 2.1. Hence we have $\mathbf{R}_{BS} = \mathbf{I}_{N_t}$ and $\mathbf{R}_{MS} = \mathbf{I}_{N_r}$. Furthermore, the matrix $\mathbf{R}_D$ is a diagonal matrix given by $\mathbf{R}_D(\ell,\ell) = \sigma_\ell^2$ and $\sum_{\ell=0}^{L} \sigma_\ell^2 = 1$. The number of subcarriers in the MIMO-OFDM subsystem is assumed to be $P \leq N_t(L+1)$ and $P > N_t$. Because the maximal rank of the matrix (4.9) is $\min(N_r N_t(L+1), N_r P)$, the maximum achievable transmit diversity is P including full spatial diversity order but partial frequency diversity order.

By utilizing these assumptions and definitions, the covariance matrix $\mathbf{\Lambda}$ in (4.9) is given by

$$\mathbf{\Lambda} = \mathbf{I}_{N_r} \otimes \left\{ (\Delta\tilde{\mathbf{S}}\Delta\tilde{\mathbf{S}}^\dagger) \circ (\mathbf{W}\mathbf{R}_D\mathbf{W}^\dagger) \right\} \tag{4.12}$$

where the matrix $\mathbf{W}$ is given by equation (2.20). And if the covariance matrix $\mathbf{\Lambda}$ is of full rank, the determinant of $\mathbf{\Lambda}$ is given by

1. if $P = N_t(L+1)$ (full spatial and frequency diversity as achieved in [9]), or $\mathbf{R}_D = \frac{1}{L+1}\mathbf{I}_{L+1}$ (uniform PDP as adopted in [8]), we have

$$\det(\mathbf{\Lambda}) = \left(\prod_{\ell=0}^{L}\sigma_\ell^2\right)^{N_tN_r} \|\det(\mathbf{\Omega})\|^{2N_r}, \tag{4.13}$$

where $\mathbf{\Omega}$ is a $P \times N_t(L+1)$ complex square matrix and reconstructed as

$$\mathbf{\Omega} = [(\Delta\tilde{\mathbf{S}}^1 \circ \mathbf{w}^0), \cdots, (\Delta\tilde{\mathbf{S}}^{N_t} \circ \mathbf{w}^0), \cdots, (\Delta\tilde{\mathbf{S}}^1 \circ \mathbf{w}^L), \cdots, (\Delta\tilde{\mathbf{S}}^{N_t} \circ \mathbf{w}^L)]$$

where $\Delta\tilde{\mathbf{S}}^m$ is the mth column vector from matrix $\Delta\tilde{\mathbf{S}}$;

2. if $N_t < P < N_t(L+1)$ and $\mathbf{R}_D$ is not an identity matrix, we have

$$\det(\mathbf{\Lambda}) = \left\{\det(\mathbf{\Omega}\mathbf{\Omega}^\dagger)\right\}^{N_r} \tag{4.14}$$

where $\mathbf{\Omega}$ is a $P \times N_t(L+1)$ complex matrix that is reconstructed as

$$\mathbf{\Omega} = [(\sigma_0\Delta\tilde{\mathbf{S}}^1 \circ \mathbf{w}^0), \cdots, (\sigma_0\Delta\tilde{\mathbf{S}}^{N_t} \circ \mathbf{w}^0), \cdots, (\sigma_L\Delta\tilde{\mathbf{S}}^1 \circ \mathbf{w}^L), \cdots, (\sigma_L\Delta\tilde{\mathbf{S}}^{N_t} \circ \mathbf{w}^L)].$$

The derivation of equation (4.13) and (4.14) is shown in Appendix B.

Remark 1: Equations (4.13)-(4.14) show that the design of SFBC is separable from the delay power σ_ℓ only if $P = N_t(L+1)$ or $\mathbf{R}_D$ is an identity matrix. Hence two types of matrix $\mathbf{\Omega}$ are given, without σ_ℓ as shown in (4.13), or more generally with σ_ℓ as shown in (4.14). Moreover, the matrix $\mathbf{\Omega}$ reveals the characteristics of repetition and rotation patterns of the SFBC which do not exist in the traditional STBC design. The matrix $\mathbf{\Omega}$ is a pattern of $\Delta\tilde{\mathbf{S}}$ which is repeated $L+1$ times within the matrix column by column. Each copy is also rotated by a specific column vector $\mathbf{w}^\ell$ and further shaped by scalar σ_ℓ for some cases. Hence if $P = N_t(L+1)$, the matrix $\mathbf{\Omega}$ is a square matrix. The goal of the design is simplified into optimizing $\mathbf{\Omega}$ in (4.13) so that $\mathbf{\Omega}$ should be full rank (full spatial and frequency diversity) and $\|\det(\mathbf{\Omega})\|$ needs to be maximized. If $N_t < P < N_t(L+1)$, the goal of design is to optimize $\mathbf{\Omega}$ in (4.14) so that $\mathbf{\Omega}\mathbf{\Omega}^\dagger$ has full rank of P (full spatial diversity but partial frequency diversity) and $\|\det(\mathbf{\Omega}\mathbf{\Omega}^\dagger)\|$ needs to be maximized.

A similar expression to (4.9) can be found in [9]. However the Hadamard product

within (4.9) may conceal some valuable characteristics. The Hadamard product in (4.13) and (4.14) is used as a product of column vectors, rather than matrices like (4.9). Hence proposed repetition and rotation patterns (4.13) and (4.14) can simplify the design process and give an internal observation of each specific SFBC. For example, the rate one SFBC in [8] with the assumptions of $L+1=2$, $N_t=2$ and $P=4$ is simplified as a problem of optimizing the determinant of the following matrix:

$$\mathbf{\Omega}=\begin{bmatrix} w_1^0\Delta s_{1,1} & 0 & w_1^1\Delta s_{1,1} & 0 \\ 0 & w_2^0\alpha^1\Delta s_{2,2} & 0 & w_2^1\Delta s_{2,2} \\ w_3^0\Delta s_{3,1} & 0 & w_3^1\Delta s_{3,1} & 0 \\ 0 & w_4^0\alpha^3\Delta s_{4,2} & 0 & w_4^1\Delta s_{4,2} \end{bmatrix} \tag{4.15}$$

where $\Delta s_{2,1}=\Delta s_{4,1}=\Delta s_{1,2}=\Delta s_{3,2}=0$ in [8]. Then the determinant of the matrix $\mathbf{\Omega}$ is given by $\|\det(\mathbf{\Omega})\|=\|1-\phi^2\|^2\|\Delta s_{1,1}\Delta s_{2,1}\Delta s_{3,2}\Delta s_{4,2}\|$ where $\phi=e^{j2\pi\delta(\tau_1-\tau_0)/T_s}$. The proposed SFBC in [8] will lose the diversity gain for specific channel PDP or subcarrier interval δ, e.g. $\phi=\pm1$ when $\delta(\tau_1-\tau_0)/T_s=0.5$. The problem of diversity loss is not given much attention because of the relatively complex design structure involving Hadamard product. In order to overcome this problem, an optimization process was proposed in [9] that adjusted the subcarrier interval δ.

Moreover when comparing STBC and SFBC designs, the STBC could be considered as a special application of the SFBC with highly correlated subcarriers in the MIMO-OFDM subsystem. Hence we have $\mathbf{w}^0=\mathbf{w}^\ell=\mathbf{w}^L$. Then the matrix $\mathbf{\Omega}$ has the maximal diversity gain N_t (spatial diversity only). The frequency diversity can be achieved by a proper SFBC because of repetition/rotation patterns shown in (4.13) and (4.14).

The minimum value of $\|\det(\mathbf{\Lambda})\|$ over all possible codeword error matrices $\mathbf{\Delta C}=\tilde{\mathbf{C}}-\mathbf{C}$, for a specific constellation $\mathcal{A}$, is denoted as coding gain ξ which is given by:

$$\xi=\min_{\mathbf{\Delta C}}\frac{1}{\sqrt{N_t}}\left[\det\left(\mathbf{\Lambda}\right)\right]^{\frac{1}{2PN_r}}. \tag{4.16}$$

4.4.3 Structure Analysis with Limited PDP

The channel PDP is assumed be perfectly known by the transmitters in [9] for the purpose of optimization, and also in [4] for the purpose of high transmission rate. This assumption might be feasible for an indoor propagation scenario with relatively slow variation of channel second order statistics. However, it is infeasible for an outdoor propagation scenario in which there are no fixed surrounding scatterers, but large channel orders, e.g. $L+1=20$ in [11]. Moreover for a multiuser scenario, each user has its own particular PDP, which increases the burden of feedback significantly.

Hence it is more reasonable to assume that only partial PDP, e.g. a limited number of paths with dominant delay power, is available to the transmitters through data feedback or uplink transmission.

Moreover, it is shown in Equations (4.13) and (4.14) that if $P = N_t(L+1)$ (which could be very large), the design process is separable from the delay powers σ_ℓ. However, the number of subcarriers P for a MIMO-OFDM subsystem might be limited by the system complexity and efficiency. So the value of P could be much smaller than $N_t(L+1)$. Hence it is feasible to utilize some of the propagation paths, rather than all paths, to reduce the design complexity and make the SFBC more practical.

Similarly, the indoor propagation is still considered since the channel PDP of such a scenario usually has dominant paths so that the rest of the unimportant paths can be ignored by the transmitters. Therefore it is assumed that limited PDP, only the first largest σ_ℓ^2 and corresponding delays τ_ℓ where $\ell \in [0, \cdots, \Gamma-1]$, is known by the transmitters where $\Gamma < L+1$ and $\sum_{\ell=0}^{\Gamma-1} \sigma_\ell^2 \leq 1$.

For simplicity P is assumed to be an integer multiple of N_t (not a prerequisite) and $P = N_t\Gamma < N_t(L+1)$. Therefore equation (4.14) should be a starting point. The first P column vectors within the matrix $\mathbf{\Omega}$ defined in (4.14) are chosen to form a new matrix $\mathbf{\Omega}_1$. The remaining $N_t(L+1) - P$ column vectors of $\mathbf{\Omega}$ are further formed as a matrix $\mathbf{\Omega}_2$. Therefore, both matrices $\mathbf{\Omega}_1$ and $\mathbf{\Omega}_2$ are subblock matrices of $\mathbf{\Omega}$. The column vector permutation will not change the determinant of $\mathbf{\Omega}\mathbf{\Omega}^\dagger$ so that $\det(\mathbf{\Omega}\mathbf{\Omega}) = \det(\mathbf{\Omega}_1\mathbf{\Omega}_1^\dagger + \mathbf{\Omega}_2\mathbf{\Omega}_2^\dagger)$. Let eigenvalues $\lambda_i(\mathbf{A})$ of an arbitrary matrix $\mathbf{A}$ be arranged in increasing order. Since $\mathbf{\Omega}\mathbf{\Omega}^\dagger$, $\mathbf{\Omega}_1\mathbf{\Omega}_1^\dagger$ and $\mathbf{\Omega}_2\mathbf{\Omega}_2^\dagger$ are Hermitian matrices and also positive semidefinite, $\lambda_i(\mathbf{\Omega}\mathbf{\Omega}^\dagger) = \lambda_i(\mathbf{\Omega}_1\mathbf{\Omega}_1{}^\dagger + \mathbf{\Omega}_2\mathbf{\Omega}_2{}^\dagger) \geq \lambda_i(\mathbf{\Omega}_1\mathbf{\Omega}_1{}^\dagger) \geq 0$ where $i \in [1, \cdots, P]$ [84,85] . Therefore we have $\det(\mathbf{\Omega}\mathbf{\Omega}^\dagger) \geq \det(\mathbf{\Omega}_1\mathbf{\Omega}_1^\dagger) = \|\det(\mathbf{\Omega}_1)\|^2$. Then the determinant of $\mathbf{\Omega}\mathbf{\Omega}^\dagger$ has a lowerbound which can be expressed as

$$\|\det(\mathbf{\Omega}\mathbf{\Omega}^\dagger)\| \geq \|\det(\mathbf{\Omega}_1)\|^2 = \left\{\prod_{\ell=0}^{\Gamma-1} \sigma_\ell^2\right\}^{N_t} \|\det(\mathbf{\Psi})\|^2 \tag{4.17}$$

where the matrix $\mathbf{\Psi}$ is shown as

$$\begin{aligned}\mathbf{\Psi} = \; & [\Delta\tilde{\mathbf{S}}_1 \circ \mathbf{w}^0, \cdots, \Delta\tilde{\mathbf{S}}_{N_t} \circ \mathbf{w}^0, \cdots, \\ & \Delta\tilde{\mathbf{S}}_1 \circ \mathbf{w}^{\Gamma-1}, \cdots, \Delta\tilde{\mathbf{S}}_{N_t} \circ \mathbf{w}^{\Gamma-1}].\end{aligned}$$

Therefore the coding gain lowerbound $\check{\xi}$ for a specific SFBC can be expressed as

$$\xi \geq \check{\xi} = \frac{1}{\sqrt{N_t}} \|\det(\mathbf{\Psi})\|^{\frac{1}{P}} \prod_{\ell=0}^{\Gamma-1} \sigma_\ell^{\frac{1}{\Gamma}}. \tag{4.18}$$

This shows that the design of SFBC can be converted into optimizing the matrix Ψ in (4.17) so as to improve the coding gain lowerbound $\check{\xi}$ given by (4.18). Perfect knowledge of channel PDP is unnecessary (or infeasible), but full transmit diversity order of P can be guaranteed always by optimizing the coding gain lowerbound.

Generally the powers of delay paths are less important than the time delays in a SFBC design. Time delays σ_ℓ are directly involved in the construction of the matrix Ψ. On the other hand, the knowledge of average power of path σ_ℓ^2 is generally hard to achieve in a dynamic real-time system. So it might be easier to feedback the information of time delays into the transmit side, rather than whole channel PDP. Therefore the SFBC designs proposed in this chapter will be based on the coding gain lowerbound with only limited knowledge of PDP at the transmit side.

4.5 Rate One Matched Rotation Precoding

In this section a rate one SFBC with MRP is proposed. The rate one MRP has a relatively simple structure and easy optimization process when compared to high rate SFBC ($R > 1$). The corresponding optimization process is also discussed.

4.5.1 Rate One SFBC

The construction of the rate one MRP is proposed here to optimize the coding gain lowerbound $\check{\xi}$ in (4.18) . Assuming that $s_{p,m} = \bar{s}_p e^{j\phi_{p,m}}$ and $\bar{\mathbf{S}} = [\bar{s}_1, \cdots, \bar{s}_P]^T$, we have $\Delta s_{p,m} = \Delta\bar{s}_p e^{j\phi_{p,m}}$ and

$$\Delta\tilde{\mathbf{S}}^m = \Delta\bar{\mathbf{S}} \circ \mathbf{\Phi}^m \tag{4.19}$$

where $\Delta\bar{\mathbf{S}} = [\Delta\bar{s}_1, \cdots, \Delta\bar{s}_P]^T$, $\mathbf{\Phi}^m = [e^{j\phi_{1,m}}, \cdots, e^{j\phi_{P,m}}]^T$ and $m \in [1, \cdots, N_t]$. Then the matrix Ψ in (4.18) can be expressed as

$$\begin{aligned}\Psi = [&\Delta\bar{\mathbf{S}} \circ \mathbf{\Phi}^1 \circ \mathbf{w}^0, \cdots, \Delta\bar{\mathbf{S}} \circ \mathbf{\Phi}^{N_t} \circ \mathbf{w}^0, \cdots, \\ &\Delta\bar{\mathbf{S}} \circ \mathbf{\Phi}^1 \circ \mathbf{w}^{\Gamma-1}, \cdots, \Delta\bar{\mathbf{S}} \circ \mathbf{\Phi}^{N_t} \circ \mathbf{w}^{\Gamma-1}].\end{aligned} \tag{4.20}$$

The $P \times N_t$ matrix $\mathbf{\Phi}$ is defined as

$$\mathbf{\Phi} = [\mathbf{\Phi}^1, \cdots, \mathbf{\Phi}^{N_t}] = \begin{bmatrix} e^{j\phi_{1,1}} & \cdots & e^{j\phi_{1,N_t}} \\ \vdots & \vdots & \vdots \\ e^{j\phi_{P,1}} & \cdots & e^{j\phi_{P,N_t}} \end{bmatrix}. \tag{4.21}$$

$$\mathbf{V} = \begin{bmatrix} w_1^0 e^{j\phi_{1,1}} & \cdots & w_1^0 e^{j\phi_{1,N_t}} & \cdots & w_1^{\Gamma-1} e^{j\phi_{1,1}} & \cdots & w_1^{\Gamma-1} e^{j\phi_{1,N_t}} \\ \vdots & \cdots & \vdots & \cdots & \vdots & \cdots & \vdots \\ w_P^0 e^{j\phi_{P,1}} & \cdots & w_P^0 e^{j\phi_{P,N_t}} & \cdots & w_P^{\Gamma-1} e^{j\phi_{P,1}} & \cdots & w_P^{\Gamma-1} e^{j\phi_{P,N_t}} \end{bmatrix} \tag{4.23}$$

$$\begin{aligned} \mathbf{V}\mathbf{V}^\dagger = & \begin{bmatrix} \Gamma & \sum_{\ell=0}^{\Gamma-1} e^{-j2\pi\delta\tau_\ell/T_s} & \cdots & \sum_{\ell=0}^{\Gamma-1} e^{-j2(P-1)\pi\delta\tau_\ell/T_s} \\ \sum_{\ell=0}^{\Gamma-1} e^{j2\pi\delta\tau_\ell/T_s} & \Gamma & \cdots & \sum_{\ell=0}^{\Gamma-1} e^{-j2\pi(P-2)\delta\tau_\ell/T_s} \\ \vdots & \vdots & \vdots & \vdots \\ \sum_{\ell=0}^{\Gamma-1} e^{j2\pi(P-1)\delta\tau_\ell/T_s} & \sum_{\ell=0}^{\Gamma-1} e^{j2\pi(P-2)\delta\tau_\ell/T_s} & \cdots & \Gamma \end{bmatrix} \\ & \circ \begin{bmatrix} N_t & \sum_{m=1}^{N_t} e^{j(\phi_{1,m}-\phi_{2,m})} & \cdots & \sum_{m=1}^{N_t} e^{j(\phi_{1,m}-\phi_{P,m})} \\ \sum_{m=1}^{N_t} e^{j(\phi_{2,m}-\phi_{1,m})} & N_t & \cdots & \sum_{m=1}^{N_t} e^{j(\phi_{2,m}-\phi_{P,m})} \\ \vdots & \vdots & \vdots & \vdots \\ \sum_{m=1}^{N_t} e^{j(\phi_{P,m}-\phi_{1,m})} & \sum_{m=1}^{N_t} e^{j(\phi_{P,m}-\phi_{2,m})} & \cdots & N_t \end{bmatrix} \\ = & \mathbf{R}_\delta \circ \mathbf{R}_\phi \end{aligned} \tag{4.24}$$

Hence each specific rotation angle $\phi_{p,m}$ in $\mathbf{\Phi}$ is assigned to the pth subcarrier and the mth transmitter. Then we have

$$\det(\mathbf{\Psi}\mathbf{\Psi}^\dagger) = \det(\mathbf{V}\mathbf{V}^\dagger) \prod_{p=1}^{P} \|\Delta\bar{s}_p\|^2 \tag{4.22}$$

where the square matrix $\mathbf{V}$ and the Hermitian matrix $\mathbf{V}\mathbf{V}^\dagger$ are shown at the top of next page. The matrix $\mathbf{R}_\delta$ in (4.24) is a Hermitian Toeplitz matrix and related to time delays τ_ℓ of dominant paths, where $\ell \in [0, \cdots, \Gamma-1]$, and given subcarrier interval δ. The matrix $\mathbf{R}_\phi = \mathbf{\Phi}\mathbf{\Phi}^\dagger$ is a Hermitian matrix and related to rotation angles $\phi_{p,m}$.

Therefore to optimize (4.22), rotation angles $\phi_{p,m}$ of $\mathbf{\Phi}$ are actually affected by both time delays of propagation channel and subcarrier interval of specific subsystem. Furthermore the precoding process demonstrated in [8] can be regarded as a special application of rotation and power normalization for $\mathbf{\Phi}$ given by

$$\mathbf{\Phi} = [\mathbf{\Phi}^1, \mathbf{\Phi}^2] = \begin{bmatrix} \sqrt{2} & 0 \\ 0 & \sqrt{2} \\ \sqrt{2} & 0 \\ 0 & \sqrt{2} \end{bmatrix} \tag{4.25}$$

and the precoding process demonstrated in [9] can also be summarized as

$$\mathbf{\Phi} = [\mathbf{\Phi}^1, \mathbf{\Phi}^2] = \begin{bmatrix} \sqrt{2} & 0 \\ \sqrt{2} & 0 \\ 0 & \sqrt{2} \\ 0 & \sqrt{2} \end{bmatrix} \tag{4.26}$$

along with the extra optimization process of subcarrier interval δ for given PDP. The power normalization of $\mathbf{\Phi}$ provides a concise mathematical representation of both subcarrier interleaving and antenna interleaving. Although it is not further discussed in this thesis, this may be a good research direction in the future.

It is also evident in (4.22) that the question of maximizing the coding gain lowerbound in (4.18) yields two independent optimization problems: $\max_{\mathcal{A}} \prod_{p=1}^{P} \|\Delta\bar{s}_p\|$ for specific constellation $\mathcal{A}$ and $\max_{\phi} \|\det(\mathbf{V}\mathbf{V}^\dagger)\|$ for specific correlation matrix $\mathbf{R}_\delta$. Hence, we denote that

$$\check{\xi}_{\mathcal{A}} = \max_{\mathcal{A}} \prod_{p=1}^{P} \|\Delta\bar{s}_p\|^{\frac{1}{P}} \tag{4.27}$$

and

$$\check{\xi}_{ECG} = \frac{1}{\sqrt{N_t}} \|\det(\mathbf{V})\|^{\frac{1}{P}} \prod_{\ell=0}^{\Gamma} \sigma_\ell^{\frac{1}{\Gamma}} \tag{4.28}$$

which is also called as extrinsic coding gain (ECG) in [9], and is always less than one. Therefore the coding gain lowerbound can be expressed as

$$\check{\xi} = \check{\xi}_{\mathcal{A}} \check{\xi}_{ECG}. \tag{4.29}$$

Thus the principle is to construct a proper matrix $\mathbf{R}_\phi$ to match with the correlation matrix $\mathbf{R}_\delta$ so as to maximize the coding gain lowerbound. Be aware that $\mathbf{R}_\delta$ is not a physical correlation matrix of frequency domain.

4.5.2 Optimization process for $\check{\xi}_{\mathcal{A}}$

To maximize $\check{\xi}_{\mathcal{A}}$ for a given constellation $\mathcal{A}$, a linear dispersion code is proposed for flat fading channels [6] and adopted by some SFBCs [8,9,26]. The codeword $\mathbf{C}$ with specific constellation $\mathcal{A}$ is precoded by a complex unitary square matrix $\mathbf{\Theta}$ so that

$$\bar{\mathbf{S}} = \mathbf{C}\mathbf{\Theta}. \tag{4.30}$$

where the codeword $\mathbf{C} = [c_1, \cdots, c_P]$ is a $1 \times P$ vector where $c_1, \cdots, c_P$ are complex scalars chosen from a particular r-PSK or r-QAM constellation $\mathcal{A}$. It is assumed that both the real parts and the imaginary parts of $c_1, \cdots, c_P$ have a variance of $1/2$ and

are uncorrelated, so we have $\mathbb{E}[c_i c_i^*] = 1$ and $\mathbb{E}[c_i^2] = 0$ where $i \in [1, \cdots, P]$.

We will not discuss construction details of Θ here which can be found in [6]. The matrix Θ is assumed to be a Vandermonde matrix and is given by

$$\Theta = \frac{1}{\sqrt{P}} \begin{bmatrix} 1 & \cdots & 1 & \cdots & 1 \\ \theta_1 & \cdots & \theta_i & \cdots & \theta_P \\ \vdots & \vdots & \vdots & \vdots & \vdots \\ \theta_1^{P-1} & \cdots & \theta_i^{P-1} & \cdots & \theta_P^{P-1} \end{bmatrix} \tag{4.31}$$

where for a QAM constellation and $P = 2^t (t \geq 1)$, the parameters θ_i are given by $\theta_i = e^{j\frac{4i-3}{2P}\pi}$ where $i \in [1, \cdots, P]$. If $P = 2^t \times 3 (t \geq 0)$, the parameters $\theta_i = e^{j\frac{6i-1}{3P}\pi}$. Moreover, if $P = 2^t 3^q (t \geq 1, q \geq 1)$, the parameters θ_i are given by $\theta_i = e^{j\frac{6i-5}{3P}\pi}$. Therefore we have $\check{\xi}_{\mathcal{A}} = \Delta_{\min}/\beta$ where $\Delta_{\min}$ is the minimum Euclidean distance in constellation $\mathcal{A}$ and $\beta^2 = P$ if P is an Euler number or a power of two; otherwise $\beta^2 = 1/(2^{1/P} - 1)$.

Recently some precoding matrices of linear dispersion codes were introduced for the case of P which are a power of two [6]. If P is not a power of two but $P = \varphi(J)$ for some J with $J \neq 4$, $\theta_i = e^{j\frac{2m_i}{J}\pi}$ where $gcd(m_i, J) = 1$ and $1 \leq m_i < J$. The $\varphi(J)$ is denoted as the number of integers $k (1 \leq k < J)$, such that $gcd(k, J) = 1$. The $gcd(a, b)$ is the greatest common divisor between a and b. For example, when P is $6, 10, 12, 18$, the corresponding J is $7, 11, 13, 19$ respectively. For these case, $\theta_i = e^{j(2i\pi/J)}$. When for some odd P, e.g. $P = 5, 7, 9$, an experimental result was also given as

$$\theta_i = 2^{\frac{1}{2P}} e^{j\frac{8i-7}{4P}\pi} \tag{4.32}$$

and a normalization factor $\sqrt{(2^{1/P} - 1)}$ is applied for these cases.

The optimization process of $\check{\xi}_{\mathcal{A}}$ is not our main task and can be found in other research literature, e.g. [50]. The optimal Vandermonde matrix designed for some specific values of P can not be found yet, but it is separable from the whole design process. So the results are only quoted and used here. For more details refer to [6].

4.5.3 Optimization Process for $\check{\xi}_{ECG}$

The optimization process of the rate one MRP will focus on $\check{\xi}_{ECG}$ given by (4.28). Hence it is an optimization process strongly related to the channel parameters, e.g. σ_ℓ and w_p^ℓ where $p = [1, \cdots, P]$, $\ell \in [0, \cdots, \Gamma - 1]$. Therefore a proper rotation matrix $\mathbf{\Phi}$ is designed to adjust the matrix $\mathbf{R}_\Phi = \mathbf{\Phi}\mathbf{\Phi}^\dagger$ so as to maximize the coding gain lowerbound $\check{\xi}$ for a given channel correlation matrix $\mathbf{R}_\delta$. In contrast, the optimization in [9] will fix the matrix $\mathbf{\Phi}$ and consequently the matrix $\mathbf{R}_\Phi$ is unchanged. It can be

regarded as an optimization process of matrix $\mathbf{R}_\delta$ by adjusting the value of δ for a given $\mathbf{R}_\Phi$.

Adjusting the subcarrier interval δ is an efficient way of improving the system performance since the receive side only needs to know the indexes of allocated subcarriers for each MIMO-OFDM subsystem by system scheduler. However in order to guarantee one-to-one mapping during the subcarrier grouping (for the reason of efficiency), the subcarrier interval should be a factor of F. Moreover, in a multiuser scenario, each user performs an independent optimization process. So the optimal subcarrier intervals for users are varied because users are experiencing different wireless propagation. Consequently, there is a difficulty of subcarrier allocation in a multiuser scenario which is forced to balance the system efficiency and user priority since each user (each subsystem) wishes to occupy the best "seat".

In this section we focus on an optimization process by adjusting the matrix $\mathbf{\Phi}$, which can be specially designed for each user so that the performance of each user and each subsystem can be improved simultaneously. Moreover, it does not have the trouble of subcarrier grouping since a special subcarrier interval is not required. The construction method of rotation angles $\phi_{p,m}$ might not be unique, but here for simplicity we assume that $\phi_{2,1} = 0$ and $\phi_{p,m} = (p-1)\phi_{2,m}$ for $\forall p, m$. Therefore, the determinant of $\mathbf{V}\mathbf{V}^\dagger$ is a function with $N_t - 1$ variables $\phi_{1,m}$ where $m \in [2, \cdots, N_t]$. Then the matrix $\mathbf{V}$ in (4.23) is an Vandermonde matrix. If $\lambda_1, \cdots, \lambda_n \in \mathbb{C}$, the determinant of an Vandermonde matrix is given by [84]:

$$\det \begin{bmatrix} 1 & 1 & \cdots & 1 \\ \lambda_1 & \lambda_2 & \cdots & \lambda_n \\ \vdots & \vdots & \vdots & \vdots \\ \lambda_1^{n-1} & \lambda_2^{m-1} & \cdots & \lambda_n^{m-1} \end{bmatrix} = \prod_{j<i} (\lambda_i - \lambda_j). \tag{4.33}$$

Therefore, the coding gain lowerbound for the proposed rate one MRP is given as

$$\begin{aligned} \check{\xi} &= \check{\xi}_{\mathcal{A}} \check{\xi}_{ECG} \\ &= \frac{\Delta_{\min}}{\beta\sqrt{N_t}} \prod_{\ell=0}^{\Gamma-1} \sigma_\ell^{\frac{1}{\Gamma}} \times \prod_{\ell>\ell'(m>m')} \left\| 2\sin\left(\frac{\pi\delta\tau_\ell}{T_s} - \frac{\pi\delta\tau_{\ell'}}{T_s} + \frac{\phi_{2,m} - \phi_{2,m'}}{2} \right) \right\|^{\frac{1}{P}} \\ &\leq \frac{\sqrt{\Gamma}\Delta_{\min}}{\beta} \prod_{\ell=0}^{\Gamma-1} \sigma_\ell^{\frac{1}{\Gamma}} \\ &\leq \frac{\Delta_{\min}}{\beta} \end{aligned} \tag{4.34}$$

where ℓ, ℓ', m, m' are integrals, $\ell, \ell' \in [0, \cdots, \Gamma - 1]$ and $m, m' \in [1, \cdots, N_t]$.

The first upperbound in (4.34) can be achieved only with certain conditions and

specific channel PDP. We have an upperbound given by

$$\prod_{\ell>\ell'(m>m')} \left\| 2\sin\left(\frac{\pi\delta\tau_\ell}{T_s} - \frac{\pi\delta\tau_{\ell'}}{T_s} + \frac{\phi_{2,m}-\phi_{2,m'}}{2}\right)\right\|^{\frac{1}{P}} \leq \sqrt{P}. \tag{4.35}$$

The upperbound can be achieved only by equally separated angles $\frac{2\pi\delta\tau_\ell}{T_s} + \phi_{2,m}$ where $\ell \in [0,\cdots,\Gamma-1]$ and $m \in [1,\cdots,N_t]$. The optimization process can be visualized later so that such an upperbound can be demonstrated more clearly. For instance, if $P = N_t\Gamma = 10$, then a total of 10 angles formed by $\frac{2\pi\delta\tau_\ell}{T_s} + \phi_{2,m}$ should be equally distributed with exact interval $\pi/5$.

Moreover the second upperbound in (4.34) can be achieved with a further condition of uniform delay power so that $\sigma_\ell^2 = 1/\Gamma$ for $\forall \ell \in [0,\cdots,\Gamma-1]$. Using the inequality of geometric mean, we know that

$$\prod_{\ell=0}^{\Gamma-1} \sigma_\ell^{\frac{1}{\Gamma}} = \left\{\prod_{\ell=0}^{\Gamma-1}\sigma_\ell^2\right\}^{\frac{1}{2\Gamma}} \leq \left\{\frac{1}{\Gamma}\sum_{\ell=0}^{\Gamma-1}\sigma_\ell^2\right\}^{\frac{1}{2}} \leq \frac{1}{\sqrt{\Gamma}} \tag{4.36}$$

As an example, the case of $P = 4$ and $N_t = 2$ is considered. The candidates of optimal rotation angle $\phi_{2,2}$ can be derived by differentiation of (4.34) and are given by

$$\phi_{2,2} = k\pi, 2\arccos\sqrt{\frac{1}{2}+\frac{1}{2}\cos^2\left(\frac{\pi\delta}{T_s}(\tau_0-\tau_1)\right)} + k\pi \tag{4.37}$$

where $k \in \mathbb{Z}$. Then the optimal rotation angle $\phi_{2,2}$ can be obtained by comparing the coding gain lowerbound using these candidates.

For the case that P is not an integer multiple of N_t and $P < N_t\Gamma$, the process of optimization is not much different. The matrix $\mathbf{\Omega}_1$ in (4.17) is constructed by truncating first P column vectors from the matrix $\mathbf{\Omega}$ which then yields the coding gain lowerbound $\check{\xi}$. Therefore the matrix $\mathbf{V}$ will be similar to equation (4.23), but the coding gain lowerbound $\check{\xi}$ given by (4.34) will be slightly different. For example, if $P = 3$ and $N_t = 2$, the targeted matrix $\mathbf{V}$ in the optimization process for the rate one MRP is given by

$$\mathbf{V} = \begin{bmatrix} w_1^0 e^{j\phi_{1,1}} & w_1^0 e^{j\phi_{1,2}} & w_1^1 e^{j\phi_{1,1}} \\ w_2^0 e^{j\phi_{2,1}} & w_2^0 e^{j\phi_{2,2}} & w_2^1 e^{j\phi_{2,1}} \\ w_3^0 e^{j\phi_{3,1}} & w_3^0 e^{j\phi_{3,2}} & w_3^1 e^{j\phi_{3,1}} \end{bmatrix}. \tag{4.38}$$

The corresponding optimal rotation angle $\phi_{2,2}$ is given by

$$\phi_{2,2} = k\pi - \frac{\pi\delta}{T_s}(\tau_0-\tau_1) \tag{4.39}$$

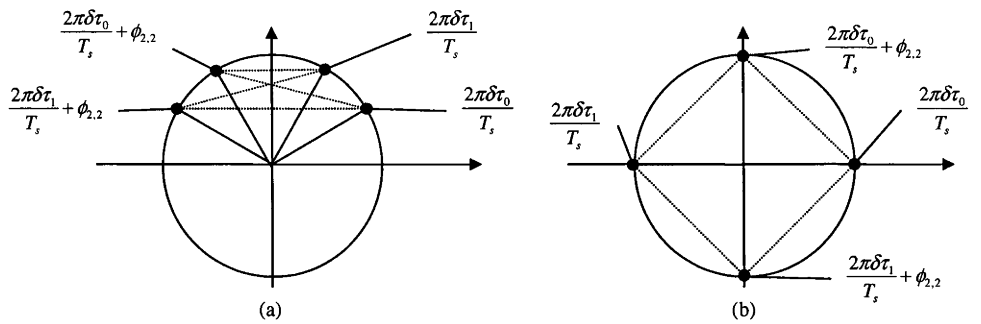

Figure 4.2: Visualization of optimization for the case of $P = 4$ and $N_t = 2$

where $k \in \mathbb{Z}$.

4.5.4 Visualization of Optimization

The optimization process for the rate one MRP can be visualized by diagrams, which can provide a better understanding. Two examples are demonstrated here. It would be interesting to observe the optimization process for the case of $P = 4$ and $N_t = 2$ through Figure 4.2(a) which describes two delay paths as two points in the unit circle located in the first quadrant. Each point represents one dominant delay path. After being rotated by a certain angle $\phi_{2,2}$ clockwise, two points are then moved into the second quadrant. Hence the optimization process is to look for a best rotation angle $\phi_{2,2}$ that can maximize the product of lengths of the four dashed lines connecting these four points in Figure 4.2 (a). Through the visualization of optimization process, it is feasible to get optimal rotation angles instinctively for some cases without complicated calculation. For example, it is easy to obtain the optimal rotation angle $\phi_{2,2} = \pi$ through Figure 4.2 (a) and another optimal rotation angle $\phi_{2,2} = \pi/2$ through Figure 4.2(b).

The visualization of optimization contains two step: the first step is to put Γ points in the unit circle whose angles, $\frac{2\pi\delta\tau_\ell}{T_s}$ where $\ell \in [0, \cdots, \Gamma - 1]$, are determined by corresponding time delays and subcarrier interval. The second step is to rotate these points simultaneously with the same rotation angle $\phi_{2,m}$ where $m \in [1, \cdots, N_t]$. Such rotation is repeated N_t times and each will create a new set of Γ points. Therefore after these rotations, a total of N_t sets corresponding to $N_t\Gamma$ points are created and spread around the unit circle. Therefore there are $\Gamma^2 N_t(N_t - 1)/2$ lines connecting these points among different sets, e.g. four lines in Figure 4.2. Beware that the connection lines between points within a same set are useless for the optimization process because they are determined by the time delays and can not be changed artificially. Moreover the angle $\phi_{2,1}$ is assumed to be zero here so that only $N_t - 1$ rotations are

Table 4.1: Optimal Rotation Angles $\phi_{2,2}$ for COST207

P	$\phi_{2,2}$	$\check{\xi}_{ECG}$
3	$107\pi/180$	0.6865
4	π	0.7566
5	$129\pi/180$	0.5228
6	$141\pi/180$	0.7082

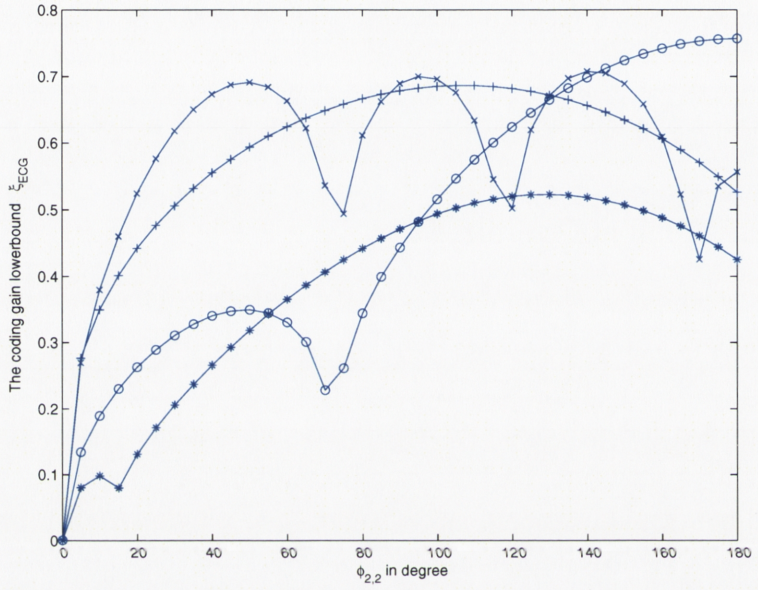

Figure 4.3: $\check{\xi}_{ECG}$ of rate one MRP vs rotation angle $\phi_{2,2}$ for a MIMO-OFDM system with $\delta = \lfloor 512/P \rfloor$, $N_t = 2$, $F = 512$, and given COST207 typical urban six-ray power delay profile

needed in this thesis.

The optimization process is to maximize the product of lengths of these connection lines. The optimal case is that total $N_t\Gamma$ points are uniformly distributed around the unit circle with an exact separation angle $2\pi/(N_t\Gamma)$. It gives the best performance for the specific subsystem and achieves the coding gain upperbound derived in [8]. Moreover, the STBC proposed in [49] has some similarity with the rate one MRP in terms of optimization strategy. The optimal constellation rotation in [49] is designed for a particular constellation with a single rotation and space diversity, but the rate one MRP is designed for particular propagation channel (independent of constellation) with multiple rotations and space-frequency diversity. Hence the rate one MRP can be visualized as a SFBC optimizing "channel Euclidean distance".

4.5.5 Examples

As an example we determine optimal rotation angles for a multipath fading model, COST207 six-ray power delay profile for typical urban scenario [33] described in Table 2.1. The power of delays of COST207 is sorted in a decreasing order. The MIMO-OFDM system has two transmitters, 512 subcarriers and a bandwidth of 16MHz. The subcarrier interval δ in the MIMO-OFDM subsystem is assumed to be $\delta = \lfloor \frac{512}{P} \rfloor$. Then the MRP has only one unknown variable $\phi_{2,2}$, and $\phi_{p,2} = (p-1)\phi_{2,2}$ for $\forall p \in [1, \cdots, P]$. It is assumed that only limited PDP of COST207 MIMO channel, that is time delay τ_ℓ shown in Table 2.1 where $\ell \in [0, \cdots, \Gamma - 1]$, is actually known by the transmitter. It is also assumed that $\Gamma = \lceil P/N_t \rceil$ where $\lceil a \rceil$ denotes the smallest integer greater or equal to a. Hence if $P = 3, 4$, then $\Gamma = 2$ delays are known by the transmitters. And if $P = 5, 6$ then $\Gamma = 3$.

Since the proposed rate one MRP is composed of two independent optimization processes and $\check{\xi}_{\mathcal{A}}$ is only related to the constellation $\mathcal{A}$, we focus on $\check{\xi}_{ECG}$ only which is highly related to the specific channel PDP known by the transmitters. Figure 4.3 shows the variations of $\check{\xi}_{ECG}$ of the MRP for a variety of values of $\phi_{2,2}$ and P. All peak points in Figure 4.3 with corresponding coordinates of $\phi_{2,2}$ and $\check{\xi}_{ECG}$ are summarized in Table 4.1. The optimization of coding gain lowerbound $\check{\xi}$ can be used to search for an approaching optimal performance since only partial PDP is known. But full transmit diversity can always be guaranteed. Moreover, full transmit diversity is achieved for same cases even if the coding gain lowerbound $\check{\xi}$ equals to zero. Hence the condition that the lowerbound $\check{\xi}$ should be greater than zero is a sufficient condition to achieve full transmit diversity. The optimal rotation angle $\phi_{2,2}$ is varied from case to case. At last the selection of column vectors for $\mathbf{\Omega}_1$ will affect the design process and results of optimization. The first Γ paths are chosen because of the largest power so that the $\prod_{\ell=0}^{\Gamma-1} \sigma_\ell^2$ is maximized. Moreover, it is known that if more column vectors are built inside $\mathbf{\Omega}_1$ (also meaning better knowledge of PDP at the transmitters and $\mathbf{\Omega}_1 \Longrightarrow \mathbf{\Omega}$), the optimization process will be closer to the global optimal.

On the other hand the optimization process of subcarrier interval δ is still feasible for the proposed rate one MRP. Figure 4.4 shows the changes of the $\check{\xi}_{ECG}$ of rate one MRP for a variety of values of $\phi_{2,2}$ and δ. For arbitrary subcarrier interval δ, the rotation angle $\phi_{2,2}$ can be adjusted to achieve the optimal performance. Subcarrier interval δ is fixed to $\lfloor \frac{F}{P} \rfloor$ in this thesis because of limited choices of subcarrier interval δ if one-to-one mapping needs to be guaranteed during subcarrier permutation, or if the performance of all users in a multiuser scenario needs to be optimized simultaneously.

Remark 2: The rate one MRP with limited PDP is proposed for the circumstance that the transmitters have only partial or imperfect knowledge of the channel PDP

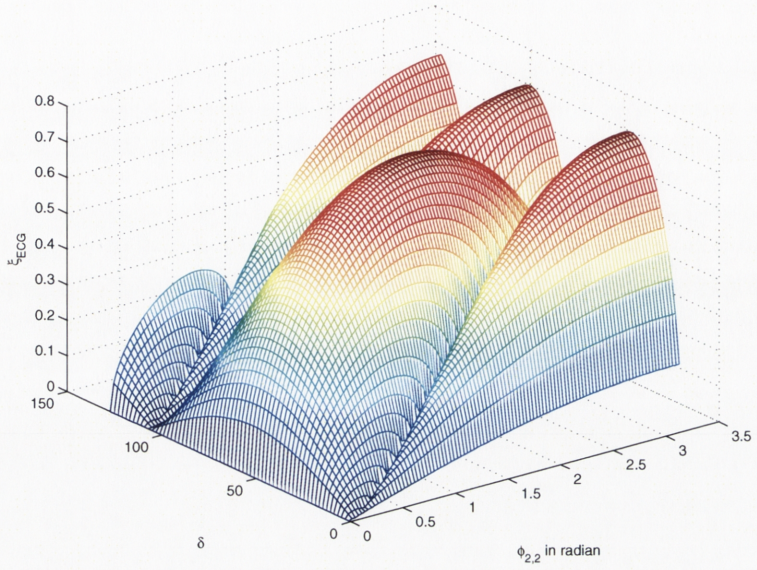

Figure 4.4: $\check{\xi}_{ECG}$ of rate one MRP vs rotation angle $\phi_{2,2}$ and δ for a MIMO-OFDM system with $P = 4$, $N_t = 2$, $F = 512$, and given COST207 typical urban six-ray power delay profile

through the feedback from the receivers or uplink transmission. It is capable of reducing both system complexity and SFBC design complexity significantly. Better optimization process requires more knowledge of channel PDP. Moreover, the rate one MRP can overcome the drawback of diversity loss in [8] for specific channel PDP, and remove the limitations of subcarrier interval and subcarrier grouping. It can always achieve full transmit diversity and get close to optimal performance.

4.6 Multirate Matched Rotation Precoding

In this section the multirate SFBC with MRP is proposed. The multirate SFBC provides a variety of symbol transmission rate without a significant change of coding process. So specific transmission rate can be dynamically determined by the system for the requirement of QoS or performance. It has better spectral efficiency when compared to the rate one MRP, and better performance if the same bit transmission rate is assumed. It also can achieve relatively smooth balance between the performance and the transmission rate without a significant configuration change. The optimization process of proposed multirate MRP is also discussed.

$$\Psi\Psi^{\dagger} = \begin{bmatrix} \Gamma & \sum_{\ell=0}^{\Gamma-1} e^{-j2\pi\delta\tau_\ell/T_s} & \cdots & \sum_{\ell=0}^{\Gamma-1} e^{-j2(P-1)\pi\delta\tau_\ell/T_s} \\ \sum_{\ell=0}^{\Gamma-1} e^{j2\pi\delta\tau_\ell/T_s} & \Gamma & \cdots & \sum_{\ell=0}^{\Gamma-1} e^{-j2\pi(P-2)\delta\tau_\ell/T_s} \\ \vdots & \vdots & \vdots & \vdots \\ \sum_{\ell=0}^{\Gamma-1} e^{j2\pi(P-1)\delta\tau_\ell/T_s} & \sum_{\ell=0}^{\Gamma-1} e^{j2\pi(P-2)\delta\tau_\ell/T_s} & \cdots & \Gamma \end{bmatrix}$$
$$\circ \begin{bmatrix} \sum_{m=1}^{N_t} \|\Delta\bar{s}_{1,m}\|^2 & \cdots & \sum_{m=1}^{N_t} \left(\Delta\bar{s}_{1,m}\Delta\bar{s}_{P,m}^{*} e^{j(\phi_{1,m}-\phi_{P,m})}\right) \\ \sum_{m=1}^{N_t} \left(\Delta\bar{s}_{2,m}\Delta\bar{s}_{1,m}^{*} e^{j(\phi_{2,m}-\phi_{1,m})}\right) & \cdots & \sum_{m=1}^{N_t} \left(\Delta\bar{s}_{2,m}\Delta\bar{s}_{p,m}^{*} e^{j(\phi_{2,m}-\phi_{P,m})}\right) \\ \vdots & \vdots & \vdots \\ \sum_{m=1}^{N_t} \left(\Delta\bar{s}_{P,m}\Delta\bar{s}_{1,m}^{*} e^{j(\phi_{P,m}-\phi_{1,m})}\right) & \cdots & \sum_{m=1}^{N_t} \|\Delta\bar{s}_{P,m}\|^2 \end{bmatrix}$$
$$= \mathbf{R}_\delta \circ \mathbf{R}_\psi \tag{4.42}$$

4.6.1 Multirate SFBC

The multirate MRP is proposed here to optimize the coding gain lowerbound $\check{\xi}$ denoted in (4.18). Assuming that $s_{p,m} = \bar{s}_{p,m}e^{j\phi_{p,m}}$ and $\bar{\mathbf{S}}^m = [\bar{s}_{1,m}, \cdots, \bar{s}_{P,m}]^T$, we have $\Delta s_{p,m} = \Delta\bar{s}_{p,m}e^{j\phi_{p,m}}$ and

$$\Delta\tilde{\mathbf{S}}_m = \Delta\bar{\mathbf{S}}^m \circ \mathbf{\Phi}^m \tag{4.40}$$

where $\Delta\bar{\mathbf{S}}^m = [\Delta\bar{s}_{1,m}, \cdots, \Delta\bar{s}_{P,m}]^T$, $\mathbf{\Phi}^m = [e^{j\phi_{1,m}}, \cdots, e^{j\phi_{P,m}}]^T$ and $m \in [1, \cdots, N_t]$. The matrix Ψ in (4.18) can be expressed as

$$\begin{aligned} \Psi = [&\Delta\bar{\mathbf{S}}^1 \circ \mathbf{\Phi}^1 \circ \mathbf{w}^0, \cdots, \Delta\bar{\mathbf{S}}^{N_t} \circ \mathbf{\Phi}^{N_t} \circ \mathbf{w}^0, \cdots, \\ &\Delta\bar{\mathbf{S}}^1 \circ \mathbf{\Phi}^1 \circ \mathbf{w}^{\Gamma-1}, \cdots, \Delta\bar{\mathbf{S}}^{N_t} \circ \mathbf{\Phi}^{N_t} \circ \mathbf{w}^{\Gamma-1}]. \end{aligned} \tag{4.41}$$

Then $\Psi\Psi^{\dagger}$ is shown in equation (4.42). The rotation matrix $\mathbf{\Phi}_R$ for the symbol transmission rate R is denoted as $\mathbf{\Phi}_R = [\mathbf{\Phi}^1, \cdots, \mathbf{\Phi}^{N_t}]$.

The Hermitian matrix $\Psi\Psi^{\dagger}$ is the Hadamard product of two matrices $\mathbf{R}_\delta$ and $\mathbf{R}_\psi$ denoted in (4.42). The matrix $\mathbf{R}_\delta$ is related to both time delays τ_ℓ of paths and subcarrier interval δ. But the matrix $\mathbf{R}_\psi$ of the multirate MRP is more complicated than the matrix $\mathbf{R}_\phi$ of the rate one MRP denoted in (4.24). It is related to the proposed rotation matrix $\mathbf{\Phi}_R$ and also the specific constellation $\mathcal{A}$.

Supposed that the vector $\bar{\mathbf{S}}$ is defined as

$$\bar{\mathbf{S}} = [(\bar{\mathbf{S}}^1)^T, \cdots, (\bar{\mathbf{S}}^{N_t})^T] = [\bar{s}_{1,1}, \cdots, \bar{s}_{P,1}, \cdots, \bar{s}_{1,N_t}, \cdots, \bar{s}_{P,N_t}]. \tag{4.43}$$

The precoding process of multirate MRP with transmission rate R is given by

$$\bar{\mathbf{S}} = \mathbf{C}\Theta_R \tag{4.44}$$

where the codeword $\mathbf{C} = [c_1, \cdots, c_Q]$ is a $1 \times Q$ vector where $c_1, \cdots, c_Q$ are complex scalars chosen from a particular r-PSK or r-QAM constellation $\mathcal{A}$. The symbol transmission rate is denoted as $R = Q/P$. It is assumed that both the real parts and the imaginary parts of $c_1, \cdots, c_Q$ have a variance of $1/2$ and are uncorrelated, so we have $\mathbb{E}[c_i c_i^*] = 1$ and $\mathbb{E}[c_i^2] = 0$ where $i \in [1, \cdots Q]$.

The matrix Θ_R is a $Q \times N_t P$ complex coding matrix satisfying the following power normalization equation:

$$\text{trace}(\Theta_R \Theta_R^\dagger) = N_t P. \tag{4.45}$$

Hence the codeword $\mathbf{C}$ is dispersed from Q dimensional vector to $N_t P$ transmission data across both frequency and space domains. The value of integer Q can be chosen from 1 to $N_t P$ so that the symbol transmission rate R can be varied from $1/P$ up to N_t.

When the MIMO-OFDM subsystem achieves the highest transmission rate $R = N_t$, then $Q = N_t P$. The matrix Θ_{N_t} is a unitary square matrix and assumed to be a Vandermonde matrix given by (4.31). Hence we have

$$\Theta_{N_t} = \Theta. \tag{4.46}$$

When the bit error rate (BER) performance of the MIMO-OFDM subsystem is lower than the expected performance, the transmission rate R can be reduced to achieve better BER performance without decreasing constellation size or significantly changing the coding structure. Thus when $R \leq N_t$, $Q = RP$ and Θ_R is a $RP \times N_t P$ matrix. The coding matrix Θ_R can be obtained by simply truncating first RP row vectors from the coding matrix Θ_{N_t} and applying power normalization using (4.45). Hence the matrix Θ_R is given by

$$\Theta_R = \sqrt{N_t/R}\Theta_{Q \times PN_t} \tag{4.47}$$

where $\Theta_{Q \times PN_t}$ is truncated matrix from $\Theta_{N_t} = \Theta$.

Matrices Θ_R and Φ_R are key matrices for the multirate MRP where the rate R ranges from $1/P$ to N_t. They can even summarize coding structures of most existing SFBCs as a variety of matrix pairs Θ_R and Φ_R. For example, the rate one MRP has a transmission rate $R = 1$. Consequently, $\Phi_R = \Phi$ which is defined in (4.21) and Θ_R is given by

$$\Theta_R = [\underbrace{\Theta, \cdots, \Theta}_{N_t}] \tag{4.48}$$

where Θ which is defined in (4.31). The rate one SFBCs proposed in [8] and [9] have the same Θ_R as shown in (4.48) but different Φ_R as defined in (4.25) and (4.26) respectively.

The matrix Θ_R can disperse the information of a codeword $\mathbf{C}$ into $N_t P$ subchan-

nels but it can not guarantee full diversity gain or optimal performance. The matrix $\mathbf{\Phi}_R$ can guarantee full transmit diversity and optimize the coding gain simultaneously for specific channel PDP known by transmitters. Hence it is strongly related to constellation $\mathcal{A}$, correlation matrix $\mathbf{R}_\delta$ and designed matrix $\mathbf{\Theta}_R$.

Remark 3: The rotation matrix $\mathbf{\Phi}_R$ for arbitrary rate R can be assumed to be the same as the matrix $\mathbf{\Phi}_{N_t}$ designed for the highest rate N_t, that is $\mathbf{\Phi}_R = \mathbf{\Phi}_{N_t}$ for $\forall R$. Therefore if matrices $\mathbf{\Theta}_{N_t}$ and $\mathbf{\Phi}_{N_t}$ can achieve full transmit diversity P at the highest rate N_t for the MIMO-OFDM subsystem, full transmit diversity can be guaranteed at each transmission rate R if the matrices $\mathbf{\Theta}_R$ are derived from $\mathbf{\Theta}_{N_t}$ and $\mathbf{\Phi}_R = \mathbf{\Phi}_{N_t}$. Hence the multirate MRP can easily generate a series of lower rate SFBC and reduce design complexity significantly. The explanation is as following.

The codeword error $\Delta\mathbf{C}$ for the transmission rate R can be obtained by assigning zeros to the last $(N_t - R)P$ symbols of $\Delta\mathbf{C}$ for the transmission rate N_t. Thus the set of $\Delta\mathbf{C}$ for the rate R actually becomes a subset of $\Delta\mathbf{C}$ for the rate N_t. Therefore, for the lower transmission rate R, the subset of $\Delta\mathbf{C}$ is smaller resulting in larger coding gain and better BER performance. The rotation matrix $\mathbf{\Phi}_R$ can be either specially designed for a specific rate R and symbol constellation $\mathcal{A}$, or kept unchanged as $\mathbf{\Phi}_{N_t}$ for simplicity. The matrix $\mathbf{\Theta}_R$ can be obtained by simply truncation and power normalization from the matrix $\mathbf{\Theta}_{N_t}$. Thus full transmit diversity of P is always guaranteed in the multirate MRP.

The principle is that the matrix $\mathbf{\Theta}_R$ disperses the information of the codeword into all subchannels, whilst the matrix $\mathbf{\Phi}_R$ guarantees full transmit diversity and optimizes the coding gain simultaneously.

4.6.2 Optimization Process

The optimization process of the multirate MRP will be more complicated than the rate one MRP. The determinant of $\mathbf{\Psi}\mathbf{\Psi}^\dagger$ given by (4.42) is affected by both matrix $\mathbf{R}_\delta$ and matrix $\mathbf{R}_\psi$. The subcarrier interval is fixed to $\delta = \lfloor F/P \rfloor$ so that the matrix $\mathbf{R}_\delta$ is unchanged during the optimization process. The matrix $\mathbf{R}_\psi$ is related to specific constellation $\mathcal{A}$, designed matrix $\mathbf{\Theta}_R$, and rotation matrix $\mathbf{\Phi}_R$. It is optimized by adjusting both matrices $\mathbf{\Theta}_R$ and $\mathbf{\Phi}_R$ simultaneously. In this thesis, the matrix $\mathbf{\Theta}_R$ is fixed at first, then the rotation matrix $\mathbf{\Phi}_R$ is adjusted from case to case.

The matrix $\mathbf{\Theta}_R$ is given by (4.46) and (4.47) according the transmission rate R. And for simplicity, we assume that $\phi_{p,m} = (p-1)(m-1)\phi_{2,2}$ for $\forall p, m$ in $\mathbf{\Phi}_R$. Therefore the determinant of $\mathbf{\Psi}\mathbf{\Psi}^\dagger$ given by (4.42) is a polynomial equation with only one variable $\phi_{2,2}$ and $\det(\mathbf{\Psi}\mathbf{\Psi}^\dagger) = \|\det(\mathbf{\Psi})\|^2$. The optimization process of the multirate MRP has only one unknown variable $\phi_{2,2}$ for an arbitrary MIMO-OFDM subsystem.

R	$\phi_{2,2}$	$\check{\xi}$	$\check{\xi}$ when $\phi_{2,2} = 168\pi/180$
1/4	π	1.07	1.0626
2/4	π	0.7566	0.7514
3/4	$164\pi/180$	0.5660	0.3493
4/4	$154\pi/180$	0.4231	0.3025
5/4	$95\pi/180$	0.3048	0.2706
6/4	$99\pi/180$	0.2641	0.2337
7/4	$165\pi/180$	0.2076	0.2004
8/4	$168\pi/180$	0.1874	0.1874

Table 4.2: Transmission rate R vs optimal rotation angle $\phi_{2,2}$ and corresponding coding gain lowerbound $\check{\xi}$ for Multirate MRP in a MIMO-OFDM subsystem with $P = 4$, $N_t = \Gamma = 2$ and QPSK for COST 207 Typical urban six-ray power delay profile

Remark 4: If $e^{j\phi_{2,2}}$ is an algebraic number of degree greater than $N_t P^2$ over $\mathcal{K}$ which is the extension field containing all the entries of Θ_R, the ring of complex integers $\mathbb{Z}(j)$, and $e^{j2\pi\delta\tau_\ell/T_s}$ where $\ell \in [0, \cdots, \Gamma - 1]$, then full transmit diversity P is guaranteed for any QAM constellation. This property can be derived from the determinant expression of Ψ denoted in (4.42).

The high rate SFBC proposed in [4] has a similar rule as above. But the proposed multirate MRP has utilized a rotation matrix Φ_R designed for the scenario with limited channel PDP, and also defined a smaller extension field $\mathcal{K}$ compared to [4]. The smaller extension field $\mathcal{K}$ will reduce the complexity of searching the optimal solutions. Moreover, despite relatively high complexity and difficulty in the optimization process, the multirate MRP always takes advantage of a portion above the information of propagation paths for arbitrary channel PDP, so that it is feasible to generate a decision table for the optimization in advance at the transmit side. Therefore such a table can be stored and re-used without the requirement of another calculation.

4.6.3 Examples

As an example the optimal rotation angle $\phi_{2,2}$ is generated for COST 207 typical urban scenario defined in Table 2.1. The MIMO-OFDM system has two transmitters, 512 subcarriers, and a bandwidth 16MHz. Each MIMO-OFDM subsystem has $P = 4$ well-separated subcarriers and the subcarrier interval is assumed to $\delta = 128$. The propagation channel knowledge is assumed to be limited so that only τ_ℓ, where $\ell \in [0, \cdots, \Gamma - 1]$, are perfectly known by the transmitters where $\Gamma = 2$.

For a QPSK constellation, the coding gain lowerbound $\check{\xi}$ of multirate MRP is maximized by a computer search over $\phi_{2,2}$ varying from 0 to π. The step size is $\pi/180$ so that the algebraic degree meets the condition of Remark 4. The optimal rotation angles $\phi_{2,2}$ for a variety of transmission rate R are shown in Table 4.2. Moreover the optimal

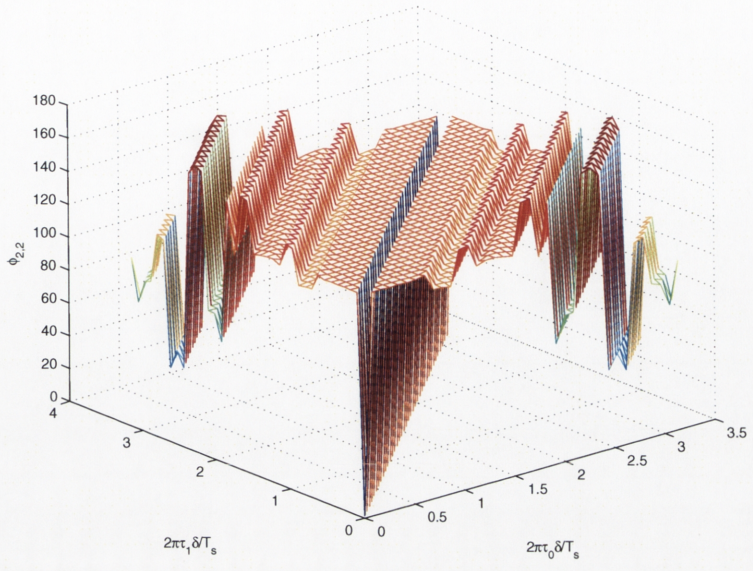

Figure 4.5: Decision Table of the optimal rotation angle $\phi_{2,2}$ for multirate MRP in a MIMO-OFDM subsystem with $P = 4$, $R = N_t = \Gamma = 2$ and BPSK constellation

rotation angle $\phi_{2,2} = 168\pi/180$ gives the largest coding gain lowerbound at the highest transmission rate $R = 2$. Hence the rotation angle $\phi_{2,2}$ can be fixed to $168\pi/180$ without jeopardizing the transmission diversity according to Remark 3. Therefore the coding gain lowerbound $\check{\xi}$ corresponding to $\phi_{2,2} = 168\pi/180$ for different rates R are also included in Table 4.2 for comparison.

It is also feasible to yield a decision table for the multirate MRP in advance since only a limited number of propagation paths are needed for the optimization process. Figure 4.5 is an example of a decision table for a BPSK constellation and the transmission rate $R = 2$. The z-axis in the figure shows the optimal rotation angle $\phi_{2,2}$ for a specific channel PDP which has two dominant delays marked by corresponding x and y coordinates. Hence it would be easy to determine the optimal rotation angle $\phi_{2,2}$ for an arbitrary MIMO-OFDM subsystem and channel PDP once such a decision table has been generated. It is also shown that if $2\pi\tau_0\delta/T_s = 2\pi\tau_1\delta/T_s + 2k\pi$ where $k \in \mathbb{Z}$, the coding gain lowerbound $\check{\xi}$ would be equal to zero with a potential loss of diversity gain.

4.7 Simulation Results

To illustrate the performance of proposed MRP, we performed some simulations and made comparisons with existing SFBC given in [8]. For example, if $P = 3$ and $N_t = 2$, transmitted symbols $\hat{\mathbf{S}}$ ($P \times N_t$ matrices) using rate one MRP and the SFBC in [8] are

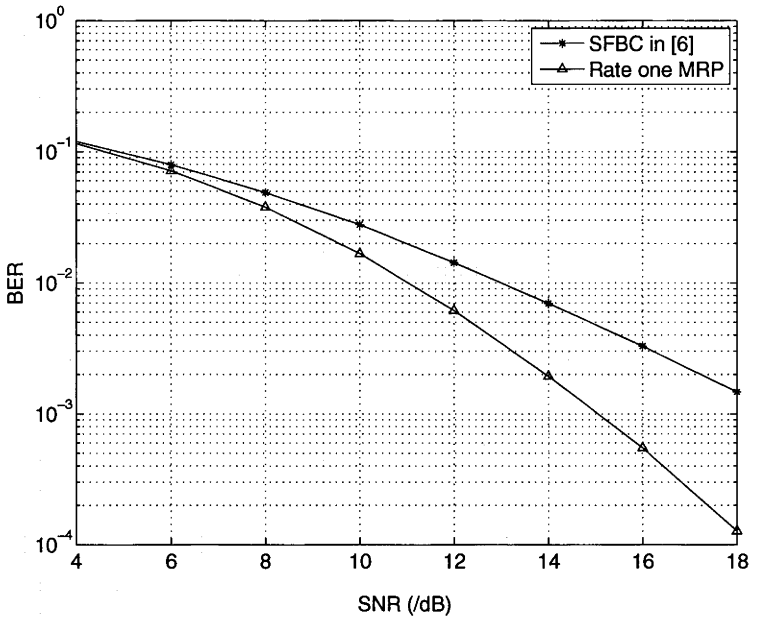

Figure 4.6: Performance of the rate one MRP and the SFBC in [8] for the MIMO-OFDM system with $N_t = 2$, $N_r = 1$, $F = 512$ and $\delta = 128$ in the propagation scenario with uniform PDP of two paths.

given by the following respectively

$$\hat{\mathbf{S}} = \begin{bmatrix} \bar{s}_1 & \bar{s}_1 \\ \bar{s}_2 & \bar{s}_2 e^{j\phi_{2,2}} \\ \bar{s}_3 & \bar{s}_3 e^{2j\phi_{2,2}} \end{bmatrix} \quad \text{and} \quad \hat{\mathbf{S}} = \begin{bmatrix} \sqrt{2}\bar{s}_1 & 0 \\ 0 & \sqrt{2}\bar{s}_2 \\ \sqrt{2}\bar{s}_3 & 0 \end{bmatrix} \tag{4.49}$$

where $\bar{\mathbf{S}} = [\bar{s}_1, \bar{s}_2, \bar{s}_3] = \mathbf{C}\boldsymbol{\Theta}$. The constellation $\mathcal{A}$ of the codeword $\mathbf{C}$ is chosen to be quaternary phase-shift keying (QPSK) or 16QAM. The precoding matrix $\boldsymbol{\Theta}$ are given by (4.31). The optimal rotation angles $\phi_{2,2}$ of the rate one MRP are given by the second column of Table 4.1. The channel state information $\tilde{\mathbf{H}}$ and the rotation angles $\phi_{2,2}$ are perfectly known by the receivers. The transmitters has a limited information of channel PDP. The decoding process is the same in all simulations and for details refer to Chapter 6. The same sphere decoding [86] is used at the receive side for each subsystem and each SFBC. The bit error rate (BER) performance is averaged over all MIMO-OFDM subsystems and channel realizations.

4.7.1 Diversity Loss

The SFBC without optimization process might lose the diversity gain for specific propagation scenarios. It has previously not been completely recognized but this problem

can be overcome by adjusting subcarrier interval δ or applying proposed MRP. We assume that the MIMO-OFDM system has $N_t = 2$, $N_r = 1$, 16MHz Bandwidth and $F = 512$ subcarriers. Each subsystem has $P = 4$ well-separated subcarriers giving a fixed subcarrier interval $\delta = 128$. The propagation scenario has two delay paths only or has two dominant delay paths. It is shown in (4.13) that for this kind of system setting and propagation scenario, the powers of paths are irrelevant to the SFBC design process. Hence it is assumed that the wireless channel has uniform delay power and $\sigma_\ell^2 = 1/2$ for simplicity. The time delays are assumed to be $\tau_0 = 0$ and $\tau_1 = 2T_s/F$. The rate one MRP is compared with the SFBC in [8] with completely the same configuration of MIMO-OFDM subsystems. The optimal rotation angle $\phi_{2,2}$ of the rate one MRP for this specific propagation scenario is $\pi/2$ which can be seen in Figure 4.2 (b).

Figure 4.6 shows clearly the improvement of the rate one MRP. The SFBC in [8] can not achieve full transmit diversity for this propagation scenario but the proposed rate one MRP can provide a significant improvement. The problem of diversity loss is not given enough attention because of the Hadamard product which conceals some properties of the frequency domain. Hence we should be cautious about judging the performance of specific SFBC, which might be good for some cases but lose diversity gain for others. The optimization process is important for all existing SFBCs because of the issue of diversity loss, through either adjusting subcarrier interval, or applying the proposed MRP, or even both if feasible.

4.7.2 Rate one MRP

To show the performance of rate one MRP with limited channel PDP, a more practical scenario COST207 typical urban six-ray PDP, is considered and defined in Table 2.1. The MIMO-OFDM system has $N_t = 2$, $N_r = 1$, 16MHz Bandwidth, and $F = 512$ subcarriers. Each subsystem has P well-separated subcarriers and a fixed subcarrier interval $\delta = \lfloor \frac{512}{P} \rfloor$. So there are $512 - P\delta < P$ subcarriers un-allocated which could be used as subcarrier guard interval. Limited knowledge is fed back to the transmitters. So it is assumed that only time delays τ_ℓ where $\ell \in [0, \cdots, \Gamma - 1]$ are known by the transmitters. It is also assumed that $\Gamma = \lceil P/N_t \rceil$.

It is shown in Figure 4.7 that the performance of the rate one MRP has better performance than the SFBC in [8] when $P = 3$ and 6, and the same performance when $P = 4$ for COST207 typical urban scenario. The performance gain of rate one MRP is roughly about 0.5dB at a BER of 10^{-3} when $P = 3$. The performance gain is about 0.2dB when $P = 6$. The performances of both SFBC are same when $P = 4$ but we could observe the advantage of the rate one MRP for other channel PDP from Figure 4.6. The observation confirms that the rate one MRP does improve BER performance

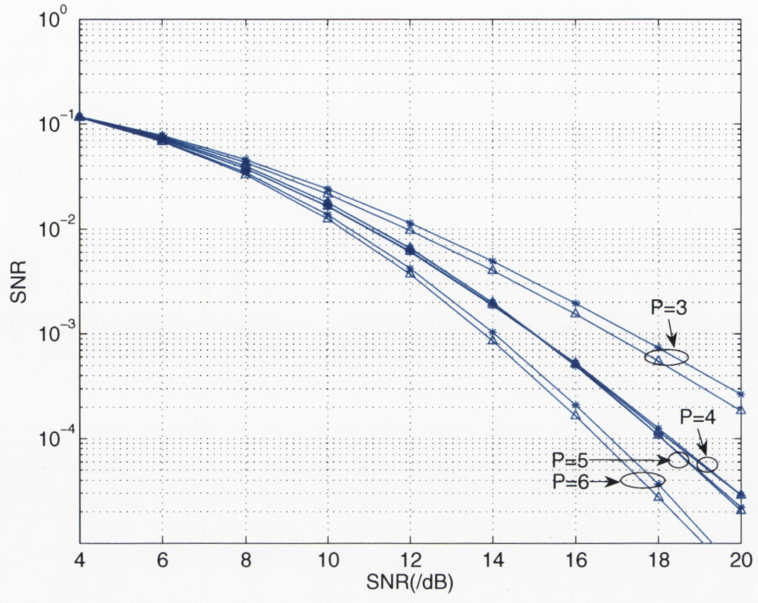

Figure 4.7: Performance of the MRP marked by △ and the SFBC in [8] marked by ∗ for the MIMO-OFDM system with $N_t = 2$, $N_r = 1$, $F = 512$ and $\delta = \lfloor \frac{512}{P} \rfloor$ in COST207 typical urban scenario.

by optimizing coding gain lowerbound $\check{\xi}$ for some cases, even when the knowledge of channel PDP is limited. Therefore the rate one MRP is capable of providing more design freedom and better system performance when compared to [8,9]. Furthermore the information required by the optimization process can be reduced by the proposed SFBC design with limited knowledge of PDP.

4.7.3 Multirate MRP

The multirate SFBC following the coding matrix (4.40) is investigated in Figure 4.8 for the MIMO-OFDM system with $N_t = 2$, $N_r = 2$, $P = 4$, $\delta = 128$ and $F = 512$. The constellations of QPSK and 16 QAM are applied. For example, transmitted symbols $\hat{\mathbf{S}}$ (a $P \times N_t$ matrix) using the multirate MRP are given by

$$\hat{\mathbf{S}} = \begin{bmatrix} \bar{s}_{1,1} & \bar{s}_{1,2} \\ \bar{s}_{2,1} & \bar{s}_{2,2}e^{j\phi_{2,2}} \\ \bar{s}_{3,1} & \bar{s}_{3,2}e^{2j\phi_{2,2}} \\ \bar{s}_{4,1} & \bar{s}_{4,2}e^{3j\phi_{2,2}} \end{bmatrix} \tag{4.50}$$

where $\bar{\mathbf{S}}$ is precoded by the matrix $\mathbf{\Theta}_R$ which is specified by (4.46) and (4.47). And the rotation angle $\phi_{2,2}$ of multirate MRP is specified by the second column in Table 4.2 for a variety of transmission rates R.

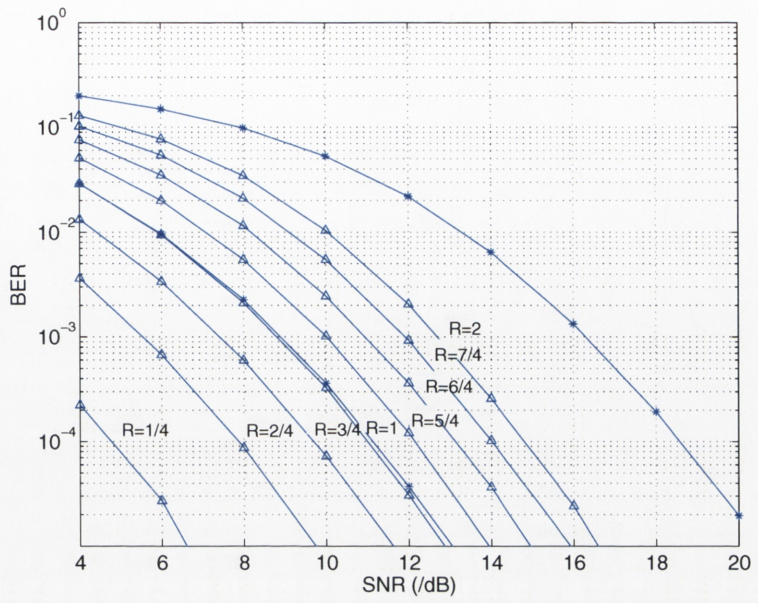

Figure 4.8: Multirate MRP simulations marked by $\triangle$ with the optimal rotation angle $\phi_{2,2}$ and the SFBC in [8] marked by $*$ for a MIMO-OFDM system with $N_t = 2$, $N_r = 2$, $F = 512$, $P = 4$ and $\delta = 128$ in COST207 typical urban scenario.

It is shown in Figure 4.8 that with the decrease of transmission rate, the coding gain lowerbound $\check{\xi}$ is increased and consequently the BER performance is better. The SNR gain is roughly 1dB for each decrease of transmission rate. Hence the coding matrix (4.40) shows a flexible structure so that targeted BER performance can be achieved by smoothly reducing the transmission rate. Moreover, in Figure 4.8 the multirate SFBC is also compared with the rate one SFBC in [8] with QPSK and 16QAM constellation. The SFBC in [8] with 16QAM is compared with multirate SFBC with $R = 2$ since both SFBCs have the same spectral efficiency of 4bps/Hz. It is shown that the multirate SFBC with $R = 2$ has about 4 dB gain. On the other hand the SFBC in [8] with QPSK is compared with multirate SFBC with $R = 1$ since both SFBCs have same spectral efficiency of 2bps/Hz. It is shown that the multirate SFBC with $R = 1$ has about 0.2dB gain of BER performance. Hence the multirate MRP achieves a better spectral efficiency and a smoother balance between the transmission rate and BER performance.

4.8 Summary

The rate one MRP and the multirate MRP are proposed for MIMO-OFDM systems in this chapter. Their characteristics can be summarized as following:

- The SFBC proposed in this chapter can easily and logically be extended into a

STFBC if temporal diversity needs to be achieved, and if the application is not sensitive to the delay. The only difference is that the matrix Θ needs to be extended across temporal domain as well, e.g. the STFBC proposed [31]. However this kind of extension is not worthwhile. The channel frequency response of all symbol periods need to be known by the receivers resulting in a longer delay. The time-invariant channel PDP needs to be known by the transmitters at the same time. All these assumptions increase the system complexity significantly, with the only advantage of higher diversity order. Hence the value in this respective is questionable.

- The knowledge of channel PDP required by the transmit side can be realized by the uplink transmission, or by data feedback. Moreover, such knowledge is also valuable to help the system making decisions, e.g. which codes should be loaded, the size of subsystem for each user, or subcarrier allocation strategy, etc. However in order to achieve such knowledge the propagation scenario should also have relatively stable surrounding scatterers, e.g. indoor propagation, so that the second order characteristics would not be changed rapidly.

- The rate one MRP and the multirate MRP with the channel PDP are capable of achieving full transmit diversity always for an arbitrary number of transmitters, subcarrier grouping and subcarrier interval. They have more design freedom and do not require a complicated subcarrier grouping strategy. The subcarriers in the subsystem are simply uniformly separated as far as possible.

- The proposed MRP demonstrates the feasibility of the SFBC design even if the transmitters do not have full channel PDP, or if the channel PDP is dominated by a limited number of delays. Consequently it can reduce the complexity of system feedback and the design of pilot sequences. The partial frequency diversity order can be captured whilst full transmit diversity can be guaranteed.

- The proposed MRP can overcome the potential loss of diversity order for specific channel PDP, and improve the system performance always independent of the configuration of subsystem.

- The proposed rate one MRP has a relatively simple optimization process, which can be visualized and solved instinctively for some cases. The visualization can provide a better and explicit observation for each SFBC, so that advantages and disadvantages can be found more easily. Moreover the optimal rotation angles may be calculated in real-time for each MIMO-OFDM subsystem and each user, since direct solutions may be available.

- The multirate MRP has a relatively complex optimization process. However the multirate MRP has better spectral efficiency when the transmission rate is greater than one. Hence the performance will be improved if same bit transmission rate is assumed. The complexity of optimization can be minimized by pre-calculation. The multirate MRP only takes advantage of limited information above channel PDP, so a dedicated decision table of optimization results can be generated and stored.

- The rate-one MRP and the multirate MRP are particulary suitable for a scenario which has a limited number of dominant paths, for example relatively close to transmitter, microcell and indoor coverage. The goal of both proposed strategies is to design an optimal or suboptimal coding method in order to maximize achievable diversity gain and coding gain by utilizing already known channel information. However if the propagation scenario is complex and has a large number of propagation paths with even power, e.g. for cell edge users, the rate-one MRP and the multirate MRP might not be a good strategy. Although they are still applicable, the performance gain would be relatively marginal, compared to increased system complexity.

The potential research directions or questions emanating from the material in this chapter are:

- The stability of SFBCs within different types of wireless propagation scenarios, e.g. urban macro, suburban macro, or indoor is rarely touched. Previous analysis has shown that the diversity might be lost for specific scenarios, but not always. Hence it is necessary to observe the severity of this problem, and also compare the performance in different wireless channel models.

- All existing SFBCs have an assumption of uncorrelated AoA and AoD, so that a concise structure can be used in the design process. However, generally the indoor propagation has strong LoS so that the AoA and AoD is correlated. Hence the next potential step is to develop a suitable design structure for this case. The MRP may be further developed.

- The MRP only considers the rotation angles $\phi_{2,m}$. Allocated power for each subcarrier and each transmitter can be modified according to the eigenvalues of correlation matrices to improve performance with the same total transmission power. Hence a more generalized optimization process can be developed, including MRP and adaptive power adjustment.

- The channel PDP or partial PDP is assumed to be known at the transmit side. However it might be difficult to satisfy this condition for some cases. Hence it is feasible to assume that the transmitters have a knowledge of the instant snapshot of a channel rather than the second order characteristics, such as channel frequency response for each symbol period. The MRP design can be adjusted according to this assumption. However the issue of diversity order can not be clarified at present. The first step in clarification could be made from comparisons made by simulations with different channel assumptions.

4.9 Conclusions

A rate one matched rotation precoding and a multirate matched rotation precoding are proposed for MIMO-OFDM systems. Both MRPs are capable of achieving full transmit diversity for an arbitrary number of transmit antennas, subcarrier grouping and subcarrier interval. Moreover, the proposed rate one MRP and multirate MRP demonstrate the feasibility of the SFBC design, even if the transmit antennas do not have full knowledge of channel PDP, or if the channel PDP is dominated by a limited number of delays. Both of SFBCs have more design freedom, mitigate the requirement upon subcarrier interval and subcarrier grouping, and also overcome the potential loss of diversity for specific propagation channels. The proposed rate one MRP has a relatively simple optimization process, which can be visualized, while the proposed multirate MRP has better spectral efficiency and provides a relatively smooth balance between system performance and transmission rate. We will extend the space-time design into another dimension by exploiting the frequency domain to create flexible space-time-frequency codes in the next chapter.

Chapter 5

Space-Time-Frequency Block Codes

In this chapter we will extend concepts of space-time block codes and space-frequency block codes into all three space, time and frequency domains. A multirate STFBC with full transmit diversity for a variety of transmission rates (code rates) is presented. It provides a relatively smooth tradeoff between the performance and the transmission rate. The multirate STFBC is suitable and useful for a system which needs to provide a stable quality of service (QoS) to users under time-varying channel conditions. The concept of multirate can, therefore, provide an alternative strategy to precisely adjust achievable performance from feedback information. Varying constellation size is not an optimal solution and has less granularity. The multirate STFBC can also be used to design multirate STBCs. The proposed multirate STFBC can achieve relatively smooth balance between the performance and the transmission rate for a given constellation size. Design of a STBC is presented as a special case of the proposed multirate STFBC, which performs better than some of the existing STBCs, with the added benefit of more flexibility. Moreover, optimized multirate STFBCs have also been compared with some of the existing STFBCs. Simulation results show that the design parameter gives sufficient flexibility to achieve improved performance with reduced computational complexity.

5.1 Introduction

The SFBC, as discussed in Chapter 4, is capable of achieving full spatial and frequency diversity and providing high throughput in a MIMO-OFDM system. On the other hand all space-time-frequency (STF) domains can be utilized for the data transmission by STFBC. STFBC can achieve diversity order higher than that of SFBC and STBC, with a proper code design. Moreover, the use of more domains demonstrates more design flexibility, but as a consequence the coding and decoding will be more complex.

It was shown in the previous chapter that the SFBC has the drawback of diversity loss for specific propagation scenarios, and also requires a large number of subcar-

riers in a MIMO-OFDM subsystem if full frequency diversity needs to be achieved. The estimation process of the channel power delay profile (PDP) will significantly increase the system complexity, and the system performance can not be determined without the knowledge of channel PDP. Generally, if the transmission power of signals is spread across more propagation paths, the optimization process for a SFBC has a lesser contribution towards the improvement of system performance. The proposed STFBC is capable of relieving the requirement of channel PDP knowledge at the transmitters, reducing the required number of subcarriers, and exploiting all potential STF diversities.

There is a distinct difference between SFBCs discussed in the pervious chapter and STFBCs discussed in this chapter. The SFBC usually does not have coherent subchannels (or static subchannels) in a MIMO-OFDM subsystem, but the STFBC discussion here has static subchannels across the temporal domain, or frequency domain, or both domains by domain switching. For simplicity, it is assumed that the channel frequency response coefficient remains static within several adjacent symbol periods. Therefore the temporal diversity can not be achieved. The SF domains are capable of providing high diversity order if needed. The achievement of temporal diversity increases the MIMO-OFDM system complexity dramatically, e.g. in the channel parameter estimation, decoding process and feedback process.

The rest of chapter is organized as follows. Existing STFBCs are briefly summarized in Section 5.2. An overview of the MIMO-OFDM channel is presented in Section 5.3. Section 5.4 describes the proposed multirate STFBC coding scheme. Simulations results and the performance comparisons with existing codes are presented in Section 5.5. Section 5.6 concludes that the proposed STFBC performs better than some of the existing STBCs, and adaptively changes the rate depending on the quality of service (QoS) requirements. Potential research directions and problems are also proposed in this section.

5.2 Brief survey of Space-Time-Frequency Block Codes

There are plenty of publications on space-time block coding (STBC) in the open literature [5–7, 14, 48, 52]. The first ever STBC proposed in [5] can achieve full transmit and receive diversity for a MIMO system with two transmit antennas ($N_t = 2$) and multiple receivers. The quasi-orthogonal coding for MIMO system with more than two transmit antennas is proposed in [48]. A rate one STBC for arbitrary number of transmit antennas is derived in [6]. High rate (up to N_t) full diversity STBC can improve the spectral efficiency further [7, 14, 52].

Traditionally, a static channel for several adjacent time periods is assumed in de-

signing a STBC. However considering the relatively long OFDM symbol duration, the STFBCs in [8–10, 31] are designed assuming non-static channels between OFDM symbols. Under this assumption, the similarity of the temporal and frequency domains shows that the space-frequency block coding (SFBC) can be easily extended to the STFBC. These STFBCs/SFBCs with the assumption of non-static symbol periods require OFDM symbols with a large number of subcarriers. This is a major characteristics of such STFBCs/SFBCs. The number of subcarriers has to be greater than $N_t(L+1)$ to achieve full transmit diversity above STF domains, where L is the fixed channel order (number of paths). The channel order gives a upper-bound for the rank of the frequency correlation matrix. Hence by employing more than "necessary" subcarriers, full spatial diversity is achieved. The channel order can be very large ($L+1 = 22$ for scenarios such as NLoS B3 channel in [11]). The order can also be time-varying in real propagation scenarios. A code designed for a fixed channel order would not have stable performance in such channels.

On the other hand, some STFBCs have been proposed in [26, 61, 87] with the assumption of static symbol periods, or the use of adjacent subcarriers to replace adjacent symbol periods. For example, the Alamouti code [5] is proposed in LTE system [2]. The major characteristics of these STFBCs and traditional STBCs is the requirement of static channel coefficients to achieve full spatial diversity. Non-static adjacent symbol periods or subcarriers will degrade system performance at relatively low SNR range. The use of more highly correlated adjacent symbol periods or subcarriers would move this degradation into a higher SNR region.

5.3 MIMO-OFDM System Modelling

Consider a MIMO-OFDM system with N_t transmitters, N_r receivers, F subcarriers and K symbol periods ($K \geq N_t$). The frequency selective channel is assumed to be static for consecutive K OFDM symbol periods. Each transmit and receive pair has $L+1$ resolvable delay paths with the same PDP. A block of data symbols transmitted over each transmitter passes through an F point IFFT during each symbol period. A cyclic prefix (CP) is appended. The length of CP is chosen to be long enough to remove the ISI. At each receiver, the CP is removed and then a FFT is applied. Hence the frequency selective MIMO channel is decoupled into F parallel flat fading channels.

A MIMO-OFDM system is partitioned into $\delta = \lfloor F/P \rfloor$ MIMO-OFDM subsystems at first in order to reduce the system complexity where P is the number of subcarriers in the MIMO-OFDM subsystem. Hence each subsystem contains P subcarriers, where $P \leq L+1$, N_t transmitters, N_r receivers, and K symbol periods. The subcarriers in the subsystem are well separated so that frequency diversity and frequency correlation

structure can be exploited efficiently. Therefore, full transmit diversity for a MIMO-OFDM system or subsystem is PN_t.

The channel frequency response over the pth subcarrier between the mth transmitter and the nth receiver in the MIMO-OFDM subsystem is given by

$$h_{mn}(f) = \sum_{\ell=0}^{L} \hbar_{mn,\ell} \times e^{-j2\pi((p-1)\delta+1)\tau_\ell/T_s} \tag{5.1}$$

where $m \in [1, \cdots, N_t]$, $n \in [1, \cdots, N_r]$, and $p \in [1, \cdots, P]$. Since the channel frequency response will be static for a period of time, the notation of k for the OFDM symbol period is ignored in the channel frequency response for simplicity. And τ_ℓ and $\hbar_\ell$ are the delay and complex amplitude of the ℓth path between transmitters and receivers respectively. In this chapter we assume that taps τ_ℓ are independent of each other. Moreover, the elements of $\hbar_\ell$ are assumed to be uncorrelated circularly symmetric complex Gaussian random variables with zero mean and variance σ_ℓ^2 given by the PDP of the channel.

Because of the relatively long OFDM symbol period, the wireless propagation channel might not remain static during the whole K consecutive symbol periods. However the similarity between frequency and time domains reveals that consecutive subcarriers can be used to replace part of (or all) consecutive symbol periods if the OFDM system has a large number of subcarriers, eg., 1024 in [88]. For example, K symbol periods can be replaced by K consecutive subcarriers. Then a total of KP subcarriers are required in a MIMO-OFDM subsystem, and are separated into P groups, each of which have K consecutive subcarriers. Alamouti code [5] is proposed to be deployed in the LTE system [2] so that a STBC is converted into a SFBC safely and efficiently. Such domain switching also gives rise to high robustness to user mobility. The system performance degrades at relatively high SNR. Hence the effect of implementation of frequency-time domain switching is closely related to channel correlation structure and the targeted performance.

5.4 Multirate STFBC coding scheme

The effect of subcarrier grouping described in [26, 64] is highly related to the channel frequency correlation which is also discussed in Chapter 2. The multirate STFBC is proposed in this section to optimize the system performance with the full transmit diversity and an adaptive transmission rate.

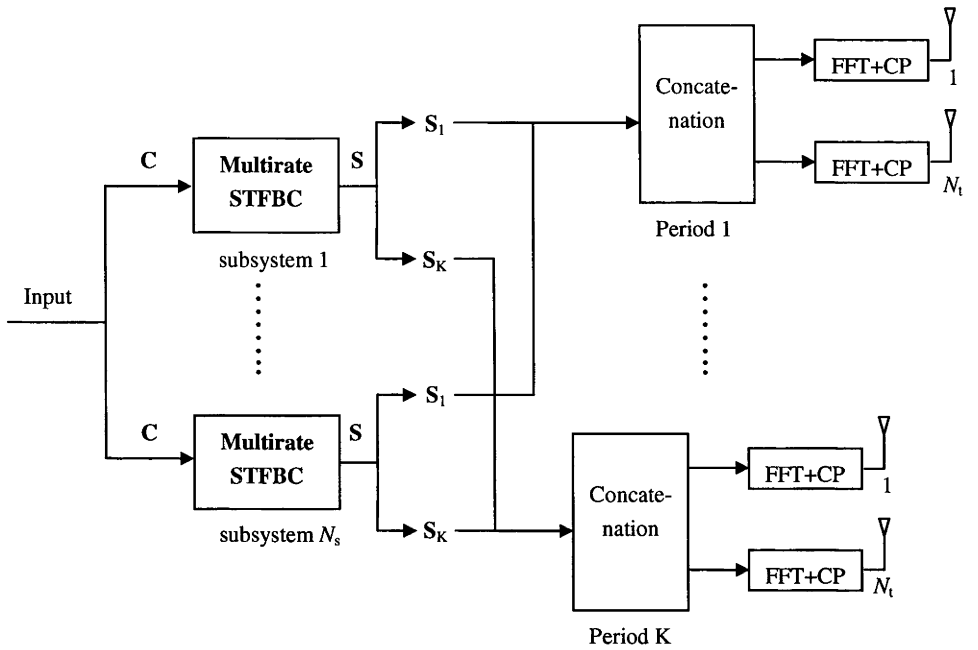

Figure 5.1: Multirate STFBC processing scheme for a MIMO-OFDM system

5.4.1 Coding Process

A multirate STFBC with transmission rate R is given by:

$$\begin{aligned} s_k^q &= \mathbf{C}\Theta_{Ak,R}^q + \mathbf{C}^*\Theta_{Bk,R}^q; \\ \mathbf{S}_k &= \mathbf{C}\Theta_{Ak,R} + \mathbf{C}^*\Theta_{Bk,R}; \\ \mathbf{S} &= \mathbf{C}\Theta_{A,R} + \mathbf{C}^*\Theta_{B,R}; \end{aligned} \tag{5.2}$$

where the codeword $\mathbf{C} = [c_1, \cdots, c_Q]$ is a $1 \times Q$ vector where $c_1, \cdots, c_Q$ are complex scalars chosen from a particularly r-PSK or r-QAM constellation $\mathcal{A}$, $Q = RPK$. Every pair of $\Theta_{Ak,R}$ and $\Theta_{Bk,R}$ are $Q \times N_tP$ complex coding matrices to be specified later. $\Theta_{Ak,R}^q$ and $\Theta_{Bk,R}^q$, where $q \in [1, \cdots, N_tP]$, are the qth column vectors of $\Theta_{Ak,R}$ and $\Theta_{Bk,R}$ respectively. $\Theta_{A,R} = [\Theta_{A1,R}, \cdots, \Theta_{AK,R}]$ and $\Theta_{B,R} = [\Theta_{B1,R}, \cdots, \Theta_{BK,R}]$ are $Q \times N_tPK$ matrices. Also $\mathbf{S} = [\mathbf{S}_1, \cdots, \mathbf{S}_k, \cdots, \mathbf{S}_K]$ is a $1 \times N_tPK$ matrix with $k \in [1, \cdots, K]$.

Equation (5.2) shows that the codeword $\mathbf{C}$ is precoded by both $\Theta_{A,R}$ and $\Theta_{B,R}$ matrices and dispersed from Q dimensional to N_tPK dimensional transmission data. Each $\mathbf{S}_k$ is transmitted by P subcarriers and N_t transmitters at the kth symbol period. The same codeword $\mathbf{C}$ is coded K times by K pairs of coding matrices $\Theta_{Ak,R}$ and $\Theta_{Bk,R}$. Therefore a transmission block coding scheme is specifically determined by a set of pairs of coding matrices $\Theta_{Ak,R}$ and $\Theta_{Bk,R}$, or a pair of $\Theta_{A,R}$ and $\Theta_{B,R}$. Symbol

$$\Lambda = \mathbf{R}_{MS} \otimes \begin{bmatrix} \Delta\tilde{\mathbf{S}}_1 (\mathbf{R}_F \otimes \mathbf{R}_{BS}) \Delta\tilde{\mathbf{S}}_1^\dagger & \cdots & \Delta\tilde{\mathbf{S}}_1 (\mathbf{R}_F \otimes \mathbf{R}_{BS}) \Delta\tilde{\mathbf{S}}_K^\dagger \\ \vdots & \vdots & \vdots \\ \Delta\tilde{\mathbf{S}}_K (\mathbf{R}_F \otimes \mathbf{R}_{BS}) \Delta\tilde{\mathbf{S}}_1^\dagger & \cdots & \Delta\tilde{\mathbf{S}}_K (\mathbf{R}_F \otimes \mathbf{R}_{BS}) \Delta\tilde{\mathbf{S}}_K^\dagger \end{bmatrix} \tag{5.5}$$

transmission rate is denoted as $R = Q/(PK)$. The value of integer Q can be chosen from 1 to $N_t PK$ so that the symbol transmission rate R can be varied from $1/(PK)$ up to N_t. The proposed multirate STFBC processing scheme for a MIMO-OFDM system is shown in Figure 5.1.

Assuming that both the real parts and the imaginary parts of $c_1, \cdots, c_Q$ have a variance of $1/2$ and are uncorrelated, we have $\mathbb{E}[c_i c_i^*] = 1$ and $\mathbb{E}[c_i^2] = 0$ where $i \in [1, \cdots, Q]$, and $\mathbb{E}[\cdot]$ is the mathematical expectation. The transmitted symbol matrix $\mathbf{S}$ is normalized such that $\mathbb{E}[\mathbf{S}\mathbf{S}^\dagger] = N_t PK$. This leads to the normalization for the proposed multirate STFBC given by:

$$\begin{aligned} &\text{trace}\left(\Theta_{A,R}\Theta_{A,R}^\dagger + \Theta_{B,R}\Theta_{B,R}^\dagger\right) \\ &= \sum_{k=1}^{K} \text{trace}\left(\Theta_{Ak,R}\Theta_{Ak,R}^\dagger + \Theta_{Bk,R}\Theta_{Bk,R}^\dagger\right) = N_t PK. \end{aligned} \tag{5.3}$$

5.4.2 Coding Gain

Suppose that the transmitted codeword $\mathbf{C}$ is decoded as $\tilde{\mathbf{C}}$ at the receivers with the codeword error $\Delta\mathbf{C} = \mathbf{C} - \tilde{\mathbf{C}}$, then the errors in the transmitted symbols invoked by the codeword error $\Delta\mathbf{C}$ is given by:

$$\begin{aligned} \Delta s_k^q &= \Delta\mathbf{C}\Theta_{Ak,R}^q + \Delta\mathbf{C}^*\Theta_{Bk,R}^q; \\ \Delta\mathbf{S}_k &= \Delta\mathbf{C}\Theta_{Ak,R} + \Delta\mathbf{C}^*\Theta_{Bk,R}; \\ \Delta\mathbf{S} &= \Delta\mathbf{C}\Theta_{A,R} + \Delta\mathbf{C}^*\Theta_{B,R}; \end{aligned} \tag{5.4}$$

where $\Delta\mathbf{S} = [\Delta\mathbf{S}_1, \cdots, \Delta\mathbf{S}_K]$.

The averaged pairwise error probability (PEP) between $\mathbf{C}$ and $\tilde{\mathbf{C}}$ over all channel realizations can be upper bounded [29], and determined by the eigenvalues of the covariance matrix Λ given by (5.5) where $\Delta\tilde{\mathbf{S}}_k = (\mathbf{I}_P \otimes \mathbf{1}_{1\times N_t}) \circ (\mathbf{1}_{P\times 1} \otimes \Delta\mathbf{S}_k)$. For details of the covariance matrix Λ of the MIMO-OFDM subsystem with arbitrary space-time-frequency correlation structure refer to Chapter 2. And if $K = 1$, the covariance matrix Λ given by (5.5) can be simplified to (4.9) and the STFBC has no difference with the SFBC discussed in Chapter 4.

The effect of subcarrier grouping described in [26,64] is highly related to the chan-

nel frequency correlation. Since $P \leq L+1$, frequency correlation matrix $\mathbf{R}_F$, transmitter spatial correlation matrix $\mathbf{R}_{BS}$ and receiver spatial correlation matrix $\mathbf{R}_{MS}$ for the MIMO-OFDM subsystem are assumed to be identity matrices. The frequency correlation matrix can not be assumed to be an identity matrix if $P > L+1$. Such assumptions will not jeopardize the design process of the STFBC. Hence the covariance matrix $\mathbf{\Lambda}$ in (5.5) is simplified as

$$\mathbf{\Lambda} = \mathbf{I}_{N_r} \otimes \begin{bmatrix} \Delta\tilde{\mathbf{S}}_1 \Delta\tilde{\mathbf{S}}_1^\dagger & \cdots & \Delta\tilde{\mathbf{S}}_1 \Delta\tilde{\mathbf{S}}_K^\dagger \\ \vdots & \vdots & \vdots \\ \Delta\tilde{\mathbf{S}}_K \Delta\tilde{\mathbf{S}}_1^\dagger & \cdots & \Delta\tilde{\mathbf{S}}_K \Delta\tilde{\mathbf{S}}_K^\dagger \end{bmatrix} \tag{5.6}$$

The coding gain ζ is further defined as

$$\zeta = \arg \min_{\Delta\mathbf{C} \neq \Delta\tilde{\mathbf{C}}} \det(\mathbf{\Lambda})^{\frac{1}{N_r N_t P K}}. \tag{5.7}$$

If $P = 1$, $\Delta\tilde{\mathbf{S}}_k = \Delta\mathbf{S}_k$. Then the MIMO-OFDM subsystem is converted into a MIMO system with a single subcarrier. Thus the coding gain of the MIMO-OFDM subsystem is simplified and determined by the specific STBC coding strategy.

5.4.3 Coding Design

Previous discussion shows the primary mission of the multirate STFBC design is to find the pair of coding matrices $\mathbf{\Theta}_{A,R}$ and $\mathbf{\Theta}_{B,R}$ in (5.2) for a given constellation and transmission rate R. Full transmit diversity $N_t P$ is guaranteed always. Moreover, the coding gain ζ in (5.7) should be maximized by the coding matrices for every transmission rate.

When the MIMO-OFDM subsystem achieves the highest transmission rate N_t, $Q = N_t P K$. In this chapter $\mathbf{\Theta}_{B,N_t}$ is assumed to be zero for simplicity. $\mathbf{\Theta}_{A,N_t}$ is a unitary square matrix satisfying the power constraint condition of (5.3) and designed as following

$$\mathbf{\Theta}_{A,N_t} = \mathbf{V}_{Q\times Q}\mathbf{D} \tag{5.8}$$

where $\mathbf{V}_{Q\times Q}$ is a $Q \times Q$ Vandermonde matrix given by

$$\begin{aligned} \mathbf{V}_{Q\times Q} &= [\mathbf{V}^1_{Q\times Q}, \cdots, \mathbf{V}^i_{Q\times Q}, \cdots, \mathbf{V}^Q_{Q\times Q}] \\ &= \frac{1}{\sqrt{Q}} \begin{bmatrix} 1 & \cdots & 1 & \cdots & 1 \\ \theta_1 & \cdots & \theta_i & \cdots & \theta_Q \\ \vdots & \vdots & \vdots & \vdots & \vdots \\ \theta_1^{Q-1} & \cdots & \theta_i^{Q-1} & \cdots & \theta_Q^{Q-1} \end{bmatrix} \end{aligned} \tag{5.9}$$

where $\mathbf{V}^i_{Q\times Q}$ is the ith column vector of square matrix $\mathbf{V}_{Q\times Q}$ and $i \in [1, \cdots, Q]$. The matrix $\mathbf{D}$ is a $Q \times Q$ diagonal matrix given by

$$\begin{aligned}\mathbf{D} = \text{Diag}(1, e^{j\phi}, \cdots, e^{j\phi \bmod(q+k-2,N_t)}, \cdots, \\ e^{j\phi \bmod(N_tP+k-2,N_t)}, \cdots, e^{j\phi \bmod(N_tP+K-2,N_t)})\end{aligned} \tag{5.10}$$

where $q \in [1, \cdots, N_tP]$, $k \in [1, \cdots, K]$, $\phi \in [-\pi, \pi]$ and $\bmod(a, b)$ gives the remainder on division of a by b.

The coding matrix $\mathbf{\Theta}_{A,N_t}$ constitutes the product of two complex matrices, Vandermonde matrix $\mathbf{V}_{Q\times Q}$ which guarantees full frequency diversity and diagonal matrix $\mathbf{D}$ which guarantees full spatial diversity. The design of matrix $\mathbf{V}_{Q\times Q}$ has been discussed in [6, 64] for an OFDM system or a MIMO system. The Vandermonde matrix specifications in [6] are used in this paper. Moreover, the coding gain ζ is optimized by the parameter ϕ of the diagonal matrix $\mathbf{D}$. For a QAM constellation and $Q = N_tPK = 2^s (s \geq 1)$, the parameters θ_i are given by $\theta_i = e^{j\frac{4i-3}{2Q}\pi}$ where $i \in [1, \cdots, Q]$ [6]. If $Q = N_tPK = 2^s \times 3^t (s \geq 1, t \geq 1)$, the parameters θ_i are given by $\theta_i = e^{j\frac{6i-5}{3Q}\pi}$. Moreover $\Delta\mathbf{C}\mathbf{V}^i_{Q\times Q} = 0$ only if $\Delta\mathbf{C} = \mathbf{0}_{1\times Q}$ or $\mathbf{C} = \tilde{\mathbf{C}}$.

Remark 1: If $e^{j\phi}$ is an algebraic number of degree greater than $(N_t - 1)N_t$ over $\mathcal{K}$ which is the extension field containing all the entries of $\mathbf{V}_{Q\times Q}$ and the ring of complex integers $\mathbb{Z}(j)$, then full transmit diversity is guaranteed over all QAM constellations. For details of proof refer to Appendix C. Hence it provides the freedom to design a MIMO-OFDM system with full transmit diversity.

When the bit error rate (BER) of the MIMO-OFDM subsystem is worse than designed performance, the transmission rate R can be reduced to achieve better BER performance without decreasing constellation size, or significantly changing the coding structure. Thus $Q = RPK$ and $\mathbf{\Theta}_{A,R}$ is $RPK \times N_tPK$ matrix where $R \leq N_t$. The coding matrix $\mathbf{\Theta}_{A,R}$ for a specific rate R can be obtained by simply truncating first RPK row vectors from the coding matrix $\mathbf{\Theta}_{A,N_t}$ and normalization using (5.3). Hence the matric $\mathbf{\Theta}_{A,R}$ is given by

$$\mathbf{\Theta}_{A,R} = \sqrt{N_t/R}\mathbf{V}_{Q\times N_tPK}\mathbf{D} \tag{5.11}$$

where

$$\mathbf{V}_{Q\times N_tPK} = [\mathbf{V}^1_{Q\times N_tPK}, \cdots, \mathbf{V}^i_{Q\times N_tPK}, \cdots, \mathbf{V}^{N_tPK}_{Q\times N_tPK}]$$

The vector $\mathbf{V}^i_{Q\times N_tPK}$ is the ith column vector ($i \in [1, \cdots, N_tPK]$) of matrix $\mathbf{V}_{Q\times N_tPK}$ which is truncated matrix from $\mathbf{V}_{Q\times Q}$ in (5.9). And $\sqrt{N_t/R}$ is the power normalization factor. The structure of matrix $\mathbf{D}$ is unchanged. However the optimal scalar ϕ_{opt}

for the MIMO-OFDM subsystem can be designed for a specific rate R and symbol constellation $\mathcal{A}$. Furthermore, if Θ_{A,N_t} can guarantee the full transmit diversity at rate N_t, full transmit diversity is still guaranteed at each transmission rate R without the change of ϕ. Hence if Θ_{A,N_t} is specified, a series of transmission rates for the MIMO-OFDM system and corresponding coding matrices $\Theta_{A,R}$ can be obtained by a direct truncation process.

Remark 2: If the coding matrix Θ_{A,N_t} is capable of achieving full transmit diversity in the MIMO-OFDM system with the rate N_t, truncated coding matrix $\Theta_{A,R}$ from Θ_{A,N_t} can guarantee full transmit diversity for the system with a rate R ($R \leq N_t$). The codeword error $\Delta\mathbf{C}$ for the transmission rate R can be obtained by assigning zeros to the last $(N_t - R)PK$ symbols of $\Delta\mathbf{C}$ for the transmission rate N_t. Thus the set of $\Delta\mathbf{C}$ for the rate R actually becomes a subset of the set of $\Delta\mathbf{C}$ for the rate N_t. Therefore, for the lower transmission rate R, the subset of $\Delta\mathbf{C}$ is smaller resulting in a larger coding gain.

5.4.4 Example of the multirate STFBC

Here we show an example of multirate STFBC for the MIMO-OFDM subsystem with two transmitters, two receivers, two subcarriers and two symbol periods. For QPSK, the coding gain ζ is maximized by computer search over ϕ varying from 0 to $\pi/2$. The step size is chosen to be $\pi/256$ so that the algebraic degree meets the condition of *Remark 1.* The optimal ϕ_{opt} are shown in Table 5.1 for a variety of transmission rates R. The scalar ϕ_{opt} is not unique in some cases. The scalar $\phi = 119\pi/256$ gives the largest coding gain for the given MIMO-OFDM system at the highest transmission rate $R = N_t = 2$. The coding matrix $\Theta_{A,R}$ obtained by direct truncation of Θ_{A,N_t} also gives full transmit diversity as mentioned in *Remark 2.* Hence the coding gains corresponding to $\phi = 119\pi/256$ for different rates R are also included in Table 5.1 for the comparison.

When $R = 2$, $Q = N_tKP = 8$. Then coding matrices $\Theta_{Ak,2}$ for $k \in [1,2]$ are given by

$$\begin{aligned}\Theta_{A1,2} &= [\mathbf{V}^1_{8\times 8}, \phi\mathbf{V}^2_{8\times 8}, \phi\mathbf{V}^3_{8\times 8}, \mathbf{V}^4_{8\times 8}] \\ \Theta_{A2,2} &= [\mathbf{V}^5_{8\times 8}, \phi\mathbf{V}^6_{8\times 8}, \phi\mathbf{V}^7_{8\times 8}, \mathbf{V}^8_{8\times 8}]\end{aligned} \tag{5.12}$$

where $\mathbf{V}^i_{8\times 8}$ is the ith column vector of matrix $\mathbf{V}_{8\times 8}$.

When $R = 1$, $Q = RKP = 4$. Then coding matrices $\Theta_{Ak,1}$ for $k \in [1,2]$ are given

R	ϕ_{opt}	$\zeta(\phi = \phi_{opt})$	$\zeta(\phi = 119\pi/256)$
1/4	$\pi/2$	3.1623	3.1623
2/4	$\pi/2$	2	1.9878
3/4	$87\pi/256$	1.1648	0.8868
1	$\pi/2$	0.6436	0.5760
5/4	$121\pi/256$	0.2757	0.2103
6/4	$127\pi/256$	0.2211	0.1752
7/4	$126\pi/256$	0.1290	0.1024
2	$119\pi/256$	0.0896	0.0896

Table 5.1: Transmission rate R vs coding gain ζ for $\phi = \phi_{opt}$, and $\phi = 119\pi/256$ in the MIMO-OFDM system with $N_t = N_r = P = K = 2$ and QPSK.

by

$$\begin{aligned} \Theta_{A1,1} &= \sqrt{2}[\mathbf{V}^1_{4\times 8}, \phi\mathbf{V}^2_{4\times 8}, \phi\mathbf{V}^3_{4\times 8}, \mathbf{V}^4_{4\times 8}] \\ \Theta_{A2,1} &= \sqrt{2}[\mathbf{V}^5_{4\times 8}, \phi\mathbf{V}^6_{4\times 8}, \phi\mathbf{V}^7_{4\times 8}, \mathbf{V}^8_{4\times 8}] \end{aligned} \tag{5.13}$$

where $\mathbf{V}^i_{4\times 8}$ is the ith column vector of matrix $\mathbf{V}_{4\times 8}$ which is constituted by truncating first four row vectors from the matrix $\mathbf{V}_{8\times 8}$. And $\sqrt{2}$ is the normalization factor due to truncation.

5.5 Simulations and comparisons

In this section, BER performance of a MIMO-OFDM system with two transmitters, two receivers and 512 subcarriers is investigated through computer simulations. The random channel is assumed to be a multipath channel with a uniform delay profile composed of $L+1$ independently identically distributed complex Gaussian paths with zero mean and equal variance of $1/(L+1)$. We choose $L = 3$ and $P = 2$. Subcarriers for each MIMO-OFDM subsystem are well-separated. The second order characteristics of such an MIMO-OFDM subsystem is presented in [24] and Chapter 2. All STFBCs/STBCs are unified at first, and for details about decoding process refer to Chapter 6. The same sphere decoding is used at the receiver [86,89].

If $P = 1$, the MIMO-OFDM subsystem is actually a narrowband MIMO system. Hence a STBC is a special case of STFBC. The coding matrix (5.8) for the STFBC can be used to design a STBC and then compared with other STBCs in [7,52], which also can be unified into the same structure of (5.2). These STBCs have the same transmission rate of two. The scalar ϕ in the coding matrix (5.8) for the STBC is optimized for the 2×2 MIMO system. It gives $\phi_{opt} = 73\pi/256$ if a QPSK constellation is employed and

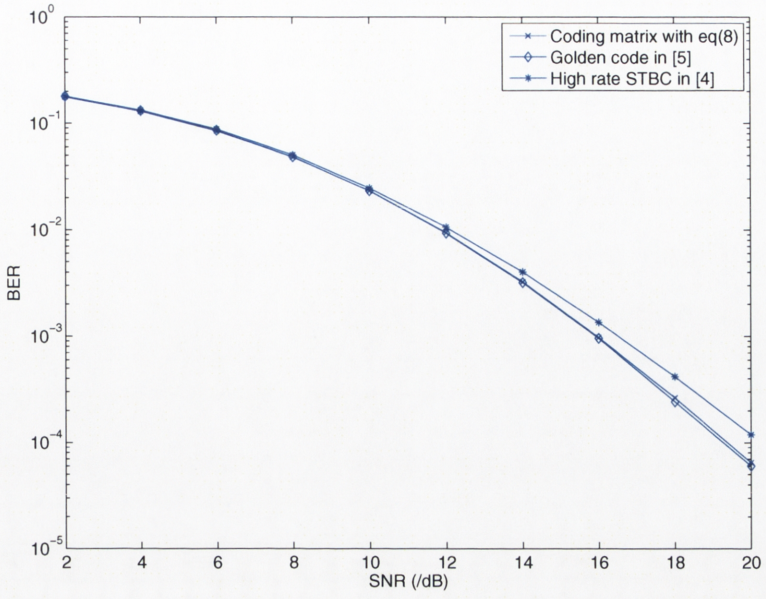

Figure 5.2: Comparisons of BER performance of the coding matrix (5.8), the golden code [7] and high rate STBC [52] for a MIMO-OFDM system where $N_t = N_r = K = 2$ and $P = 1$ and QPSK

correspondingly a coding gain $\zeta = 0.8203$. For comparison, the golden code in [7] and high rate STBC in [52] give a coding gain $\zeta = 0.9457$ and $\zeta = 0.6883$ respectively. The coding gain defined in this paper is slightly different to [7,52]. Simulations for these STBCs in the MIMO-OFDM system are shown in Figure 5.2 where frequency diversity is not achieved since $P = 1$. It is shown that the STBC with the coding matrix (5.8) has performance very close to the golden code in [7] (about 0.1dB difference), but better performance than high rate STBC in [52] (about 0.8dB difference). Simulations confirm that the coding matrix (5.8) can achieve relatively large coding gain and good performance compared with some existing STBCs known to have good performance.

The multirate STFBC following the coding matrix (5.11) is investigated in Figure 5.3 for the MIMO-OFDM system with $N_t = N_r = P = K = 2$ and QPSK constellation. The scalar $\phi = \phi_{opt}$ is specified in Table 5.1 for a variety of transmission rates R. It is shown that with the decrease of transmission rate, the coding gain is increased and consequently the BER performance is better. And similar slopes of plots in Figure 5.3 indicate similar diversity gains which have been achieved by all transmission rates. The SNR gain is roughly 1.5dB for each decrease of transmission rate. Hence the coding matrix (5.11) shows a flexible structure such that targeted BER performance can be achieved by smoothly reducing the transmission rate. Moreover, in Figure 5.3 the multirate STFBC is also compared with the rate one STFBC in [26] with QPSK and 16QAM constellation. The STFBC in [26] with 16QAM is compared with the multirate

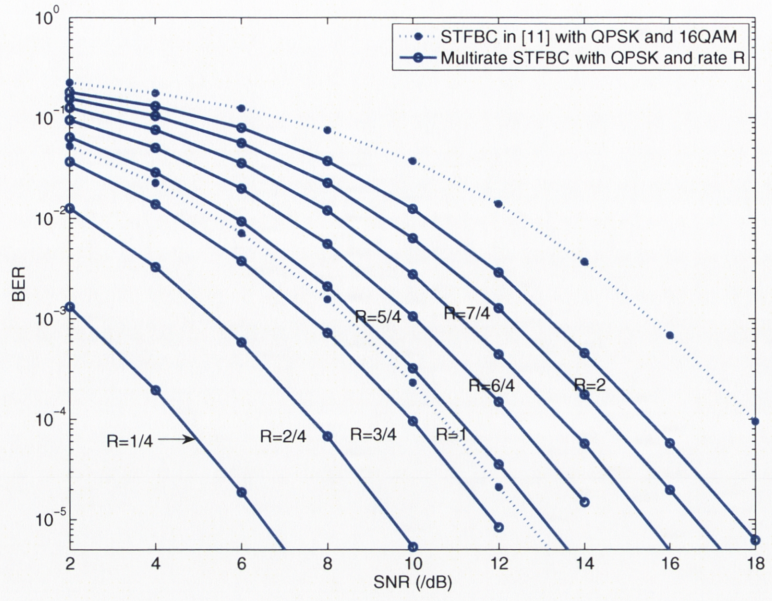

Figure 5.3: Simulations of multirate STFBC with $\phi = \phi_{opt}$ and STFBC in [26] for the MIMO-OFDM system where $N_t = N_r = K = P = 2$

STFBC with $R = 2$ since both STFBCs have same spectral efficiency of 4 bit/s/Hz. It is shown that the multirate STFBC with $R = 2$ has about 2.5dB gain. On the other hand, the STFBC in [26] with QPSK is compared with the multirate STFBC with $R = 1$ since both STFBCs have same spectral efficiency of 2 bit/s/Hz. It is shown that the multirate STFBC with $R = 1$ has about 0.3dB loss of BER performance because the efficient rate one Alamouti code is embedded in the STFBC [26]. However the change of constellation size from QPSK to 16QAM for the STFBC [26] leads to a significant degradation of system performance. Hence the multirate STFBC can achieve a smoother balance between the transmission rate and BER performance.

The effect of the scalar ϕ on the coding gain ζ is shown in Figure 5.4. The coding gain in (5.7) for the MIMO-OFDM subsystem is calculated for a QPSK constellation. The multirate STFBC with $R = 1$ gives larger and smoother coding gain than the multirate STFBC with $R = 2$ because of lower transmission rate. Simulations show that the full transmit diversity of the MIMO-OFDM system is achieved for every scalar ϕ. Hence with the increase of algebraic degree of ϕ, the full diversity is easily achieved in the MIMO-OFDM system. Both lines in Figure 5.4 show repeated deep troughs in the coding gain. The oscillations between deep troughs are relatively small. Hence in general the BER performance is not significantly sensitive to the scalar ϕ for a ranges of values between these troughs. Therefore some particular and easily calculated values, eg. $\phi = \pi/2$ and $e^{j\phi} = j$, can be chosen without seriously degrading the system performance.

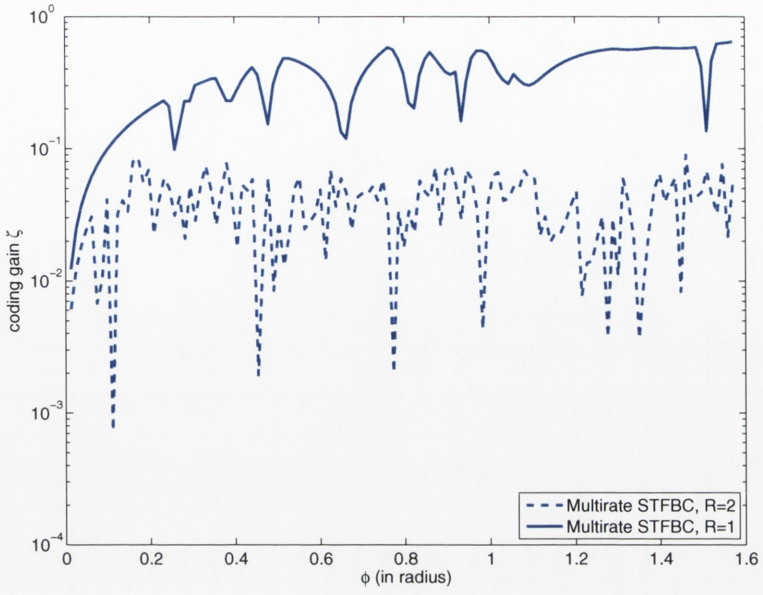

Figure 5.4: Coding gain ζ vs the scalar ϕ with QPSK for the MIMO-OFDM system where $N_t = N_r = K = P = 2$

5.6 Summary

Characteristics of the multirate STFBC proposed for the MIMO-OFDM system in this chapter is summarized below:

- The presented design of a multirate STFBC scheme can achieve full transmit diversity at an arbitrary transmission rate. A variety of rate adaptive coding matrices are obtained by a simple truncation of the coding matrix, $\mathbf{\Theta}_{A,N_t}$, or by parameter optimization for coding matrices for a given transmission rate and constellation.

- Since all STBCs are only special applications of the proposed multirate STFBC, the coding equation (5.2) is a generalized version of STBC/SFBC/STFBC. Therefore the structure of the STFBC can be used to design STBCs, which show a close or better performance than some of the existing STBCs. It also means that it can be used to design a high rate STBC with an arbitrary number of transmitters and have optimal or close-to-optimal performance without a significant structure change of the code. It appears that the golden codes are optimal for a two by two MIMO system but they are hard to extend into a MIMO system with more than two transmitters [14].

- The proposed multirate STFBC can achieve relatively smooth balance between the transmission rate (or the code rate) and the performance without the need to

change constellation size. It has a relatively smooth coding gain for small variations in the design parameter. This gives the flexibility to select certain special values at, or close to, the optimum design parameter to reduce the computation complexity without significant sacrifice of the performance.

The potential research directions or questions are:

- The coding matrix, Θ_{B,N_t}, is assumed to be zero in this chapter for simplicity. However there is no doubt that if it is properly designed, it can improve BER performance further. The matrix Θ_{B,N_t} can disperse the conjugate of the codeword into all subchannels. The matrix Θ_{A,N_t} only manipulates the original codeword. However designing matrix Θ_{B,N_t} is difficult for a MIMO system with more than two transmitters (considering the STBC as a special application of STFBC), and will be more difficult for a MIMO-OFDM system with multiple subcarriers. There is no clear design method yet, but it is definitely worth exploring further. It is still an open question of how to balance the system complexity with the potential performance gain.

5.7 Conclusions

This chapter presents a novel multi-rate Space-Time-Frequency code design for MIMO-OFDM systems. A variety of rate adaptive coding matrices are obtained by a simple truncation of the coding matrix or by parameter optimization for coding matrices for a given transmission rate and constellation. The structure of the STFBC is also used to design STBCs, which show a close or better performance than some of the existing STBCs. The proposed multirate STFBC can achieve relatively smooth balance between the transmission rate and the performance without the need to change constellation size. It has a relatively smooth coding gain for small variations in the design parameter giving us the flexibility to select certain special values close to the optimum design parameter to reduce the computation complexity without sacrificing the performance significantly. A novel low-complexity decoding schemes for MIMO-OFDM systems will be discussed in the next chapter.

Chapter 6

Simplified Decoding for MIMO-OFDM Systems

Coding processes of the MIMO-OFDM system which are designed for optimizing the diversity gain and coding gain were discussed in previous chapters. The default decoding process of these STBC/SFBC/STFBC codes is the maximum-likelihood decoding or the sphere decoding. Such decoding methods are prohibited in most practical communication systems because of high complexity and time delay. Hence in this chapter the decoding process of the MIMO-OFDM system is further analyzed. Decoding strategies to achieve a trade-off between the system performance and complexity is developed for MIMO-OFDM systems and MIMO systems. A novel decoding scheme called "compensation decoding" which is at least twice as fast as the sphere decoding is presented.

6.1 Introduction

The optimal detection schemes such as maximum-likelihood decoding (MLD) of signals demands computational resources that are beyond the capabilities of most practical systems. The performance of the sphere decoding (SD) approaches the MLD performance with a reduced complexity. Alternatively the zero-forcing decoding and MMSE has the lowest lower decoding complexity but has the worst performance, compared to MLD and SD. Hence in this chapter we investigate strategies to trade-off between system performance and complexity, so that the performance can be improved with the help of extra information or a special design process, but without a significant increase in decoding complexity.

Firstly, a unified decoding process of STFBC/STBC/SFBC is proposed for a fair comparison. Moreover, the proposed unified decoding process also provides an intrinsic observation of each code and the theoretic basis for further reduction of decod-

ing complexity.

Secondly, a novel compensation decoding (CD) scheme for a given space-time-frequency linear block code is presented, exploiting the simplicity of zero forcing equalization, and special characteristics of the precoding matrix. The proposed decoding procedure is relatively simple and straightforward in comparison to maximum likelihood decoding and sphere decoding. The bit-error-rate performance of the proposed scheme is better than zero forcing decoding, and close to MLD and SD for a low to medium signal-to-noise ratio range. Both MLD and SD are impractical for mobile network considering extremely limited battery life of user equipment. So ZFD and similar decoding strategies are common used, e.g. LTE [2]. Proposed CD can provide much better performance than ZFD whilst remaining similar decoding complexity.

Finally, a low complexity detection scheme, classifier based decoding (CBD), is proposed for MIMO systems incorporating spatial multiplexing. The CBD is a hybrid of an equalizer-based technique and an algorithmic search stage. Based on an error matrix and its probability density functions for different classes of error, a particular search region is selected for the algorithmic stage. As the probability of occurrence of error classes with larger search regions is small, overall complexity of the proposed technique remains low, while providing a significant improvement in error performance. Limitations of CBD arising from the requirement of priori probability of class will restrict the application of CBD to a static environment, e.g. indoor coverage using Femto in LTE [1].

The rest of chapter is organized as follows. Selected decoding processes of MIMO-OFDM system are briefly summarized in Section 6.2. Then a unified decoding process is proposed in Section 6.3 based on the coding strategies discussed in previous chapters. A novel compensation decoding scheme for a given space-time-frequency linear block code is presented in Section 6.4, and a low complexity detection scheme for MIMO systems is presented in Section 6.5. Section 6.6 summarizes this chapter and makes a comparison among the decoding processes to reveal the motivation behind each strategy, and finally potential research directions are proposed.

6.2 Summary of Decoding

In order to achieve full space-time-frequency (STF) diversity of MIMO-OFDM systems, subcarrier grouping or frequency grouping [26,31,64] is usually used to reduce the system complexity and reuse well-developed space-time (ST) coding schemes. Moreover, STF coding schemes proposed in [10,26,31,64,83] are capable of achieving full STF diversities using maximum likelihood decoding (MLD) or sphere decoding (SD) [86,90]. The complexity of SD and MLD increases dramatically as the number of

subcarriers increases. On the other hand, zero forcing decoding (ZFD) [82] has much a simpler decoding procedure at the expense of performance compared with MLD and SD, and alternatively requires redundant subcarriers and a complex matrix inversion. Hence there is a trade-off between system performance and complexity, which we propose to address by a new method that simplifies the decoding procedure into element by element decoding for a slightly modified STF coding scheme as presented in [26].

6.3 Unified Decoding

The STBC discussed in open literature, the SFBCs discussed in Chapter 4 and STFBCs discussed in Chapter 5 have linear precoding processes. They can be summarized in (5.2) and each of them has specialized matrices $\Theta_{A,R}$ and $\Theta_{B,R}$. Hence the decoding process of these codes are unified at first so that simulations of MIMO-OFDM systems can be easily implemented and fairly compared by substituting specific pair of matrices $\Theta_{A,R}$ and $\Theta_{B,R}$ with given transmission rate R and constellation $\mathcal{C}$.

The matrix $\mathbf{H}_D$ is constructed by stacking up P channel frequency response matrices $\mathbf{H}(p)$ in the MIMO-OFDM subsystem diagonally after subcarrier grouping. The decoding process is executed for each individual subsystem. The overall system performance is the averaged performance of all subsystems. The matrix $\mathbf{H}(p)$ is a $N_t \times N_r$ matrix defined in (4.2) for the pth subcarrier in a given MIMO-OFDM subsystem. The matrix $\mathbf{H}_D$ is defined as

$$\mathbf{H}_D = \mathrm{Diag}[\mathbf{H}(1), \cdots, \mathbf{H}(P)]. \tag{6.1}$$

The channel equation for each symbol period is reorganized as

$$\mathbf{Y}_k = \sqrt{\frac{\rho}{N_t}}(\mathbf{C}\Theta_{Ak,R} + \mathbf{C}^*\Theta_{Bk,R})\mathbf{H}_D + \mathbf{Z}_k \tag{6.2}$$

where $k \in [1, \cdots, K]$. $\mathbf{Y}_k$ and $\mathbf{Z}_k$ are the received signal vector and noise vector at P subcarriers during the kth symbol period respectively. The vector $\mathbf{Z}_k$ denotes the additive white complex Gaussian (AWGN) noise with zero mean and unit variance. After some manipulations and combination, we rewrite and merge K channel complex equations into one real equation as following

$$\begin{aligned}&[\mathrm{Re}(\mathbf{Y}_1), \mathrm{Im}(\mathbf{Y}_1), \cdots, \mathrm{Re}(\mathbf{Y}_K), \mathrm{Im}(\mathbf{Y}_K)] \\ &= \sqrt{\frac{\rho}{N_t}}[\mathrm{Re}(\mathbf{C}), \mathrm{Im}(\mathbf{C})][\mathbf{H}_{R1}, \mathbf{H}_{I1}, , \cdots, \mathbf{H}_{RK}, \mathbf{H}_{IK}] + [\mathrm{Re}(\mathbf{Z}), \mathrm{Im}(\mathbf{Z})]\end{aligned} \tag{6.3}$$

where Re and Im are real and imaginary component of a vector respectively,

$$\mathbf{H}_{Rk} = \begin{bmatrix} \mathrm{Re}(\Theta_{Ak,R}) & \mathrm{Re}(\Theta_{Bk,R}) & -\mathrm{Im}(\Theta_{Ak,R}) & -\mathrm{Im}(\Theta_{Bk,R}) \\ -\mathrm{Im}(\Theta_{Ak,R}) & \mathrm{Im}(\Theta_{Bk,R}) & -\mathrm{Re}(\Theta_{Ak,R}) & \mathrm{Re}(\Theta_{Bk,R}) \end{bmatrix} \times \begin{bmatrix} \mathrm{Re}(\mathbf{H}_D) \\ \mathrm{Re}(\mathbf{H}_D) \\ \mathrm{Im}(\mathbf{H}_D) \\ \mathrm{Im}(\mathbf{H}_D) \end{bmatrix}$$

and

$$\mathbf{H}_{Ik} = \begin{bmatrix} \mathrm{Im}(\Theta_{Ak,R}) & \mathrm{Im}(\Theta_{Bk,R}) & \mathrm{Re}(\Theta_{Ak,R}) & \mathrm{Re}(\Theta_{Bk,R}) \\ \mathrm{Re}(\Theta_{Ak,R}) & -\mathrm{Re}(\Theta_{Bk,R}) & -\mathrm{Im}(\Theta_{Ak,R}) & \mathrm{Im}(\Theta_{Bk,R}) \end{bmatrix} \times \begin{bmatrix} \mathrm{Re}(\mathbf{H}_D) \\ \mathrm{Re}(\mathbf{H}_D) \\ \mathrm{Im}(\mathbf{H}_D) \\ \mathrm{Im}(\mathbf{H}_D) \end{bmatrix}.$$

The equation (6.3) gives a unified decoding equation with $2Q$ dimensions and real parameters for a variety of transmission rates R and STBC/SFBC/STFBC. Moreover, to achieve the full transmit and receive diversity performance, the MLD should be used for these codes. Considering high transmission rate R and large value of $Q = RPK$, the SD in [86, 89] is adopted for each code in this thesis to achieve near MLD performance.

The unified decoding does not provide any simplification for the decoding process but rather a unified decoding structure, which can be applied into arbitrary STBC/SFBC/STFBC. The zero-forcing decoding and iterative interference cancelation can be used in the practical implementations because of their high efficiency and simplicity. However they can not achieve full diversity order so that the performance of the code can not be compared fairly. Hence only SD is adopted to compare the performance of the codes presented in previous chapters.

6.4 Compensation Decoding

To address the decoding complexity, a new method of decoding is proposed in this section to achieve a tradeoff between desired performance and affordable complexity.

6.4.1 Channel Modelling and Coding

Here we consider a frequency selective MIMO-OFDM system with $N_t = 2$ transmitters, $N_r \geq 1$ receivers, $F \geq 2$ subcarriers and $K = 2$ symbol periods. The channel is assumed to be quasi-static over two symbol periods. Each pair of transmitter and receiver has $L + 1$ resolvable delay paths. The data sequence over each transmitter first passes through a F-point inverse fast Fourier transform after which a cyclic prefix (CP)

is added. At each receiver, the CP is removed at first and followed by a fast Fourier transform. The length of cyclic prefix is chosen to be long enough (greater than the channel length at least) so that the frequency selective MIMO channel is decoupled into F parallel flat fading MIMO channels between each transmit and receive pair.

It is impractical and inefficient to put all F subcarriers into one precoding scheme. Therefore, subcarrier grouping or frequency grouping is necessary in order to reduce the design and decoding complexity, while preserving most of the diversity and the coding gains. The method of subcarrier grouping has been well researched [26, 31, 64]. The basic principle is that each group consists of several uniformly separated subcarriers from all available subcarriers. Therefore we assume that P subcarriers are employed for the precoding scheme in each group by subcarrier grouping.

Reference [26] has proved that full space-frequency diversity of N_tP and rate one can be achieved if $P \leq (L+1)$ and $N_t = 2$. The popular decoding method, SD, is also suggested in [26]. It has been adopt by many researchers, e.g. [10,26,64] etc. The ZFD is proposed in [82], but it requires redundant subcarriers and matrix inversion in order to deal with subcarrier selection. As a result, decoding complexity is still high and the transmission rate has to be reduced to less than one. In this section we adopt part of the precoding procedure in [26] to develop a simpler, element by element decoding method for the case of two transmitters.

Applying Alamouti coding for space and time domains, we have the following transmission scheme

$$\mathbf{S} = \begin{bmatrix} s_{11} & s_{21} & \cdots & s_{1P} & s_{2P} \\ -s_{21}^* & s_{11}^* & \cdots & -s_{2P}^* & s_{1P}^* \end{bmatrix} \tag{6.4}$$

The first row of $\mathbf{S}$ is transmitted during the first symbol period by two transmitters through P subcarriers. Complex scalars s_{1p} and s_{2p} are symbols transmitted by the first and second transmitters respectively from the pth subcarrier where $p \in [1, \cdots, P]$. Similarly the second row of $\mathbf{S}$ is transmitted during the second symbol period by two transmitters through P subcarriers. However during the second period, $-s_{2p}^*$ and s_{1p}^* are transmitted by the first and second transmitter respectively from the pth subcarrier, where $*$ is the complex conjugate operation.

Therefore the MIMO-OFDM channel equation at the pth subcarrier is given by

$$\begin{cases} \mathbf{Y}_{1p} = \sqrt{\frac{\rho}{2}} \left(s_{1p}\mathbf{H}_{1p} + s_{2p}\mathbf{H}_{2p} \right) + \mathbf{n}_{1p} & ; \\ \mathbf{Y}_{2p} = \sqrt{\frac{\rho}{2}} \left(-s_{2p}^*\mathbf{H}_{1p} + s_{1p}^*\mathbf{H}_{2p} \right) + \mathbf{n}_{2p} & . \end{cases} \tag{6.5}$$

where $\mathbf{Y}_{kp}$ for $k \in [1, \cdots, 2]$ and $p \in [1, \cdots, P]$ is $1 \times N_r$ received signal vector by N_r receivers during the kth symbol period at the pth subcarrier. And $\mathbf{H}_{mp}$ where $m \in [1, \cdots, 2]$ and $p \in [1, \cdots, P]$ is $1 \times N_r$ channel frequency response vector of

wireless propagation from the mth transmitter to N_r receivers at the pth subcarrier. We assume that the channel state information $\mathbf{H}_{mp}$ is perfectly known at receivers, but not at transmitters. The ρ is the average signal-to-noise ratio (SNR) at each receiver with same transmission power, independent of the number of transmitters, receivers and subcarriers. $\mathbf{n}_{kp}$ is $1 \times N_r$ noise vector during the kth symbol period at the pth subcarrier. Each entry of $\mathbf{n}_{kp}$ denotes independent complex additive white Gaussian noise (AWGN) with zero mean and unit variance.

Although, the code presented in (6.4) can achieve space diversity, it can not achieve any frequency diversity without further precoding. The Vandermonde matrix has been proved to have the maximal coding gain and full diversity for precoding across the frequency domain [6,26,64]. However in this section we propose to employ a real matrix $\mathbf{\Phi}$ as proposed in [50] so that the full frequency diversity is still achieved, but the coding gain may not be optimal. The real matrix $\mathbf{\Phi}$ will simplify the following decoding procedure. Hence we have

$$[s_{11}, \cdots, s_{1P}] = \mathbf{C}_1\mathbf{\Phi}, \quad [s_{21}, \cdots, s_{2P}] = \mathbf{C}_2\mathbf{\Phi} \tag{6.6}$$

where $\mathbf{\Phi}$ is $P \times P$ real matrix and $\mathbf{\Phi}_p$ is defined as the pth column vector of $\mathbf{\Phi}$. Each entry of the codeword vectors $\mathbf{C}_1$ and $\mathbf{C}_2$ is a complex scalar chosen from a given constellation $\mathcal{A}$. They are defined as $\mathbf{C}_1 = [c_1, \cdots, c_P]$ and $\mathbf{C}_2 = [c_{P+1}, \cdots, c_{2P}]$ so that symbol transmission rate equals unity for this STF block coding scheme.

The real matrix $\mathbf{\Phi}$ is restricted by:

$$\mathbf{\Phi}\mathbf{\Phi}^T = \mathbf{I}, \quad \mathbf{\Phi}^T\mathbf{\Phi} = \mathbf{I} \tag{6.7}$$

where $(.)^T$ is the transpose operation of a matrix and $\mathbf{I}$ is defined as an identity matrix.

From (6.6) the transmitted symbol s_{kp} for $k \in [1, \cdots, 2]$ and $p \in [1, \cdots, P]$ can be expressed as $s_{kp} = \mathbf{C}_k\mathbf{\Phi}_p$, which is then substituted into (6.5). And after applying a complex conjugate operation (6.5) can be given by

$$\begin{cases} \mathbf{Y}_{1p} = \sqrt{\frac{\rho}{2}}\left(\mathbf{C}_1\mathbf{\Phi}_p\mathbf{H}_{1p} + \mathbf{C}_2\mathbf{\Phi}_p\mathbf{H}_{2p}\right) + \mathbf{n}_{1p} & ; \\ \mathbf{Y}^*_{2p} = \sqrt{\frac{\rho}{2}}\left(-\mathbf{C}_2\mathbf{\Phi}_p\mathbf{H}^*_{1p} + \mathbf{C}_1\mathbf{\Phi}_p\mathbf{H}^*_{2p}\right) + \mathbf{n}^*_{2p} & . \end{cases} \tag{6.8}$$

Combining the above equations for different subcarriers into one equation we

have

$$\begin{bmatrix} \mathbf{Y}_{11} & \mathbf{Y}_{21}^* & \cdots & \mathbf{Y}_{1P} & \mathbf{Y}_{2P}^* \end{bmatrix} = [\mathbf{C}_1, \mathbf{C}_2] \times \begin{bmatrix} \mathbf{\Phi}_1\mathbf{H}_{11} & \mathbf{\Phi}_1\mathbf{H}_{21}^* & \cdots & \mathbf{\Phi}_P\mathbf{H}_{1P} & \mathbf{\Phi}_P\mathbf{H}_{2P}^* \\ \mathbf{\Phi}_1\mathbf{H}_{21} & -\mathbf{\Phi}_1\mathbf{H}_{11}^* & \cdots & \mathbf{\Phi}_P\mathbf{H}_{2P} & -\mathbf{\Phi}_P\mathbf{H}_{1P}^* \end{bmatrix} + \begin{bmatrix} \mathbf{n}_{11} & \mathbf{n}_{21}^* & \cdots & \mathbf{n}_{1P} & \mathbf{n}_{2P}^* \end{bmatrix} \tag{6.9}$$

Redefining (6.9), we have an equivalent channel equation given by following

$$\tilde{\mathbf{Y}} = [\mathbf{C}_1, \mathbf{C}_2]\tilde{\mathbf{H}} + \tilde{\mathbf{N}} \tag{6.10}$$

where

$$\begin{aligned} \tilde{\mathbf{Y}} &= \begin{bmatrix} \mathbf{Y}_{11} & \mathbf{Y}_{21}^* & \cdots & \mathbf{Y}_{1P} & \mathbf{Y}_{2P}^* \end{bmatrix} \\ \tilde{\mathbf{H}} &= \begin{bmatrix} \mathbf{\Phi}_1\mathbf{H}_{11} & \mathbf{\Phi}_1\mathbf{H}_{21}^* & \cdots & \mathbf{\Phi}_P\mathbf{H}_{1P} & \mathbf{\Phi}_P\mathbf{H}_{2P}^* \\ \mathbf{\Phi}_1\mathbf{H}_{21} & -\mathbf{\Phi}_1\mathbf{H}_{11}^* & \cdots & \mathbf{\Phi}_P\mathbf{H}_{2P} & -\mathbf{\Phi}_P\mathbf{H}_{1P}^* \end{bmatrix} \\ \tilde{\mathbf{N}} &= \begin{bmatrix} \mathbf{n}_{11} & \mathbf{n}_{21}^* & \cdots & \mathbf{n}_{1P} & \mathbf{n}_{2P}^* \end{bmatrix} \end{aligned}$$

and $\tilde{\mathbf{N}}$ is complex AWGN.

6.4.2 MIMO-OFDM Decoding

Starting from the channel equation (6.10), we propose a novel decoding scheme, compensation decoding (CD), for this particular STF block coding scheme.

Multiplying both sides of (6.10) by $\tilde{\mathbf{H}}^\dagger$ and using the properties of (6.7), we have

$$\tilde{\mathbf{Y}}\tilde{\mathbf{H}}^\dagger = [\mathbf{C}_1, \mathbf{C}_2] \times \begin{bmatrix} \sum_{p=1}^{P} \left(\mathbf{H}_{1p}\mathbf{H}_{1p}^\dagger + \mathbf{H}_{2p}\mathbf{H}_{2p}^\dagger\right) \mathbf{\Phi}_p\mathbf{\Phi}_p^T, \mathbf{0}_{P\times P} \\ \mathbf{0}_{P\times P}, \sum_{p=1}^{P} \left(\mathbf{H}_{1p}\mathbf{H}_{1p}^\dagger + \mathbf{H}_{2p}\mathbf{H}_{2p}^\dagger\right) \mathbf{\Phi}_p\mathbf{\Phi}_p^T \end{bmatrix} + \tilde{\mathbf{N}}\tilde{\mathbf{H}}^\dagger \tag{6.11}$$

where $(.)^\dagger$ is complex conjugate transpose and $\mathbf{0}_{P\times P}$ is the $P \times P$ dimensional zero matrix. $\mathbf{H}_{1p}\mathbf{H}_{1p}^\dagger + \mathbf{H}_{2p}\mathbf{H}_{2p}^\dagger$ for any $p \in [1, \cdots, P]$ is a scalar and defined as $\tilde{h}_p$. We also define the matrix $\sum_{p=1}^{P} \tilde{h}_p\mathbf{\Phi}_p\mathbf{\Phi}_p^T$ in (6.11) as $\hat{\mathbf{H}}$. Hence $\hat{\mathbf{H}} = \mathbf{\Phi}\text{Diag}[\tilde{h}_1, \cdots, \tilde{h}_P]\mathbf{\Phi}^T$ where Diag constitutes a diagonal matrix with entries $[\tilde{h}_1, \cdots, \tilde{h}_P]$. Because of (6.7), we can have

$$\begin{cases} \hat{\mathbf{H}}^{1/2} = \mathbf{\Phi}\text{Diag}[\tilde{h}_1^{1/2}, \cdots, \tilde{h}_P^{1/2}]\mathbf{\Phi}^T & ; \\ \hat{\mathbf{H}}^{-1/2} = \mathbf{\Phi}\text{Diag}[\tilde{h}_1^{-1/2}, \cdots, \tilde{h}_P^{-1/2}]\mathbf{\Phi}^T & . \end{cases} \tag{6.12}$$

Note that $\tilde{\mathbf{N}}\tilde{\mathbf{H}}^\dagger$ in (6.11) is colored Gaussian noise, hence by multiplying $(\tilde{\mathbf{H}}\tilde{\mathbf{H}}^\dagger)^{-1/2}$

at both sides of (6.11), we have

$$\tilde{\mathbf{Y}}\tilde{\mathbf{H}}^{\dagger}\begin{bmatrix}\hat{\mathbf{H}}^{-1/2} & \mathbf{0}_{P\times P}\\ \mathbf{0}_{P\times P} & \hat{\mathbf{H}}^{-1/2}\end{bmatrix} = [\mathbf{C}_1,\mathbf{C}_2]\begin{bmatrix}\hat{\mathbf{H}}^{1/2} & \mathbf{0}_{P\times P}\\ \mathbf{0}_{P\times P} & \hat{\mathbf{H}}^{1/2}\end{bmatrix} + \tilde{\mathbf{N}} \tag{6.13}$$

Because $\tilde{\mathbf{H}}^{\dagger}(\tilde{\mathbf{H}}\tilde{\mathbf{H}}^{\dagger})^{-1/2}$ is the unitary matrix, $\tilde{\mathbf{N}}$ in (6.13) is still complex AWGN.

Both $\tilde{\mathbf{Y}}\tilde{\mathbf{H}}^{\dagger}$ and $\tilde{\mathbf{N}}$ are then split up into two vectors equally so that $\tilde{\mathbf{Y}}\tilde{\mathbf{H}}^{\dagger} = [\hat{\mathbf{Y}}_1, \hat{\mathbf{Y}}_2]$ and $\tilde{\mathbf{N}} = [\mathbf{N}_1, \mathbf{N}_2]$. Hence (6.13) can be rewritten as

$$\begin{cases} \hat{\mathbf{Y}}_1\hat{\mathbf{H}}^{-1/2} = \mathbf{C}_1\hat{\mathbf{H}}^{1/2} + \mathbf{N}_1 & ; \\ \hat{\mathbf{Y}}_2\hat{\mathbf{H}}^{-1/2} = \mathbf{C}_2\hat{\mathbf{H}}^{1/2} + \mathbf{N}_2 & . \end{cases} \tag{6.14}$$

where $\mathbf{N}_1$ and $\mathbf{N}_2$ are complex AWGN.

Note that both $\hat{\mathbf{H}}^{-1/2}$ and $\hat{\mathbf{H}}^{1/2}$ are real matrices. Therefore the above equation can be split up further as real and imaginary parts easily so that we have

$$\begin{cases} real(\hat{\mathbf{Y}}_1)\hat{\mathbf{H}}^{-1/2} = real(\mathbf{C}_1)\hat{\mathbf{H}}^{1/2} + real(\mathbf{N}_1) & ; \\ imag(\hat{\mathbf{Y}}_1)\hat{\mathbf{H}}^{-1/2} = imag(\mathbf{C}_1)\hat{\mathbf{H}}^{1/2} + imag(\mathbf{N}_1) & ; \\ real(\hat{\mathbf{Y}}_2)\hat{\mathbf{H}}^{-1/2} = real(\mathbf{C}_2)\hat{\mathbf{H}}^{1/2} + real(\mathbf{N}_2) & ; \\ imag(\hat{\mathbf{Y}}_2)\hat{\mathbf{H}}^{-1/2} = imag(\mathbf{C}_2)\hat{\mathbf{H}}^{1/2} + imag(\mathbf{N}_2) & . \end{cases} \tag{6.15}$$

In (6.15) we have split up (6.10) into four independent sub-equations after some manipulation. Hence we only use the first equation of (6.15) as an example and decode the real component of $\mathbf{C}_1$. And the decoding of rest sub-equations will follow exactly same procedure. For simplicity, we denote that $\mathbf{Y} = real(\hat{\mathbf{Y}}_1)$, $\mathbf{C} = real(\mathbf{C}_1)$ and $\mathbf{N} = real(\mathbf{N}_1)$ which is independent real AWGN with zero mean and 0.5 variance. Thus the first equation of (6.15) is represented by

$$\mathbf{Y}\hat{\mathbf{H}}^{-1/2} = \mathbf{C}\hat{\mathbf{H}}^{1/2} + \mathbf{N} \tag{6.16}$$

By multiplying $\hat{\mathbf{H}}^{-1/2}$ at both sides of (6.16), we have

$$\mathbf{Y}\Phi\mathrm{Diag}[\tilde{h}_1^{-1},\cdots,\tilde{h}_P^{-1}]\Phi^T = \mathbf{C} + \mathbf{N}\hat{\mathbf{H}}^{-1/2} \tag{6.17}$$

Then we are able to use left side of (6.17) to get the first estimation $\tilde{\mathbf{C}}$ of $\mathbf{C}$ by hard decision on real domain of the constellation $\mathcal{A}$.

$\tilde{\mathbf{C}}$ might not be a good estimation because $\mathbf{N}\hat{\mathbf{H}}^{-1/2}$ in (6.17) is colored Gaussian noise and the decoding of $\tilde{\mathbf{C}}$ is simply based on the ZFD. Hence if there exists a better estimation, then the estimation can be expressed as $\tilde{\mathbf{C}} + \Delta\mathbf{C}$. $\Delta\mathbf{C}$ is the compensation vector respective to $\tilde{\mathbf{C}}$. Then our new target is to search such non-zero compensation

vector $\Delta\mathbf{C}$ so that we could get a better estimation $\tilde{\mathbf{C}} + \Delta\mathbf{C}$. $\Delta\mathbf{C}$ also needs to satisfy

$$\|\mathbf{Y}\hat{\mathbf{H}}^{-1/2} - (\tilde{\mathbf{C}} + \Delta\mathbf{C})\hat{\mathbf{H}}^{1/2}\|^2 < \|\mathbf{Y}\hat{\mathbf{H}}^{-1/2} - \tilde{\mathbf{C}}\hat{\mathbf{H}}^{1/2}\|^2 \tag{6.18}$$

which is under the condition of the MLD of (6.16). If $\tilde{\mathbf{C}}$ is the decoding result from the MLD, non-zero $\Delta\mathbf{C}$ satisfying (6.18) can not be found. $\tilde{\mathbf{C}} + \Delta\mathbf{C}$ should be limited in the range of constellation $\mathcal{A}$.

We simplify (6.18) to

$$\begin{aligned} &\Delta\mathbf{C}\mathbf{\Phi}\text{Diag}[\tilde{h}_1, \cdots, \tilde{h}_P]\mathbf{\Phi}^T\Delta\mathbf{C}^T < \\ &\quad 2\Delta\mathbf{C}\left(\mathbf{Y}^T - \mathbf{\Phi}\text{Diag}[\tilde{h}_1, \cdots, \tilde{h}_P]\mathbf{\Phi}^T\tilde{\mathbf{C}}^T\right) \end{aligned} \tag{6.19}$$

Define $P \times 1$ vector $\mathbf{\Lambda}$ as

$$\mathbf{\Lambda} = 2\left(\mathbf{Y}^T - \mathbf{\Phi}\text{Diag}[\tilde{h}_1, \cdots, \tilde{h}_P]\mathbf{\Phi}^T\tilde{\mathbf{C}}^T\right) \cdot / \left(\mathbf{\Phi}^{\cdot 2}[\tilde{h}_1, \cdots, \tilde{h}_P]^T\right) \tag{6.20}$$

where $\cdot^2$ and $\cdot/$ are element by element matrix multiplication and division respectively. If $\mathbf{\Phi}$ is chosen to be a Hadamard matrix, we have a simpler version of $\mathbf{\Lambda}$ given by

$$\mathbf{\Lambda} = 2\left(\mathbf{Y}^T - \mathbf{\Phi}\text{Diag}[\tilde{h}_1, \cdots, \tilde{h}_P]\mathbf{\Phi}^T\tilde{\mathbf{C}}^T\right) / \sum_{p=1}^{P} \tilde{h}_p \tag{6.21}$$

Supposed that the compensation vector $\Delta\mathbf{C}$ contains only one non-zero entry. It means there is only one mistake among decoded vector $\tilde{\mathbf{C}}$. Hence we define $\Delta\mathbf{C} = [0, \cdots, \Delta c_i, \cdots, 0]$ where $i \in [1, \cdots, P]$. The scalar Δc_i is defined as the ith compensation entry of $\Delta\mathbf{C}$. Hence if $\tilde{\mathbf{C}}$ has one decoding error, (6.19) can be simplified further as

$$\begin{cases} 0 < \Delta c_i < \mathbf{\Lambda}_i, & ; \\ 0 > \Delta c_i > \mathbf{\Lambda}_i, & . \end{cases} \tag{6.22}$$

where $\mathbf{\Lambda}_i$ is the ith entry of $\mathbf{\Lambda}$. Therefore if we are able to find a Δc_i satisfying (6.22), we can use Δc_i to compensate and correct the ith entry of $\tilde{\mathbf{C}}$ denoted as $\tilde{c}_i$. The possible values of Δc_i are related with particular constellation $\mathcal{A}$. And the possibilities of Δc_i are also limited. For example, $\Delta c_i = \pm\sqrt{2}$ for QPSK and $\Delta c_i = \pm 2/\sqrt{10}, \pm 4/\sqrt{10}, or \pm 6/\sqrt{10}$ for 16QAM. Therefore the decoding of Δc_i becomes another kind of hard decision based on a new constellation. For example, if QPSK is employed, (6.22) gives us $\Delta c_i = \sqrt{2}$ if $\mathbf{\Lambda}_i > \sqrt{2}$ and $\Delta c_i = -\sqrt{2}$ if $\mathbf{\Lambda}_i < -\sqrt{2}$.

The decoding procedure of CD is summarized in Figure 6.1 where $[*]_1$ is the hard decision of real or imaginary part of constellation $\mathcal{A}$ and $[*]_2$ is the hard decision based on (6.22). Moreover the position i is chosen as the position with the largest absolute

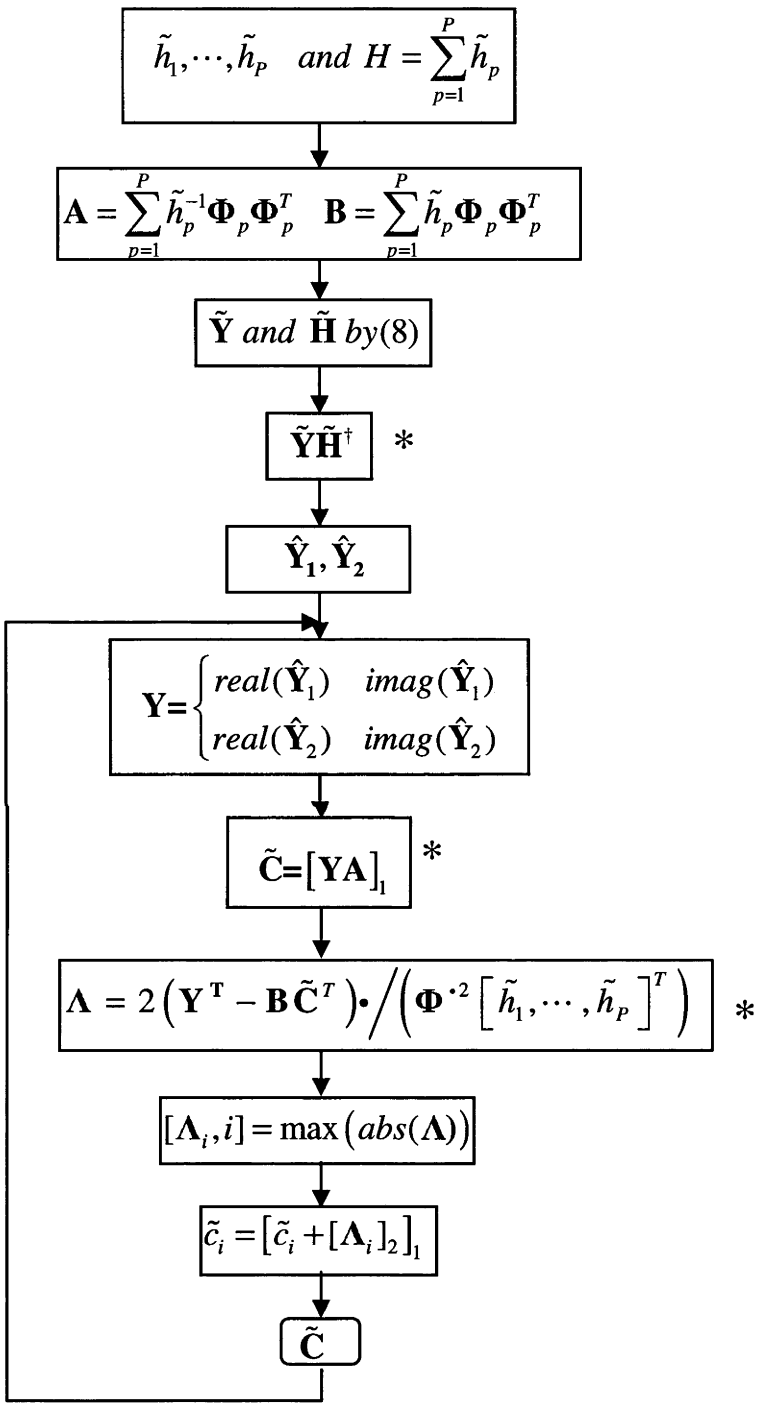

Figure 6.1: Flow of Compensation Decoding

value of the vector $\mathbf{\Lambda}$. Also $\tilde{c}_i + \Delta c_i$ should be bounded within given constellation $\mathcal{A}$ otherwise $\tilde{c}_i + \Delta c_i$ is out of range. Each loop in Figure 6.1 will decode the real or imaginary component of $\mathbf{C}_1$ or $\mathbf{C}_2$ so that total four loops are needed.

The advantage of the CD is that the calculation of channel matrix inverse of (6.10) is simplified as a direct real matrix product shown in (6.17). The real precoding matrices $\mathbf{\Phi}$, $\mathbf{\Phi}^T$ and $\mathbf{\Phi}^{\cdot 2}$ can be stored at receivers in advance. We also split up the whole decoding procedure into four independent parts so that the complexity of decoding is reduced. Only real calculations are involved during the decoding of each part. The calculation in real domain is simpler than the calculation in complex domain. Moreover the decoding of $\tilde{\mathbf{C}}$ and $\Delta\mathbf{C}$ are two hard decisions in real domain. The complexity of the CD is unrelated to the constellation size of $\mathcal{A}$ except for the two hard decisions. Full receive diversity is achieved by ZFD because of Alamouti coding. Increasing the number of receivers requires only small amount of extra calculations at the first step of Figure 6.1. Major calculations are focused on one complex and two real matrix multiplications shown in Figure 6.1 and marked with $*$. A number of simulations show that the proposed CD is roughly two or three times faster than the SD due to reduced computational complexity. The disadvantage is that the CD still can not achieve full frequency diversity so that the performance of decoding is worse than the MLD and SD. Hence we sacrifice the decoding ability to gain a simpler and faster decoding procedure.

6.4.3 Simulations and Comparisons

In this section we present simulations to investigate the decoding ability of the proposed method. We will compare the BER performance of SD in [86], the MLD, the ZFD, with that of the proposed CD. The ZFD is the decoding procedure without compensation $\Delta\mathbf{C}$. Hence only (6.17) is required for the ZFD. The SD and MLD are based on the equivalent channel equation (6.10). The QPSK constellation is employed in every simulation. Figures 6.2 and 6.3 are averaged bit error rate (BER) over large number of channel realizations. The random channel is assumed to be a multi-path channel. It has the uniform power delay profile composed of $L+1$ independent identically distributed complex Gaussian paths with zero mean and equal variance ($\frac{1}{L+1}$). We choose $F = 128$ and $L = 3$. The second order characteristics of such a MIMO-OFDM system is presented in [24] and Chapter 2. It shows that this ideal MIMO-OFDM system is able to employ at most $L+1$ slightly correlated subcarriers within a subcarrier group. Hence subcarrier grouping here is formed by choosing subcarriers equally separated. More subcarriers ($P \leq L+1$) can achieve higher frequency diversity. Considering a feasible number of subcarriers and practical low and median SNR scenarios, we focus

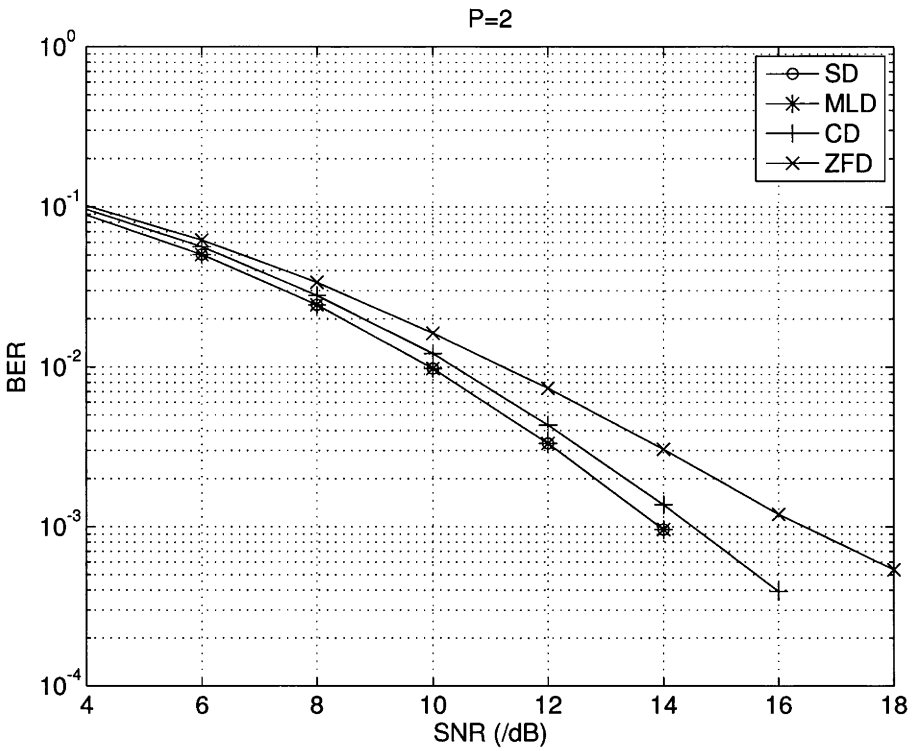

Figure 6.2: MIMO-OFDM system with two subcarriers and one receiver

on the cases of $P = 2$ and $P = 4$ at SNR $\leq$ 15dB.

The performances of ZFD are much worse than the CD, MLD and SD in both Figure 6.2 and Figure 6.3. The ZFD can not achieve full frequency diversity. But increasing number of subcarrier is still capable of achieving a little improvement by the ZFD. At $SNR = 14dB$, the CD can achieve roughly 2dB gain compared with ZFD in both figures with the expense of extra calculations of the compensation vector.

Simulation results in Figure 6.2 and Figure 6.3 also show that the proposed CD can approach the performance of MLD better than the ZFD. It proves that the compensation vector $\Delta\mathbf{C}$ improve the decoding result of the ZFD to a certain degree. However full frequency diversity can not be achieved by the CD, just like the ZFD. The MLD (the SD) has about 0.5dB and 2.5dB gains compared with the CD and ZFD respectively at BER of 10^{-3} in Figure 6.2. Moreover the MLD (the SD) has about 1.5dB and 3.3dB gains compared with the CD and ZFD respectively at BER of 10^{-3} in Figure 6.3. Hence for given BER, the difference between the CD and the MLD gets larger as more subcarriers are employed. The reason is that most of decoded $\tilde{\mathbf{C}}$s for OFDM systems with two subcarriers are either error-free or one error. Such situations are suited to the decoding ability of proposed CD. Hence for the MIMO-OFDM systems with two subcarriers, the CD becomes a good candidate for decoding because of its

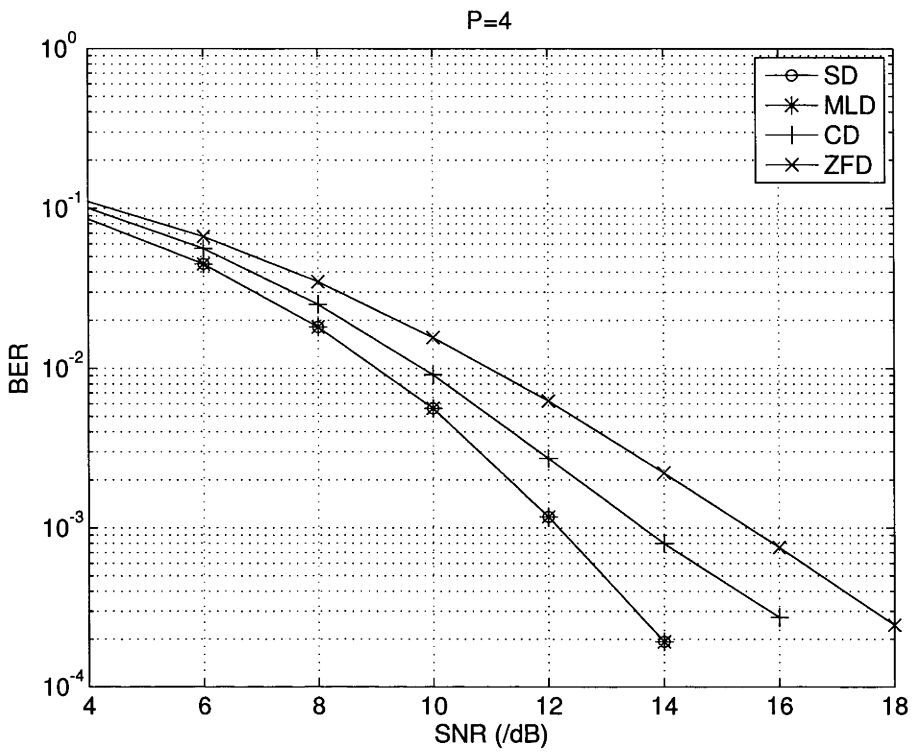

Figure 6.3: MIMO-OFDM system with four subcarriers and one receiver

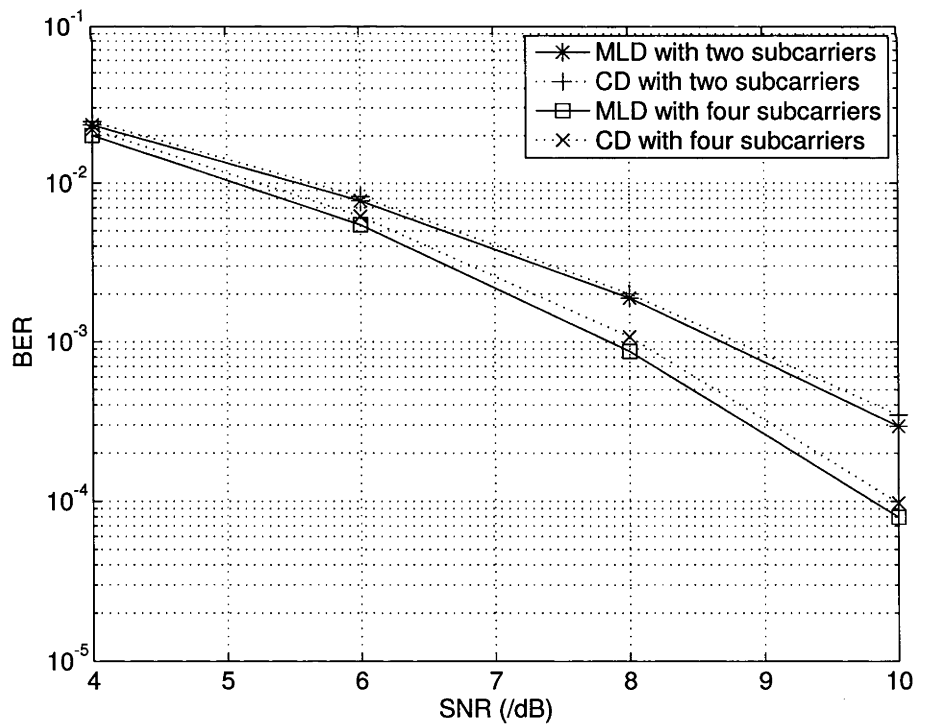

Figure 6.4: MIMO-OFDM system with two or four subcarriers and two receivers

lowest complexity and relatively good performance for MIMO-OFDM systems at low and medium SNR.

Increasing the number of receivers will not significantly affect the complexity of the CD. More calculations are only needed at the first step of Figure 6.1. Although the CD can not achieve full frequency diversity, full receiver diversity can still be guaranteed. Hence increasing the number of receivers will increase the achievable STF diversity of the CD. This forces the performances of the CD and MLD to get closer at given BER as shown in Figure 6.4. The figure shows that the MLD has about 0.1dB and 0.2dB gains compared with the CD for the cases of two subcarriers and four subcarriers groupings respectively at BER of 10^{-3} if two receivers are employed. Therefore at a given BER the difference between the CD and the MLD becomes smaller if more receivers are employed. The CD is still a good candidate for decoding because of its lowest complexity and the relatively good performance for MIMO-OFDM systems at low and medium SNR.

6.5 Classifier Based Decoding

In this section, we propose a low complexity detection scheme, called classifier based decoding (CBD), for MIMO systems incorporating spatial multiplexing.

The optimal detection schemes such as MLD of MIMO signals demands computational resources that are beyond the capabilities of most practical systems. Although several reduced complexity MIMO detection techniques have been proposed, e.g, SD [90], the complexity of such algorithmic schemes are in general much higher than that of the equalizer-based techniques, e.g. ZFD or MMSE. On the other hand, equalizer based techniques perform relatively poor in terms of error rate. In this section, we propose a hybrid of an equalizer-based technique and an algorithmic search stage. Based on an error matrix and its probability density functions (PDF) for different classes of error, a particular search region is selected for the algorithmic stage. As the probability of occurrence of error classes with larger search regions is small, overall complexity of the proposed technique remains low while providing a significant improvement in the error performance.

Suppose that a spatial multiplexed MIMO system with N_t transmitters and N_r receivers is considered. The transmitted symbol vector for a given time slot is taken as $\mathbf{X} = [x_1, \cdots, x_{N_t}]$ with $\sigma_x^2 = \mathbb{E}[\|x_m\|^2]$ and the received signal vector is $\mathbf{Y} = [y_1, \cdots, y_{N_r}]^T$. The channel equation is given by

$$\mathbf{Y} = \mathbf{HX} + \mathbf{W} \tag{6.23}$$

where H is a $N_r \times N_t$ containing statistically independent complex Gaussian channel values. The channel noise (AWGN) vector is given by $\mathbf{W} = [w_1, \cdots, w_{N_r}]^T$ where $\sigma_w^2 = \mathbb{E}[\|w_n\|^2]$ for $n \in [1, \cdots, N_r]$ is the noise power. The element h_{mn} corresponding to the mth row and the nth column of the matrix $\mathbf{H}$ is a uncorrelated circularly symmetric complex Gaussian random variable with zero mean and unit variance.

The equalizer-based MIMO detection can be generalized as

$$\mathbf{x}_{EQ} = \mathbf{GY} \tag{6.24}$$

where $\mathbf{G}$ is the $N_t \times N_r$ equalizer matrix. The estimated transmitted symbol vector $\hat{\mathbf{X}}$ becomes

$$\hat{\mathbf{X}}_{EQ} = Q(\mathbf{X}_{EQ}) \tag{6.25}$$

where $Q(.)$ denotes the nearest neighbor constellation demapping operation. The equalization $\mathbf{G} = \mathbf{G}_{ZF}$ of the ZFD [91] is given by

$$\mathbf{G}_{ZF} = \left(\mathbf{H}^\dagger \mathbf{H}\right)^{-1} \mathbf{H}^\dagger \tag{6.26}$$

And the equalization $\mathbf{G} = \mathbf{G}_{MMSE}$ of the MMSE [92] is given by

$$\mathbf{G}_{MMSE} = \left(\mathbf{H}^\dagger \mathbf{H} + \frac{\sigma_w^2}{\sigma_x^2}\mathbf{I}\right)^{-1} \mathbf{H}^\dagger \tag{6.27}$$

The universal set $\mathcal{G} = \mathcal{G}_0 \cup \mathcal{G}_1 \cup \cdots \cup \mathcal{G}_G$ contains all possible symbol vectors $\mathbf{X} - \hat{\mathbf{X}}_{EQ}$, thus $|\mathcal{G}| = \sum_{i=0}^{G} |\mathcal{G}_i| = \mathcal{C}^{N_t}$ where $\mathcal{C}$ is the constellation size. Therefore, the proposed classification based detector divides the total search space into $G+1$ number of mutually exhaustive and exclusive subspaces $\mathcal{G}_i$ where $i \in [0, \cdots, G]$. Every $\hat{\mathbf{X}}_{EQ}$ belongs to a unique class $\mathcal{G}_i$.

The proposed MIMO detection algorithm can be formulated as follows:

Step 1: Calculate the error measure ρ using an equalizer-based estimate of the transmitted symbol vector $\hat{\mathbf{X}}_{EQ}$ (either ZFD or MMSE):

$$\rho = \|\mathbf{Y} - \mathbf{H}\hat{\mathbf{X}}_{EQ}\| \tag{6.28}$$

where $\hat{\mathbf{X}}_{EQ}$ is given by equation (6.25).

Step 2: Given the observation of ρ, calculate according to the Bayesian classification rule the most probable index i^* of classes $\mathcal{G}_i$ that $\hat{\mathbf{X}}_{EQ}$ belongs to:

$$i^* = \arg\max_i p_{\mathcal{G}_i}(\rho|\mathcal{G}_i) P_{\mathcal{G}_i} \tag{6.29}$$

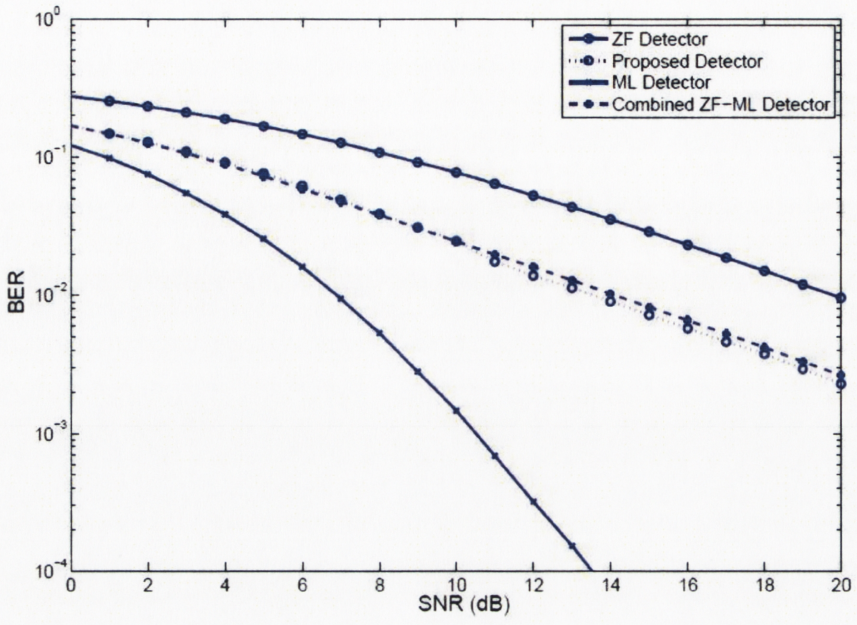

Figure 6.5: BER performance of the CBD (with ZFD) versus SNR

where $P_{\mathcal{G}_i}$ is the actual probability of occurrence of the class $\mathcal{G}_i$, independent of the classifier and depends on the linear equalizer used and the operating SNR. And the probability $p_{\mathcal{G}_i}(\rho|\mathcal{G}_i)$ is the PDF of specific class $\mathcal{G}_i$ for a given SNR ρ. A particular class associated with the estimation results of ZF (or MMSE) is identified in this step utilizing priori knowledge of MIMO channel statistics information.

Step 3: Perform a exhaustive search within the class $\mathcal{G}_{i^*}$ to find out the best estimate $\hat{\mathbf{X}}^*$ of the transmitted symbol vector:

$$\hat{\mathbf{X}}^* = \arg \min_{\hat{\mathbf{X}} \in \mathcal{G}_{i^*}} \|\mathbf{Y} - \mathbf{H}\hat{\mathbf{X}}\|^2 \tag{6.30}$$

A 4×4 MIMO system with BPSK modulation is simulated to demonstrate the performance of the proposed detection algorithm. The BER performance of the proposed classifier based detector is shown in Figure 6.5. In the same figure, the performance of the following three MIMO detectors are shown for comparison: (1) ZFD, (2) MLD and (3) combined ZF-ML detector in [91]. It can be seen in Figure 6.5 that the BER performance of the proposed classifier based MIMO detector is significantly better than that of the ZFD, i.e. at BER= 10^{-2}, a 6dB improvement can be observed. In fact, the performance of the proposed detector is closer (or marginally better) to the combined ZF-ML detector. However the proposed detector has a much lower complexity than

that of ZF-ML detector.

Some characteristics of proposed CBD are summarized here:

- The proposed CBD subdivides the full maximal-likelihood search space into a number of variable size subspaces with respect to the solution given by a linear equalizer (ZFD or MMSE).

- The CBD needs the statistics information of channel impulse response and SNR at the receivers in advance. In other words, the knowledge of $p_{\mathcal{G}_i}(\rho|\mathcal{G}_i)$ for each class and $P_{\mathcal{G}_i}$ for each SNR and equalizer should be determined at first. The subspace or class is selected based on such information. Generally, the CBD is designed for relatively slow-changed propagation environment.

- Within the selected subspace or class a MLD type search is performed to obtain the final detected vector. The computational advantage of the proposed technique results from an optimal MLD in a computationally prohibitive search space.

- The method of classification is not unique, but in this section the criteria is the number of errors of estimated symbol vector $\hat{\mathbf{X}}_{EQ}$ after an equalization process. Alterative criteria could be used, e.g. constellation distances.

- The CBD is capable of detecting some dominant errors with a limited computation. Although the classification process of estimated symbol vector is not always correct, the most likely subspace or class will be chosen every time with priori statistical information.

6.6 Summary

Two novel decoding processes for the MIMO-OFDM system and MIMO system are proposed in this chapter. Some characteristics can be summarized as following:

- The CD is proposed for a given STFBC. Taking advantage of the simplicity of zero forcing equalization, we develop a method to calculate a compensation vector for the result of ZFD. After modifying its results by the compensation vector the BER performance can be improved. The advantages of this method are firstly the decoding procedure is relatively simple and secondly the complexity is independent of the constellation size. Hence there is a trade-off between system performance and complexity. Moreover the decoding is a hard decision,

which can easily be implemented in hardware. The performance of the new decoding method is close to the optimum maximum likelihood decoding at low to medium SNR range, and gets even closer if more receivers are employed.

- The CBD is proposed for the MIMO system. The proposed CBD subdivides the full maximum-likelihood search space into a number of variable size subspaces with respect to the solution given by a linear equalizer (ZFD or MMSE). A subspace or class is selected based on the statistical information which is known by the receiver. Within the selected subspace or class a MLD type search is performed to obtain the final detected vector.
- The CBD is capable of correcting an estimated symbol vector with more than one error, however the CD can only correct an estimated symbol vectors with one error.
- The CBD is capable of correcting a partial amount of vectors in each subspace or class. However the CD can correct all vectors in one subspace but none of them in other subspaces.
- The CBD requires both channel statistical information and channel state information at the receive side. The accuracy of such priori knowledge will affect the system performance significantly. But the CD requires channel state information only in the decoding process.
- The CBD requires the calculation of a channel matrix inverse, which might not be easy in a real-time system but the CD does not have such a limitation.
- Intrinsically both CBD and CD are the simplification of the MLD in different approaches. The CBD is a MLD with a reduced search space, but the CD is a MLD with a reduced correction capability. The methodology of both detectors is similar to the examiners working on a production line. In order to speed up the testing process, the examiners could work faster and as a consequence more faulty goods are overlooked, which is similar to the proposed CD. Alternatively the examiners could simply carefully test a certain percentage of the products, but the tested products are only selected with the best guess, which is similar to the proposed CBD.

The potential research directions or questions are:

- It may be feasible to extend the CBD into the MIMO-OFDM system, and it may also be feasible to merge the CD and CBD together since they simplify the decoding process in different directions. For example, the ability of CD may be improved to correct the estimated symbol vector which has more than one errors.

Thus the classification process of the CBD would be applied to the decoding process.

- The criteria of classification should be improved, rather than a scalar as defined in (6.28).
- The CD may be applied to other STFBCs so that the performance of the MIMO-OFDM system could be improved steadily with a smoothly increased decoding complexity. Then an adaptive balance could be made between complexity and performance of the decoding process.

6.7 Conclusions

A novel compensation decoding and a low complexity classifier based decoding are proposed in this chapter for the MIMO-OFDM system and the MIMO system respectively. The CD utilizes the special characteristics of the precoding matrix and the simplicity of zero-forcing decoding to design a compensation vector. The CBD utilizes prior-known channel statistical information to improve the performance of the zero-forcing or MMSE decoding. Both methods are capable of improving the performance without a significant increase of decoding complexity.

Chapter 7

Conclusion

The objectives and contributions of this thesis with respect to SFBC/STFBC and MIMO-OFDM system design are shown as following:

FLEXIBILITY: A novel SFBC with matched rotation precoding is proposed for the MIMO-OFDM system to provide greater flexibility of resource scheduling. It is expected to provide the maximal space-frequency diversity and the optimal coding gain for an MIMO-OFDM system with an arbitrary number of transmitters, subcarrier interval, and an arbitrary subcarrier grouping strategy for an arbitrary channel power delay profile.

FEASIBILITY: The lowerbound of coding gain of the SFBC is derived in this thesis so that the SFBC can be implemented in a practical wireless system. Most existing SFBCs with achievable space-frequency diversity are too optimistic regarding to their assumptions of propagation channel, which might give rise to debatable system performance robustness in terms of achievable diversity gain and coding gain. For example, the potential of diversity loss is shown in the thesis, and the assumption of uniform power delay profile gives optimal system performance. Because the real propagation channels are time-varying and the characteristics of the channels might be significantly different from case to case, the analysis of the lowerbound can improve the feasibility of the SFBC and mitigate the requirement of system information at transmitters.

SPECTRAL EFFICIENCY: The multirate SFBC and STFBC are proposed to improve the spectral efficiency of MIMO-OFDM system, and balance the symbol transmission rate and desired BER performance without a significant change of coding structure. The designs of high rate SFBC/STFBC (greater than one) with achievable SF or STF diversity in the MIMO-OFDM system are more challenging, compared to the design of high rate STBC in the MIMO system. The design criteria of the high rate SFBC/STFBC have to be combined with coding gain, diversity gain and channel power delay profile. The proposed multirate SFBC in Chapter 4 can always achieve full SF diversity, with simplified requirements on a dynamic parameter optimization process. On the

other hand, proposed multirate STFBC in Chapter 5 can achieve partial SF diversity only, with a requirement of fixed parameter optimization. A relatively smooth balance between the transmission rate and system BER performance can be achieved by both multirate block codes, in order to provide stable user experience. On the other hand the coding gain corresponding to each transmission rate is always optimized.

DECODING COMPLEXITY: The decoding procedures of the MIMO-OFDM system are investigated. The compensation decoding and classifier based decoding are proposed to reduce the decoding complexity by a trade-off between decoding complexity and BER performance. The decoding performance can be improved with the help of an additional compensation vector or the prior statistical information known by receivers.

Future work of this doctoral thesis with respect to SFBC and the MIMO-OFDM system design are shown as following:

ENHANCED MRP: The precoding matrix in Chapter 4 is a unified structure suitable for all STBCs and SFBCs. However, most existing SFBCs only consider rotation angles like proposed MRP in the thesis, or antenna switching corresponding to a simple power allocation strategy. More complex power allocation algorithm can be adopt in the precoding matrix and might be similar to water filling algorithms developed for the STBC. Furthermore, both adaptive power allocation and proposed MRP can be combined in the MIMO-OFDM system so that a generalized optimization process can be developed. This strategy will increase the requirement of channel knowledge at the transmit side and the complexity of the optimization process. However it will improve the system performance and spectral efficiency further. Potential performance gains of enhanced MRP is hard to estimate but it will be very channel-dependent.

NETWORK MRP: A network MRP should be proposed to incorporate ongoing research of the network MIMO for LTE-Advanced, which is a candidate of IMT-advanced. The network MIMO or cooperative MIMO will utilize the multiple channel information from different sites in order to achieve improved cell interference mitigation. Existing research of network MIMO has shown a similarity between codebook-based precoding and proposed MRP. Frequency diversity and multi-cell diversity are usually achieved by scheduling in the physical Layer and layer 2 in LTE or LTE-A. However proposed MRP might have similar capability so that enhanced codebook-based precoding can be realized. Considering the requirement of optimization, TDD in LTE-A might be more feasible to exploit the concept of network MRP. Hence a powerful network SFBC can be developed to fully capture all spatial, multicell and frequency diversity in a multi-cell, multipath frequency-selective fading environment.

MULTIUSER MRP: The worth of multiuser MRP should be investigated since each specific user can be assigned with a distinct rotation pattern. This concept might be

similar with spreading codes in code division multiple access (CDMA), but it would be more suitable for the OFDM system, e.g LTE-A or WiMax. The user-specific rotation pattern acts as a user finger print. When multiple finger prints cover each other with interference, we still can extract each finger print successively since everyone is unique. From the point of coding theory, the multiuser MRP is capable of achieve multiuser diversity by spreading precoding matrices into multiple users. The complexity of decoding will be increased but the additional power consumption will be only for base stations.

Derivation of Equation (4.9)

The derivation of equation (4.9) can be shown as following:

$$\begin{aligned} \Lambda &= \mathbb{E}\left[\Delta\hat{\mathbf{S}}\text{vec}(\tilde{\mathbf{H}})\text{vec}^{\dagger}(\tilde{\mathbf{H}})\Delta\hat{\mathbf{S}}^{\dagger}\right] \\ &= \Delta\hat{\mathbf{S}}\left\{\mathbf{R}_{MS}\otimes\mathbf{R}_{F}\otimes\mathbf{R}_{BS}\right\}\Delta\hat{\mathbf{S}}^{\dagger} \end{aligned} \tag{A.1}$$

which comes from the property of (4.7). The transmitted symbol vector $\mathbf{S}$ is defined as

$$\mathbf{S} = [s_{1,1},\cdots,s_{1,N_t},\cdots,s_{P,1},\cdots,s_{P,N_t}] \tag{A.2}$$

and $\hat{\mathbf{S}} = (\mathbf{I}_{N_rP}\otimes\mathbf{1}_{1\times N_t})\circ(\mathbf{1}_{N_rP\times N_r}\otimes\mathbf{S})$. which can be rewritten as

$$\begin{aligned} \hat{\mathbf{S}} &= (\mathbf{I}_{N_rP}\otimes\mathbf{1}_{1\times N_t})\circ(\mathbf{1}_{N_rP\times N_r}\otimes\mathbf{S}) \\ &= (\mathbf{I}_{N_r}\otimes\mathbf{I}_{P}\otimes\mathbf{1}_{1\times N_t})\circ(\mathbf{1}_{N_r}\otimes\mathbf{1}_{P\times 1}\otimes\mathbf{S}) \\ &= \mathbf{I}_{N_r}\otimes\{(\mathbf{I}_{P}\otimes\mathbf{1}_{1\times N_t})\circ(\mathbf{1}_{P\times 1}\otimes\mathbf{S})\} \qquad \text{(A.3)} \\ &= \mathbf{I}_{N_r}\otimes\hat{\hat{\mathbf{S}}} \qquad \text{(A.4)} \end{aligned}$$

where $\hat{\hat{\mathbf{S}}} = \{(\mathbf{I}_{P}\otimes\mathbf{1}_{1\times N_t})\circ(\mathbf{1}_{P\times 1}\otimes\mathbf{S})\}$.

Therefore using the property of $(\mathbf{A}_1\otimes\mathbf{B}_1)(\mathbf{A}_2\otimes\mathbf{B}_2)(\mathbf{A}_3\otimes\mathbf{B}_3) = (\mathbf{A}_1\mathbf{A}_2\mathbf{A}_3)\otimes(\mathbf{B}_1\mathbf{B}_2\mathbf{B}_3)$ shown in [84], we have

$$\Lambda = \mathbf{R}_{MS}\otimes\left\{\Delta\hat{\hat{\mathbf{S}}}\left(\mathbf{R}_{F}\otimes\mathbf{R}_{BS}\right)\Delta\hat{\hat{\mathbf{S}}}^{\dagger}\right\}. \tag{A.5}$$

The transmitted symbol vector $\mathbf{S}$ can be expressed as a form of matrix:

$$\tilde{\mathbf{S}} = [\tilde{\mathbf{S}}^{1},\cdots,\tilde{\mathbf{S}}^{N_t}] = \begin{bmatrix} s_{1,1} & \cdots & s_{1,N_t} \\ \vdots & \vdots & \vdots \\ s_{P,1} & \cdots & s_{P,N_t} \end{bmatrix}. \tag{A.6}$$

Then we have

$$\begin{aligned} \mathbf{\Lambda} &= \mathbf{R}_{MS} \otimes \left\{ \Delta\hat{\tilde{\mathbf{S}}} \left(\mathbf{R}_F \otimes \mathbf{R}_{BS} \right) \Delta\hat{\tilde{\mathbf{S}}}^{\dagger} \right\} \\ &= \mathbf{R}_{MS} \otimes \left\{ \left(\Delta\tilde{\mathbf{S}} \mathbf{R}_{BS} \Delta\tilde{\mathbf{S}}^{\dagger} \right) \circ \mathbf{R}_F \right\} \end{aligned} \tag{A.7}$$

because the entry of $\mathbf{A} = \left\{ \Delta\hat{\tilde{\mathbf{S}}} \left(\mathbf{R}_F \otimes \mathbf{R}_{BS} \right) \Delta\hat{\tilde{\mathbf{S}}}^{\dagger} \right\}$ at the p_1th row and p_2th column can be expressed as

$$\mathbf{A}(p_1, p_2) = \mathbf{R}_F(p_1, p_2) \left\{ [\Delta s_{p_1,1}, \cdots, \Delta s_{p_1,N_t}] \mathbf{R}_{BS} [\Delta s_{p_2,1}, \cdots, \Delta s_{p_2,N_t}]^{\dagger} \right\} \tag{A.8}$$

which is exactly same entry of $\left\{ \left(\Delta\tilde{\mathbf{S}} \mathbf{R}_{BS} \Delta\tilde{\mathbf{S}}^{\dagger} \right) \circ \mathbf{R}_F \right\}$ at the p_1th row and p_2th column.

Therefore we have

$$\mathbf{\Lambda} = \mathbf{R}_{MS} \otimes \left\{ \left(\Delta\tilde{\mathbf{S}} \mathbf{R}_{BS} \Delta\tilde{\mathbf{S}}^{\dagger} \right) \circ \mathbf{R}_F \right\} \tag{A.9}$$

Derivation of Equation (4.14)

Because the equation (4.13) is a simplified version of (4.14), we focus on (4.14) only. It is shown that the entry of $\mathbf{A} = \mathbf{\Omega}\mathbf{\Omega}^{\dagger}$ at the p_1th row and p_2th column can be expressed as

$$\begin{aligned}
\mathbf{A}(p_1, p_2) &= [\sigma_0 \Delta s_{p_1,1} w^0_{p_1}, \cdots, \sigma_0 \Delta s_{p_1,N_t} w^0_{p_1}, \cdots, \sigma_L \Delta s_{p_1,1} w^L_{p_1}, \cdots, \sigma_L \Delta s_{p_1,N_t} w^L_{p_1}] \\
&\times [\sigma_0 \Delta s_{p_2,1} w^0_{p_2}, \cdots, \sigma_0 \Delta s_{p_2,N_t} w^0_{p_2}, \cdots, \sigma_L \Delta s_{p_2,1} w^L_{p_2}, \cdots, \sigma_L \Delta s_{p_2,N_t} w^L_{p_2}]^{\dagger} \\
&= \left(\sum_{m=1}^{N_t} \Delta s_{p_1,m} \Delta s^*_{p_2,m} \right) \left(\sum_{\ell=0}^{L} \sigma^2_{\ell} w^{\ell}_{p_1} \left(w^{\ell}_{p_2} \right)^* \right) \\
&= \left([\Delta s_{p_1,1}, \cdots, \Delta s_{p_1,N_t}] \times [\Delta s_{p_2,1}, \cdots, \Delta s_{p_2,N_t}]^{\dagger} \right) \\
&\times \left([w^0_{p_1}, \cdots, w^L_{p_1}] \mathbf{R}_{\mathrm{D}} [w^0_{p_2}, \cdots, w^L_{p_2}]^{\dagger} \right)
\end{aligned}$$

where $\left([\Delta s_{p_1,1}, \cdots, \Delta s_{p_1,N_t}] \times [\Delta s_{p_2,1}, \cdots, \Delta s_{p_2,N_t}]^{\dagger}\right)$ is the entry of $\Delta\tilde{\mathbf{S}}\Delta\tilde{\mathbf{S}}^{\dagger}$ at the p_1th row and p_2th column. And $\left([w^0_{p_1}, \cdots, w^L_{p_1}] \mathbf{R}_D [w^0_{p_2}, \cdots, w^L_{p_2}]^{\dagger}\right)$ is the entry of $\mathbf{W}\mathbf{R}_D\mathbf{W}^{\dagger}$ at the p_1th row and p_2th column.

Hence we have $\mathbf{\Lambda} = \mathbf{I}_{N_t} \otimes (\mathbf{\Omega}\mathbf{\Omega}^{\dagger})$.

Proof of Remark 1 in Chapter 5

Proof:

The covariance matrix $\mathbf{\Lambda}$ is represented as

$$\mathbf{\Lambda} = \mathbf{I}_{N_r} \otimes \begin{bmatrix} \Delta\tilde{\mathbf{S}}_1\Delta\tilde{\mathbf{S}}_1^\dagger & \cdots & \Delta\tilde{\mathbf{S}}_1\Delta\tilde{\mathbf{S}}_K^\dagger \\ \vdots & \vdots & \vdots \\ \Delta\tilde{\mathbf{S}}_K\Delta\tilde{\mathbf{S}}_1^\dagger & \cdots & \Delta\tilde{\mathbf{S}}_K\Delta\tilde{\mathbf{S}}_K^\dagger \end{bmatrix} \tag{C.1}$$

in which each block matrix $\Delta\tilde{\mathbf{S}}_k\Delta\tilde{\mathbf{S}}_{k'}^\dagger$ is a $P \times P$ diagonal matrix. The ath diagonal entry is defined as $D_a^{kk'} = \sum_{b=1}^{N_t} \Delta s_k^{aN_t+b}(\Delta s_{k'}^{aN_t+b})^*$ where $a \in [0, \cdots, P-1]$ and $k, k' \in [1, \cdots, K]$. After the manipulation of entries in $\mathbf{\Lambda}$, a block diagonal matrix $\tilde{\mathbf{\Lambda}}$ is given by

$$\tilde{\mathbf{\Lambda}} = \mathbf{I}_{N_r} \otimes \begin{bmatrix} \mathbf{D}_0 & \cdots & 0 \\ \vdots & \vdots & \vdots \\ 0 & \cdots & \mathbf{D}_{P-1} \end{bmatrix} \tag{C.2}$$

where each block matrix $\mathbf{D}_a$ is constructed by

$$\mathbf{D}_a = \begin{bmatrix} D_a^{11} & \cdots & D_a^{1K} \\ \vdots & \vdots & \vdots \\ D_a^{K1} & \cdots & D_a^{KK} \end{bmatrix}. \tag{C.3}$$

The determinant of $\mathbf{\Lambda}$ is not changed after manipulation. Therefore we have

$$\det(\mathbf{\Lambda}) = \det(\tilde{\mathbf{\Lambda}}) = \left(\prod_{a=0}^{P-1} \det(\mathbf{D}_a) \right)^{N_r}. \tag{C.4}$$

If $\det(\mathbf{\Lambda}) > 0$, $\det(\mathbf{D}_a) > 0$ for $\forall a \in [0, \cdots, P-1]$. Assuming that there exists $\Delta\mathbf{C} \neq \mathbf{0}_{1\times Q}$, $\det(\mathbf{D}_a) = 0$ for specific a. The determinant of $\mathbf{D}_a$ of multirate STFBC is shown in the next page. X_t for $t \in [0, \cdots, (N_t-1)N_t]$ are the crossing terms of $\Delta\mathbf{C}$

$$
\begin{aligned}
\det(\mathbf{D}_a) &= \det\left(\begin{bmatrix} \Delta s_1^{aN_t+1} & \cdots & \Delta s_K^{aN_t+1} \\ \vdots & \cdots & \vdots \\ \Delta s_1^{aN_t+N_t} & \cdots & \Delta s_K^{aN_t+N_t} \end{bmatrix}^{\dagger} \begin{bmatrix} \Delta s_1^{aN_t+1} & \cdots & \Delta s_K^{aN_t+1} \\ \vdots & \cdots & \vdots \\ \Delta s_1^{aN_t+N_t} & \cdots & \Delta s_K^{aN_t+N_t} \end{bmatrix}\right) \\
&= \left\| \det\left(\begin{bmatrix} \Delta\mathbf{CV}^{aN_t+1} & \cdots & e^{j\phi(N_t-1)}\Delta\mathbf{CV}^{(K-1)P+aN_t+1} \\ \vdots & \cdots & \vdots \\ e^{j\phi(N_t-1)}\Delta\mathbf{CV}^{aN_t+N_t} & \cdots & \Delta\mathbf{CV}^{(K-1)P+aN_t+N_t} \end{bmatrix}\right) \right\|^2 \\
&= \left\| X_0 + e^{j\phi}X_1 + \cdots + e^{j\phi N_t(N_t-1)}X_{N_t(N_t-1)} \right\|^2
\end{aligned}
$$

and $\mathbf{V}$ where the first and last X_t are shown as

$$
\begin{aligned}
X_0 &= \prod_{k=1}^{K} \Delta\mathbf{CV}^{(k-1)P+aN_t+k}, \\
X_{N_t(N_t-1)} &= \prod_{k=1}^{K} \Delta\mathbf{CV}^{(K-k)P+aN_t+k}.
\end{aligned} \tag{C.5}
$$

Because the $e^{j\phi}$ is an algebraic number of degree $> N_t(N_t-1)$ over $\mathcal{K}$, all X_ts equal to 0. Also because of the property of Vandermonde matrix and (C.5), $\Delta\mathbf{C} = \mathbf{0}_{1\times Q}$ which contradicts the assumption of $\Delta\mathbf{C} \neq \mathbf{0}_{1\times Q}$.

Bibliography

[1] 3GPP TR 36.913 v 8.0.1, *Requirements for further advancements for Evolved Universal Terrestrial Radio Access (E-UTRA) (LTE-Advanced)*, Mar. 2009.

[2] 3GPP TS 36.101 V8.5.1, *User Equipment (UE) radio transmission and reception for Evolved Universal Terrestrial Radio Access (E-UTRA)*, Mar. 2009.

[3] WiMax, *http://www.wimaxforum.org*.

[4] W. Zhang, X. Xia, and P. Ching, "High-rate full-diversity space-time-frequency codes for broadband MIMO block-fading channels," *IEEE Transactions on Communications*, vol. 55, no. 1, pp. 25–34, Jan. 2007.

[5] S. M. Alamouti, "A simple transmit diversity technique for wireless communications," *IEEE Journal on Select Areas in Communications*, vol. 16, no. 8, pp. 1451–1458, Oct. 1998.

[6] Y. Xin, Z. Wang, and G. B. Giannakis, "Space-time diversity systems based on linear constellation precoding," *IEEE Transactions on Wireless Communications*, vol. 2, no. 2, pp. 294–309, Mar. 2003.

[7] J. C. Belfiore, G. Rekaya, and E. Viterbo, "The golden code: a 2×2 full-rate space-time code with nonvanishing determinants," *IEEE Transactions on Information Theory*, vol. 51, no. 4, pp. 1432–1436, Apr. 2005.

[8] L. Shao and S. Roy, "Rate-one space-frequency block codes with maximum diversity for MIMO-OFDM," *IEEE Transactions on Wireless Communications*, vol. 4, no. 4, pp. 1674–1687, July 2005.

[9] W. Su, Z. Safar, and K. Liu, "Full-rate full-diversity space-frequency codes with optimum coding advantage," *IEEE Transactions on Information Theory*, vol. 51, no. 1, pp. 229–249, Jan. 2005.

[10] L. Shao, S. Roy, and S. Sandhu, "Rate-one space frequency block codes with maximum diversity gain for MIMO-OFDM," *IEEE Global Telecommunications Conference*, vol. 2, pp. 809–813, Dec. 2003.

[11] WINNER, "Final report on link level and system level channel models, d5.4 v1.4," *IST-2003-507581*.

[12] W. Zhang, X. gen Xia, and P. Ching, "High-rate full-diversity space-time-frequency codes for MIMO multipath block-fading channels," *IEEE Global Telecommunications Conference*, vol. 3, pp. 1587–1591, Nov. 2005.

[13] J. Wu and S. D. Blostein, "Linear dispersion over time and frequency," *IEEE International Conference on Communications*, vol. 1, pp. 254–258, June 2004.

[14] F. Oggier, G. Rekaya, J.-C. Belfiore, and E. Viterbo, "Perfect space-time block codes," *IEEE Transactions on Information Theory*, vol. 52, no. 9, pp. 3885–3902, Sep. 2006.

[15] H. Sampath, S. Talwar, J. Tellado, V. Erceg, and A. Paulraj, "A fourth-generation MIMO-OFDM broadband wireless system: design,performance, and field trial results," *IEEE Communications Magazine*, vol. 40, no. 9, pp. 143–149, Sep. 2002.

[16] C. Dubuc, D. Starks, T. Creasy, and Y. Hou, "A MIMO-OFDM prototype for next-generation wireless WANs," *IEEE Communications Magazine*, pp. 82–87, Dec. 2004.

[17] S. N. DIGGAVI, N. AL-DHAHIR, A. STAMOULIS, and A. R. CALDERBANK, "Great expectations: The value of spatial diversity in wireless networks," *Proceeding of the IEEE*, vol. 92, no. 2, pp. 219–270, Feb. 2004.

[18] B. Saltzberg, "Performance of an efficient parallel data transmission system," *IEEE Transactions on Communication Technology*, vol. 15, no. 6, pp. 805–811, Dec. 1967.

[19] S. B. Weinstein and P. M. Ebert, "Data transmission by frequency-division multiplexing using the discrete fourier transform," *IEEE Transactions on Communication Technology*, vol. 19, no. 5, pp. 628–634, Oct. 1971.

[20] P. A. Bello, "Selectrive fading limitations of the kathryn modem and some system design considerations," *IEEE Transactions on Communication Technology*, vol. 13, no. 3, pp. 320–333, Sep. 1965.

[21] L. J. Cimini, "Analysis and simulation of a digital mobile channel using orthogonal frequency division multiplexing," *IEEE Transactions on Communications*, vol. 33, no. 7, pp. 665–675, July 1985.

[22] W. Zhang, X.-G. Xia, and K. B. Letaief, "Space-time/frequency coding for MIMO-OFDM in next generation broadband wireless systems," *IEEE Wireless Communication*, vol. 14, no. 3, pp. 32–43, June 2007.

[23] M. Zhang, T. D. Abhayapala, D. Jayalath, D. Smith, and C. Athaudage, "Matched rotation precoding: A new paradigm in space-frequency coding," *IEEE International Conference on Communications*, pp. 1–6, 2009.

[24] X. Zhu and J. Xue, "On the correlation of subcarriers in grouped linear constellation precoding OFDM systems over frequency selective fading," *IEEE Conference on*

Vehicular Technology, vol. 3, pp. 1431–1435, Spring, 2006.

[25] M. Zhang, T. D. Abhayapala, D. Jayalath, D. Smith, and C. Athaudage, "Space-frequency block coding with matched rotation for MIMO-OFDM system with limited feedback," *Accepted by EURASIP Journal on Advances in Signal Processing*, 2009.

[26] Z. Liu, Y. Xin, and G. B. Giannakis, "Space-time-frequency coded OFDM over frequency-selective fading channels," *IEEE Transactions on Signal Processing*, vol. 50, no. 10, pp. 2465–2476, Oct. 2002.

[27] M. Zhang, T. D. Abhayapala, D. Jayalath, D. Smith, and C. Athaudage, "Multirate space-time-frequency linear block coding," *IEEE International Conference on Communications*, pp. 4084–4089, May. 2008.

[28] S. Gowrisankar and B. S. Rajan, "A rate-one full-diversity low-complexity space-time-frequency block code (STFBC) for 4-Tx MIMO-OFDM," *IEEE International Symposium on Information Theory*, pp. 2090–2094, Sep. 2005.

[29] A. K. Sadek, W. Su, and K. R. Liu, "Diversity analysis for frequency-selective MIMO-OFDM systems with general spatial and temporal correlation model," *IEEE Transactions on Communications*, vol. 54, no. 5, pp. 878–888, May. 2006.

[30] H. S. Wang and P.-C. Chang, "On verifying the first-order markovian assumption for a rayleigh fading channel model," *IEEE Transactions on Vehicular Technology*, vol. 45, no. 2, pp. 353–357, May. 1996.

[31] W. Su, Z. Safar, and K. R. Liu, "Towards maximum achievable diversity in space, time and frequency: performance analysis and code design," *IEEE Transactions on Wireless Communications*, vol. 4, no. 4, pp. 1847–1857, July 2005.

[32] T. Pollock, "Correlation modelling in MIMO systems: When can we Kronecker?" *Australian Communications Theory Workshop*, pp. 149–153, Feb. 2004.

[33] COST 207 Management Committee, "Digital land mobile radio communications," *(Final Report), Commission of the European Communities,*, 1989.

[34] 3GPP and 3GPP2, "Spatial channel model AHG," 5.0ed, Apr. 2003.

[35] M. Shafi, M. Zhang, A. L. Moustakas, P. J. Smith, A. F. Molisch, F. Tufvesson, and S. H. Simon, "Polarized MIMO Channels in 3D: Models, Measurements and Mutual information," *IEEE Journal on Select Areas in Communications*, vol. 24, no. 3, pp. 514–527, Mar. 2006.

[36] M. Zhang, P. J. Smith, and M. Shafi, "A new space-time MIMO channel model," *Australian Communications Theory Workshop*, pp. 249 – 254, Feb. 2005.

[37] K. Yu, M. Bengtsson, B. Ottersten, D. McNamara, P. Karlsson, and M. Beach, "Modeling of wide-band MIMO radio channels based on NLoS indoor measurements," *IEEE Transactions on Vehicular Technology*, vol. 53, no. 3, pp. 655–665, May. 2004.

[38] D. Gesbert, M. Shafi, D. shan Shiu, P. J. Smith, and A. Naguib, "From theory to practice: An overview of MIMO spacectime coded wireless systems," *IEEE Journal on Select Areas in Communications*, vol. 21, no. 3, pp. 281–302, Apr. 2003.

[39] V. Tarokh, H. Jafarkhani, and A. Calderbank, "Space-time block coding for wireless communications: Performance results," *IEEE Journal on Select Areas in Communications*, vol. 17, no. 3, pp. 451–459, Mar. 1999.

[40] V. Tarokh, H. Jafarkhani, and A. R. Calderbank, "Space-time block codes from orthogonal designs," *IEEE Transactions on Information Theory*, vol. 45, no. 5, pp. 1456–1467, July 1999.

[41] B. Hassibi and B. M. Hochwald, "High-rate codes that are linear in space and time," *IEEE Transactions on Information Theory*, vol. 48, no. 7, pp. 1804–1824, July 2002.

[42] P. Elia, K. R. Kumar, S. A. Pawar, P. V. Kumar, and H.-F. Lu, "Explicit space-time codes that achieve the diversity-multiplexing gain tradeoff," *IEEE Transactions on Information Theory*, vol. 52, no. 9, pp. 3869–3884, Sep. 2006.

[43] H. E. Gamal and M. O. Damen, "Universal space-time coding," *IEEE Transactions on Information Theory*, vol. 49, no. 5, pp. 1097–1119, May. 2003.

[44] H. Jafarkhani, "A quasi-orthogonal spacectime block code," *IEEE Transactions on Communications*, vol. 49, no. 1, pp. 1–4, Jan. 2001.

[45] O. Tirkkonen, A. Boariu, and A. Hottinen, "Minimal non-orthogonality rate 1 space-time block code for 3+ tx antennas," *IEEE Sixth International Symposium on Spread Spectrum Techniques and Applications*, vol. 2, pp. 429–432, Sep. 2000.

[46] C. B. Papadias and G. J. Foschini, "Capacity-approaching spacectime codes for systems employing four transmitter antennas," *IEEE Transactions on Information Theory*, vol. 49, no. 3, pp. 726–732, Mar. 2003.

[47] Y. Chang and Y. Hua, "A complete family of quasi-orthogonal space-time codes," *IEEE International Conference on Acoustics, Speech, and Signal Processing*, vol. 4, Mar. 2005.

[48] W. Su and X.-G. Xia, "Signal constellations for quasi-orthogonal space-time block codes with full diversity," *IEEE Transactions on Information Theory*, vol. 50, no. 10, pp. 2331–2347, Oct. 2004.

[49] L. Xian and H. Liu, "Optimal rotation angles for quasi-orthogonal space-time codes with PSK modulation," *IEEE Communications Letters*, vol. 9, no. 8, pp. 676– 678,

Aug. 2005.

[50] D. Rainish, "Diversity transform for fading channels," *IEEE Transactions on Communications*, vol. 44, no. 12, pp. 1653–1661, Dec. 1996.

[51] J. Boutros and E. Viterbo, "Signal space diversity: a power- and bandwidth-efficient diversity technique for the rayleigh fading channel," *IEEE Transactions on Information Theory*, vol. 44, no. 4, pp. 1453–1467, July 1998.

[52] M. O. Damen, A. Tewfik, and J. Belfiore, "A construction of a space-time code based on number theory," *IEEE Transactions on Information Theory*, vol. 48, no. 3, pp. 753–760, Mar. 2002.

[53] K. F. Lee and D. B. Williams, "A space-frequency transmitter diversity technique for OFDM systems," *IEEE Global Telecommunications Conference*, vol. 3, pp. 1473–1477, Dec. 2000.

[54] H. Bölcskei and A. J. Paulraj, "Space-frequency coded broadband OFDM systems," *IEEE Wireless Communications and Networking Conference*, vol. 1, pp. 1–6, 2000.

[55] B. Lu and X. Wang, "Space-time code design in OFDM systems," *IEEE Global Telecommunications Conference*, vol. 2, pp. 1000–1004, Nov. 2000.

[56] R. S. Blum, Y. G. Li, J. H. Winters, and Q. Yan, "Improved spacectime coding for MIMO-OFDM wireless communications," *IEEE Transactions on Communications*, vol. 49, no. 11, pp. 1873–1878, Nov. 2001.

[57] Y. Gong and K. B. Letaief, "An efficient spacecfrequency coded OFDM system for broadband wireless communications," *IEEE Transactions on Communications*, vol. 51, no. 11, pp. 2019–2029, Nov. 2003.

[58] K. Suto and T. Ohtsuki, "Performance evaluation of space-time-frequency block codes over frequency selective fading channels," *IEEE Conference on Vehicular Technology*, vol. 3, pp. 1466–1470, 2002.

[59] J. Jin, K. W. Ryu, and Y. Park, "A full rate quasi-orthogonal STF-OFDM with DAC-ZF decoder over wireless fading channels," *Electronics Telecommunications Research Inst*, vol. 28, no. 1, pp. 87–90, 2006.

[60] J. Kim and I. Lee, "Space-time coded OFDM systems with four transmit antennas," *IEEE Conference on Vehicular Technology*, vol. 4, pp. 2434–2438, Sep. 2004.

[61] J. Ong, A. Jayalath, and C. Athaudage, "Adaptive time-frequency spreading of quasi-orthogonal block codes for MIMO-OFDM systems," *IEEE Singapore International Conference on Communication Systems*, pp. 1–7, Oct. 2006.

[62] L. Wei and W. Siqi, "Space-time-frequency block coding over Rayleigh fading channels for OFDM systems," *International Conference on Communication Technology*

Proceedings, vol. 2, pp. 1008–1012, Apr. 2003.

[63] Z. Wang and G. B. Giannakis, "Linearly precoded or coded OFDM against wireless channel fades?" *IEEE Third Workshop on Signal Processing Advances in Wireless Communications*, pp. 267–270, Mar. 2001.

[64] Z. Liu, Y. Xin, and G. Giannakis, "Linear constellation precoding for OFDM with maximum multipath diversity and coding gains," *IEEE Transactions on Communications*, vol. 51, no. 3, pp. 416–427, Mar. 2003.

[65] I. Ouachani, K. Gosse, and P. Duhamel, "Trading rate versus diversity in space-time-frequency block coding schemes," *First International Symposium on Control, Communications and Signal Processing*, pp. 171–174, 2004.

[66] Y. Xin and G. B. Giannakis, "High-rate space-time layered OFDM," *IEEE Communications Letters*, vol. 6, no. 5, pp. 187–189, May. 2002.

[67] B. Gui and D. Qu, "VBLAST-OFDM system with linear constellation precoding," *IEEE Conference on Vehicular Technology*, vol. 2, pp. 733–737, May. 2004.

[68] K. T. and B. S. Rajan, "A systematic design of high-rate full-diversity space-frequency codes for MIMO-OFDM systems," *IEEE International Symposium on Information Theory*, pp. 2075–2079, Sep. 2005.

[69] C. Athaudage, J. Wang, and D. Jayalath, "An efficient framework to exploit frequency diversity in OFDM: Precoding with adaptive subcarrier selection," *The 17th Annual IEEE Inter. symposium on Personal, Indoor and Mobile Radio Comm.*, pp. 1–5, 2006.

[70] M. Kuhn, I. Hammerstroem, and A. Wittneben, "Linear scalable dispersion codes for frequency selective channels," *Proceeding of the 8th International OFDM Workshop*, pp. 753–760, Sep. 2003.

[71] S. Zhou and G. B. Giannakis, "Space-time coding with maximum diversity gains over frequency-selective fading channels," *IEEE Signal Processing Letters*, vol. 8, no. 10, pp. 269–272, Oct. 2001.

[72] X. Ma and G. B. Giannakis, "Space-time-multipath coding using digital phase sweeping or circular delay diversity," *IEEE Transactions on Signal Processing*, vol. 53, no. 3, pp. 1121–1131, Mar. 2005.

[73] L. Rugini, P.Banelli, and G. B. Giannakis, "MMSE-based local ML detection of linearly precoded OFDM signals," *IEEE International Conference on Communications*, vol. 6, pp. 3270–3275, June 2004.

[74] M. Zhang, D. Jayalath, T. D. Abhayapala, D. Smith, and C. Athaudage, "Compensation decoding in space time frequency block coding," *IEEE Communications Let-*

ters, vol. 11, no. 7, pp. 610–612, July 2007.

[75] S. Gowrisankar and B. S. Rajan, "A rate-one full-diversity low-complexity space-time-frequency block code (STFBC) for 4-Tx MIMO-OFDM," *IEEE International Symposium on Information Theory*, pp. 2090–2094, Sep. 2005.

[76] A. S. G. manuele Bizzarri and G. M. Vitetta, "Adaptive space-time-frequency coding schemes for MIMO OFDM," *IEEE Global Telecommunications Conference*, vol. 2, pp. 933–937, Dec. 2004.

[77] W. P. Siriwongpairat, W. Su, M. Olfat, and K. J. R. Liu, "Multiband-OFDM MIMO coding framework for UWB communication systems," *IEEE TRANSACTIONS ON SIGNAL PROCESSING, VOL. 54, NO. 1, JANUARY 2006*, vol. 54, no. 1, pp. 426–431, Jan. 2006.

[78] W. P. Siriwongpairat, W. Su, M. Olfat, and K. R. Liu, "Space-time-frequency coded multiband UWB communication systems," *IEEE Wireless Communications and Networking Conference*, vol. 1, pp. 426–431, Mar. 2005.

[79] W. Zhang and K. B. Letaief, "A systematic design of multiuser space-frequency codes for mimo-ofdm systems," *IEEE International Conference on Communications*, pp. 1054–1058, June 2007.

[80] H. Karaa, R. S. Adve, and A. J. Tenenbaum, "Linear precoding for multiuser MIMO-OFDM systems," *IEEE International Conference on Communications*, pp. 2797–2802, June 2007.

[81] R. Doostnejad, T. J. Lim, and E. S. Sousa, "On spreading codes for the down-link in a multiuser MIMO/OFDM system," *IEEE Conference on Vehicular Technology*, vol. 1, pp. 498–502, Oct. 2003.

[82] C. Tepedelenlioglu, "Maximum multipath diversity with linear equalization in precoded OFDM systems," *IEEE Transactions on Information Theory*, vol. 50, no. 1, pp. 232–235, Jan. 2004.

[83] A. F. Molisch, M. Z. Win, and J. H. Winters, "Space-time-frequency (STF) coding for MIMO-OFDM systems," *IEEE Communications Letters*, vol. 6, no. 9, pp. 370–372, Sep. 2002.

[84] R. A. Horn and C. Johnson, *Matrix Analysis*. Cambridge University Press, 1986.

[85] R. A. Horn and C. R. Johnson, *Topics in matrix analysis*. Cambridge University Press, 1991.

[86] K. Su, "Efficient maximum likelihood detection for communication over multiple input multiple output channels," *Technical Report, University of Cambridge, http://www.cl.cam.ac.uk/research/dtg/publications/public/ks349/Su05B.pdf*, Feb. 2005.

[87] H. Kanemaru and T. Ohtsuki, "Interference cancellation with diagonalized maximum likelihood decoder for space-time/space-frequency block coded OFDM," *IEEE Conference on Vehicular Technology*, vol. 1, pp. 525–529, May. 2004.

[88] 3GPP, "Feasibility study for orthogonal frequency division multiplexing (ofdm) for UTRAN enhancement, tr 25.892,v6.0.0," *3rd generation partnership project*, 2004.

[89] K. Su and I. J. Wassell, "A new ordering for efficient sphere decoding," *IEEE International Conference on Communications*, vol. 3, pp. 1906– 1910, May. 2005.

[90] E. Viterbo and J. Boutros, "A universal lattice code decoder for fading channels," *IEEE Transactions on Information Theory*, vol. 45, no. 5, pp. 1639–1642, July 1999.

[91] V. Pammer, Y. Delignon, W. Sawaya, and D. Boulinguez, "A low complexity suboptimal MIMO receiver: the combined ZF-MLD algorithm," *The 14th IEEE Proceedings on Personal, Indoor and Mobile Radio Communications*, vol. 3, pp. 2271–2275, Sep. 2003.

[92] L. Rugini, P. Banelli, and G. B. Giannakis, "MMSE-based local ML detection of linearly precoded OFDM signals," *IEEE International Conference on Communications*, vol. 6, pp. 3270–3275, June 2004.